

65450

**OPTIMAL CONTROL OF DIGITALLY
CONTROLLED DC MOTORS**

**A Thesis Submitted to the
Graduate School of Natural and Applied Science of
Dokuz Eylül University
In Partial Fulfillment of Requirements for
the Degree of Doctor of Philosophy in Electronics Engineering**

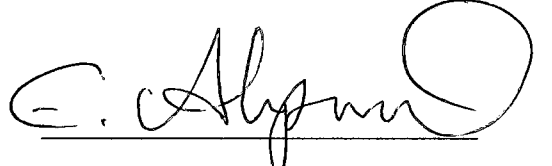
**by
Fatma GÜRBÜZ**

October, 1997


İZMİR

Ph.D. THESIS EXAMINATION RESULT FORM

We certify that we have read this thesis and that in our opinion it is fully adequate, in scope and in quality, as a thesis for the degree of Doctor of Philosophy.



Assoc. Prof. Dr. Eyüp AKPINAR
(Advisor)



(Committee Member)



(Committee Member)

Approved by the
Graduate School of Natural and Applied Sciences



Prof. Dr. Cahit HELVACI

Director

ACKNOWLEDGMENTS

I would like to express my sincere thanks to my supervisor, Assoc. Prof. Dr. Eyüp AKPINAR, for his continuous helps from the very beginning of this thesis. I am also indebted to him for his valuable suggestions, constructive criticisms and teachings on the scientific moral.

I would also like to thank to my previous supervisors for every kind of help, with whom I studied before Assoc. Prof. Dr. Eyüp AKPINAR.

I greatly appreciate the patience, understanding and support of my husband during this thesis. I especially thank to him for the help on the drawings of this thesis.

ABSTRACT

A linear model has been developed for the closed-loop control of dc motor fed by class-C chopper in z-domain including the time variation of pulsewidth modulated (PWM) waveform. This model has been used for the purpose of optimum design of the parameters of the digital proportional-integral controllers employed in the current and speed feedbacks. Therefore the entire system has been considered as a discrete linear quadratic tracker problem with output feedback. Minimization of the nonlinear cost function under the constraint of Lyapunov equation has been solved by using the Simplex algorithm. In fact, simplex algorithm is for the unconstrained nonlinear functions but it has been modified here to minimize the Lyapunov constrained cost function.

The stability analysis of the overall system under the variation of the amplitude and the chopping period of PWM waveform has been also investigated by using the root-locus method and the Jury stability test. It has been observed that the linear model developed here for the dc motor drive can be used to design the optimal values of controller parameters in the stable operating region.

Finally, the real-time simulation of the closed-loop system has been carried out to check the accuracy of the linear model develop in this thesis. For the real-time simulation, pulsewidth modulated waveform at the output of the chopper has been estimated by using the z-transformation. As a result, it has been observed that the real-time simulation results are in a consistency with the results of the analysis of the linear model.

ÖZET

C-sınıfı kısıyıcı ile sürülen doğru akım motorunun z -domain'de kapalı-çevrim kontrolü için darbe genişlik bindirimli sinyalin zaman değişimini içeren doğrusal bir model geliştirilmiştir. Bu model akım ve hız geri beslemelerinde kullanılan sayısal oransal-integral denetleyici parametrelerinin optimum tasarımı için kullanılmıştır. Dolayısıyla tüm sistem, çıkış geribeslemeli kesikli doğrusal karesel bir izleyen problemi olarak ele alınmıştır. Doğrusal olmayan maliyet fonksiyonunun Lyapunov eşitlik kısıtı altında en azlaması simplex yöntemi ile yapılmıştır. Simplex yöntemi aslında kısıtsız doğrusal olmayan fonksiyonlar için olmasına rağmen burada Lyapunov kısıtlı maliyet fonksiyonlarının en azlaması için geliştirilmiştir.

Darbe genişlik bindirimli sinyalin genlik ve periyodunun değişmesi halinde tüm sistemin kararlılık analizi de root-locus yöntemi ve Jury kararlılık testi ile yapılmıştır. DC motor sürücüsü için geliştirilen doğrusal modelin denetleyici parametrelerinin kararlı çalışma bölgesindeki optimal değerlerini bulmak için kullanılabileceği görülmüştür.

Son olarak, tezde geliştirilen doğrusal modelin geçerliliğini görmek için kapalı-çevrim sisteminin gerçek zamanda benzeşimi yapılmıştır. Bunun için kısıyıcı çıkışındaki darbe genişlik bindirimli sinyal z -transform kullanılarak üretilmiştir. Sonuçta, gerçek zaman benzeşim sonuçlarının doğrusal modelin analiz sonuçlarıyla uyumlu olduğu gözlenmiştir.

CONTENTS

	Page
Contents.....	vi
List of Figures.....	ix
List of Tables.....	xii

Chapter One

INTRODUCTION

Introduction.....	1
-------------------	---

Chapter Two

MODELING OF THE SYSTEM IN Z-DOMAIN

2.1 Introduction.....	7
2.2 Modeling of DC Motor.....	8
2.3 Modeling of Chopper.....	10
2.4 Modeling of DC Motor with Chopper Drive.....	12
2.5 Modeling of Controllers.....	17
2.5.1 Modeling of Current Controller.....	19
2.5.2 Modeling of Speed Controller.....	21

Chapter Three

OPTIMAL CONTROLLER DESIGN WITH OUTPUT FEEDBACK

3.1 Introduction.....	24
3.2 Formulation of the Entire System as a Linear Quadratic(LQ) Tracker with Output Feedback.....	26
3.3 The Performance Index and Optimal Cost.....	32
3.4 LQ Tracker Design with Output Feedback.....	37
3.4.1. Simplex Algorithm for Optimization.....	37
3.4.2 Using the Simplex Algorithm for Constrained Optimization.....	40
3.4.3 The Initial Values of Variables.....	43
3.4.4 Matlab Solution of the Optimization.....	53
3.5 Results of Analysis.....	55
3.5.1 Results of Analysis with Unlimited Duty Cycle.....	56
3.5.2 Results of Analysis with Limited Duty Cycle.....	62

Chapter Four

STABILITY ANALYSIS

4.1. Introduction.....	71
4.2. Stability Analysis for the Amplitude Control of PWM Signal by Root-Locus....	72
4.3. Jury Stability Test.....	80
4.3.1 Stability Analysis for the Amplitude Control of PWM Signal.....	82
4.3.2 Stability Analysis for the Chopping Period Control.....	87

Chapter Five
REAL TIME SIMULATION OF THE SYSTEM

5.1 Introduction.....	99
5.2 Real-time Simulation of the Closed-Loop Control of DC Drive.....	99
5.2.1 Estimation of PWM Waveform Using z-transformation.....	102
5.3 Results of the Real-time Simulation.....	103

Chapter Six
CONCLUSIONS AND FURTHERWORK

6.1 Conclusions.....	110
6.2 Furtherwork.....	111

APPENDICES

Appendix 1 Computer Programs for Optimal Controller Design.....	113
Appendix 2 Computer Programs for Stability Analysis.....	135
Appendix 3 Computer Programs for Real-Time Simulation.....	150

REFERENCES.....	156
------------------------	------------

LIST OF FIGURES

	Page
Figure 2.1 Block diagram of the dc motor speed control system.....	8
Figure 2.2 Class-C chopper circuit and related waveforms.....	11
Figure 2.3 Input-output characteristic of chopper.....	12
Figure 2.4 Pulsewidth modulated signal.....	13
Figure 2.5 Mapping of the s-plane(a) according to backward difference(b), forward difference(c), and trapezoidal rule(d) to the z-plane.....	18
Figure 2.6 Block diagram of the current controller.....	19
Figure 2.7 Block diagram of the speed controller.....	22
Figure 3.1 Block diagram representation of the system as an LQ tracker with output feedback.....	32
Figure 3.2 Possible outcomes in the simplex method.....	38
Figure 3.3 Flowchart of the simplex optimization algorithm.....	41
Figure 3.4 Flowchart of the simplex algorithm for Lyapunov constrained functions.....	43
Figure 3.5 Inner current loop of the system.....	43
Figure 3.6 Speed response for $K_{initial}$ with unlimited duty cycle.....	56
Figure 3.7 Armature current variation for $K_{initial}$ with unlimited duty cycle.....	57
Figure 3.8 Reference current variation for $K_{initial}$ with unlimited duty cycle.....	58
Figure 3.9 Speed response for K_{opt1} with unlimited duty cycle.....	59
Figure 3.10 Armature current variation for K_{opt1} with unlimited duty cycle.....	60
Figure 3.11 Reference current variation for K_{opt1} with unlimited duty cycle.....	60
Figure 3.12 Speed response for K_{opt2} with unlimited duty cycle.....	61

Figure 3.13 Armature current variation for K_{opt2} with unlimited duty cycle.....	61
Figure 3.14 Reference current variation for K_{opt2} with unlimited duty cycle.....	62
Figure 3.15 Speed response for $K_{initial}$ with limited duty cycle.....	63
Figure 3.16 Armature current variation for $K_{initial}$ with limited duty cycle.....	64
Figure 3.17 Reference current variation for $K_{initial}$ with limited duty cycle.....	64
Figure 3.18 Duty cycle variation for $K_{initial}$	65
Figure 3.19 Speed response for K_{opt1} with limited duty.....	66
Figure 3.20 Armature current variation for K_{opt1} with limited duty.....	67
Figure 3.21 Reference current variation for K_{opt1} with limited duty cycle.....	67
Figure 3.22 Duty cycle variation for K_{opt1}	68
Figure 3.23 Speed response for K_{opt2} with limited duty cycle.....	69
Figure 3.24 Armature current variation for K_{opt2} with limited duty cycle.....	69
Figure 3.25 Reference current variation for K_{opt2} with limited duty cycle.....	70
Figure 3.26 Duty cycle variation for K_{opt2}	70
Figure 4.1 Rotor speed for $K_{pwm}=545$	78
Figure 4.2 Armature current for $K_{pwm}=545$	78
Figure 4.3 Rotor speed for $K_{pwm}=555$	79
Figure 4.4 Armature current for $K_{pwm}=555$	80
Figure 4.5 Speed of the motor showing instability.....	96
Figure 4.6 Armature current denoting instability.....	96
Figure 4.7 Speed of the motor showing stability.....	97
Figure 4.8 Armature current denoting stability.....	98
Figure 5.1 Block diagram representation of the real-time simulation model.....	100
Figure 5.2 DC Motor-z subsystem in the Simulink model.....	101
Figure 5.3 Rotor speed for $K_{initial}$	104
Figure 5.4 The armature current for $K_{initial}$	104
Figure 5.5 Reference current for $K_{initial}$	105
Figure 5.6 Variation of the duty cycle for $K_{initial}$	105
Figure 5.7 Rotor speed for K_{opt1}	106
Figure 5.8 The armature current for K_{opt1}	106
Figure 5.9 Reference current for K_{opt1}	107

Figure 5.10 Variation of the duty cycle for K_{opt1}	107
Figure 5.11 Rotor speed for K_{opt2}	108
Figure 5.12 The armature current for K_{opt2}	108
Figure 5.13 Reference current for K_{opt2}	109
Figure 5.14 Variation of the duty cycle for K_{opt2}	109



LIST OF TABLES

	Page
Table 3.1 Root locations of the inner loop for different values of K_{ii}	45
Table 3.2 The absolute values of roots of the inner loop for K_{ii} in the range (0-750).....	46
Table 3.3 The absolute values of roots of the inner loop for K_{ii} in the range (45000-90000).....	48
Table 3.4 Root locations of the system for different values of K_{ig}	50
Table 4.1 Absolute values of roots for K_{pwm}	74
Table 4.2 Absolute values of roots for K_{pwm} in the range (1-5).....	76
Table 4.3 Absolute values of roots for K_{pwm} in the range (450-600).....	76
Table 4.4 Jury table for the 6th order system in thesis.....	81

CHAPTER ONE

INTRODUCTION

The purpose of this thesis is to develop a linear model of the closed loop control of dc motor fed by class-C chopper in z-domain including the time variation of pulsewidth modulated (PWM) signal and then, using this model, to design the optimum parameters of digital proportional-integral (PI) controllers employed in current and speed feedbacks. The real-time simulation is also carried out to check the accuracy of the model developed here. The stability analysis on the parameters of two controllers under the variation of chopping frequency and amplitude of PWM waveform is performed by using the root-locus method and the Jury stability test.

Although the dc machine is more expensive, the control principles and the converter equipment required are somewhat simpler compared to ac machines. The simplicity and flexibility of control of dc motors have made them suitable for adjustable speed drive applications. Also fast torque response has favored their use in high performance servo drives. The principal problem of a dc machine is its commutators and brushes and the frequent maintenance required for its operation. Thus, for several decades, attention has been diverted to develop ac drives as a viable alternative to dc drives in many applications. However, today, a considerable percentage of industrial drives use dc machines. These machines will retain its appeal for at least another one or two decades, and will continue to meet industrial needs (SEN, 1990).

The drive circuit used in this thesis is a class-C chopper. This circuit is widely used especially in the speed control of dc motors in industry. It is also used in battery-operated vehicles where energy saving and noise are the prime considerations (Sen, 1991). The early theoretical analysis studies related to choppers start in 1970's. The dynamic characteristics of a dc motor driven by thyristor choppers or rectifiers are analyzed and compared with test results (Nitta, Okitsu, Suzuki & Kinouchi, 1970). Dubey and Shepherd's paper describes certain approximations which permit the derivation of simple but analytical methods for the analysis of the dc series motor fed by a chopper, having either pulsewidth control or current limit control (Dubey & Shepherd, 1975). In the following years, digital simulation of dc motors driven by chopper has been studied. In the paper (Damle & Dubey, 1975) dc motor driven by a chopper is considered as an open loop system. The simulation was carried out by using the average value of the output voltage of the chopper. In another study, the output waveform of the chopper is taken as a square wave, and the computer simulation is performed for the open loop drive (Turner, 1988).

A microprocessor-based speed control scheme for a separately excited dc motor fed from a dc source is described in the paper (Kettleborough, Smith, Vadher & Antunes, 1991). It combines armature voltage control with spillover field weakening to provide smooth and precise control from standstill to speeds well above the base value. The function of the microprocessor, in this work, is to control the "on" times of the two choppers (one for armature control and one for field control) in order to vary the armature and field voltages in accordance with the speed control requirements by using the average value modeling of the choppers.

Since the dc motor is considered as a multi-input, multi-output system and the closed loop control system is normally built with two loops in this thesis, all controller parameters are not designed simultaneously to verify the system constraints by using the classical control theory. Instead of that, the modern control techniques allows to close the all feedback loops simultaneously in order to design the controller gains. In high performance drive applications such as in the areas of robotics, machine tools,

and rolling mills, the drive systems are required that can provide fast dynamic response, parameter insensitive control characteristics, and rapid recovery from speed drop caused by impact loads. Therefore, in recent years, intense research efforts have been focused on the use of modern control technique in drive systems (Bose, 1988).

Jing-Ping Jiang, Shen Chen and Pradip K. Sinha developed a unified methodology for real-time speed control of a thyristor-driven dc motor. For this purpose an optimal state feedback controller using the Kalman filter state estimation technique was derived. It is followed by an adaptive control algorithm to compensate the effects of noise and disturbance. The effectiveness of the optimal controller based on estimated state variables is pointed out in the paper (Jing-Ping Jiang, Shen Chen & Pradip K. Sinha, 1990).

The paper of Mota, Rognon and Le-Huy presents a digital position control system using a dc motor fed by a four quadrant transistor chopper (Mota, Rognon & Le-Huy, 1984). Both the classical and state feedback approaches are considered in this paper. Experimental results show that the classical control configuration, consisting of a position control loop with an inner speed control loop, performs better than the state feedback which is simpler to implement. The mean value of the chopper output voltage is used for the modeling of chopper.

Al-Assadi and Al-Chalabi presented a design method to find the best tuning parameters for a proportional-integral-derivative controller employed in a single feedback loop (Al-Assadi & Al-Chalabi, 1987). The procedure presented in this paper uses a time domain optimization technique to minimize the integral-squared-error response to a step input. However, the method presented in this paper has been criticized in (Fu, Olbrot & Polis, 1989).

Among all the other papers written on optimal control theory, in the paper of Umanand and Bhat, the optimal theory is applied on the design of controller parameter for the vector controlled induction-motor drive system viewed as a linear

quadratic tracker problem with output feedback, and the optimal and robust digital current controller is designed for the vector-controlled induction motor drive system (Umanand & Bhat, 1996).

In the paper of Muir and Neuman, pulsewidth modulation control of brushless dc motors is implemented with digital servomechanisms for robotic applications (Muir & Neuman, 1985). In this paper, it has been presented that the discrete-time state equation of the brushless dc motor driven by a PWM waveform can be obtained under the assumption that the pulse period is much smaller than the motor time-constants.

The principal techniques used for the stability analysis are root-locus method, Routh-Hurwitz criterion or frequency response techniques such as Nyquist criterion for the continuous time systems, and the applications of these methods are exist on the adjustable speed drives. A stability study of a rectifier-inverter induction motor drive system is performed by neglecting the harmonic content of the stator voltages and applying Nyquist stability criterion to the small-displacement equations obtained by linearization around the operating point (Lipo & Krause, 1969). The stability study of the Fallside and Wortley's paper uses eigenvalue loci and also the Routh-Hurwitz criterion (Fallside & Wortley, 1969).

For discrete time systems, on the other hand, a standart method such as z-domain analysis or pulse transfer function analysis in the s-domain in which the sampling effect is not neglected yields useful results (Kojori, Lavers & Dewan, 1993). In this thesis the first technique is used and the Jury stability test is applied. This method was a time consuming technique until the recent development in computer technology.

As it can be recognized from the brief summary of papers given above, the dc motor fed by a chopper is usually modeled by the average value of the armature terminal voltage. However this modeling does not include the ripples due to chopping of the armature voltage. In this thesis, time variation of PWM waveform is included into the model developed here for the design of the controllers' parameters for the

first time. The closed loop control of dc motor fed by a class-C chopper is considered as a discrete linear quadratic tracker problem with output feedback. The output feedback uses the only measurable states of the system and provides flexibility in choosing the controller structure. The dc motor drive has been modeled to design the optimal controller parameters by using this control theory first time.

The work presented in this thesis can be summarized as follows:

In Chapter 2, the closed loop control system is introduced firstly. Then the modeling of each subsystem is given. The dc motor is considered as a two-input two-output system. Since a class-C type chopper is used as a drive, its PWM output waveform is given. The PWM driven dc motor state equation is derived in discrete time domain. The PI controller is chosen for both the speed and current controllers in the system and their discrete time state space models are obtained using the trapezoidal integration rule.

In Chapter 3, first of all it is explained why optimal control and why output feedback are selected. Then the closed loop system is formulated in a suitable form to the Linear Quadratic Tracker design method with output feedback. The performance index and optimal cost is given. Since the simplex method is used for the minimization of the cost, an outline of the simplex method for nonlinear minimization is given. Also a modification of the simplex method for the Lyapunov constrained problems is developed. Further, finding the initial gains that stabilizes the system which is required by simplex like any other minimization algorithm is given. Finally, optimal controller gains and the results of the analysis using these gains are presented.

In Chapter 4, the amplitude and the chopping period of PWM signal are assumed to be varying and the effect of them on the stability of overall system is investigated. The effect of the amplitude of PWM signal on stability is searched by two techniques: root-locus method and Jury stability test. It is seen that the results of both methods are in consistency. On the other hand, stability analysis for the chopping period of

PWM signal is carried out by the Jury test only, because the characteristic equation of the system is not linear in T . Stability limits obtained from root-locus and Jury test are checked by analyzing the model of the system, also.

In Chapter 5, the real-time simulation of the system is carried out with the help of Simulink which is a dynamic system simulation software in Matlab. The PWM waveform is required to apply to the armature of the motor for the real-time simulation. Thus, PWM waveform is generated by a dedicated program written in Matlab using the z -transformation. Finally, real-time simulation results for the initial and local optimum controller gains are given in order to compare with the results of the analysis obtained in Chapter 3 from the linearized model.

In Chapter 6, the results and model developed in this thesis are discussed and the future work that can be performed is presented.

CHAPTER TWO

MODELING OF THE SYSTEM IN Z-DOMAIN

2.1 Introduction

For precise speed control of servo systems, closed-loop control is normally used because a closed-loop control system has the advantages of greater accuracy, improved dynamic response, and reduced effects of load disturbances. Closed-loop speed control system in this thesis consists of a separately excited direct current (DC) motor, chopper, and current and speed controllers. Block diagram of the system is as given in Figure 2 . 1. As it is seen from Figure 2 . 1, the closed-loop system has an inner current loop and an outer speed loop. The reason for including an inner loop is that a speed feedback with an inner current loop provides faster response to any disturbances in speed command, load torque, and supply voltage (Rashid, 1993). In Figure 2 . 1, the speed signal is fed into the digital controller using an analog to digital (A/D) converter or optic encoders. Armature current can also be fed into the digital controller using A/D converter or by sampling the armature current. These feedbacks can include the transducers having linear gains (k_1 and k_2) as shown in Figure 2 . 1. The separately excited DC motor has been utilized in many industrial applications where speed or torque must be controlled over a wide range, such as rolling mills, paper mills, and machine tools (Slemon & Straughen, 1980).

The pulsewidth modulation (PWM) control of dc motor is implemented with digital controllers governed by microprocessors, microcontrollers or personal computers according to the complexity of the system. The digital control systems have many advantages over analog counterparts because the hardware is simpler, it is

easy to change the control strategy and parameters using the software, and the entire system is more reliable. The most proper algorithm to model the digital systems is to use the difference equations and related transformations.

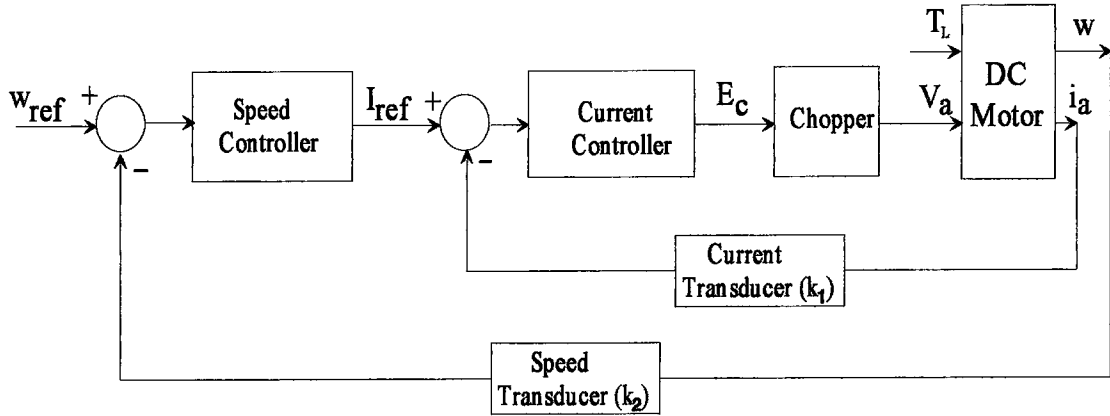


Figure 2 . 1 Block diagram of the dc motor speed control system

2.2 Modeling of DC Motor

The mechanical and electrical behaviour of a DC motor is described in continuous time domain by the following well known equations (Krause, 1986).

$$V_a = R_a \cdot i_a + L_a \cdot \frac{di_a}{dt} + E_g \quad (2-1)$$

$$E_g = K_a \cdot \phi \cdot w \quad (2-2)$$

$$T_e = T_L + J \frac{dw}{dt} + B_v \cdot w \quad (2-3)$$

$$T_e = K_a \cdot \phi \cdot i_a \quad (2-4)$$

where,

V_a : Armature voltage (Volt)

R_a : Armature resistance (Ohm)

i_a : Armature current (Amper)

L_a : Armature inductance (Henry)

E_g : Back electromotive force voltage or speed voltage (Volt)

$K_a\phi$: Back electromotive force and torque constant (Volt/rd/sec or Nt-m/Amper)

w : Motor speed (rd/sec)

T_e : Electromagnetic torque developed by the motor (Nt-m)

T_L : Load torque (Nt-m)

J : Total moment of inertia (kg-m^2)

B_v : Viscous friction constant (Nt-m/rd/sec).

Electrical and mechanical time constants of the motor are defined as $\tau_a = L_a/R_a$ and $\tau_m = J/B_v$, respectively, and the electrical time constant is much smaller compared to the mechanical time constant.

In this thesis, the field current is kept constant, thus $K_a\phi$ in Equation (2-2) and Equation (2-4) will be taken constant. The effect of armature current on the saturation has been neglected. Consequently, Equations (2-1) to (2-4) can be written in the state-space form as follows

$$\frac{d}{dt} \begin{bmatrix} i_a(t) \\ w(t) \end{bmatrix} = \begin{bmatrix} -R_a/L_a & -K_a\phi/L_a \\ K\phi/J & -B_v/J \end{bmatrix} \cdot \begin{bmatrix} i_a(t) \\ w(t) \end{bmatrix} + \begin{bmatrix} 1/L_a & 0 \\ 0 & -1/J \end{bmatrix} \cdot \begin{bmatrix} V_a(t) \\ T_L(t) \end{bmatrix} \quad (2-5)$$

or in the compact form

$$\frac{d}{dt} x_m(t) = A_m \cdot x_m(t) + B_m \cdot u_m(t). \quad (2-6)$$

where x_m is the (2x1) state vector, A_m is the (2x2) matrix consisting of motor constants, B_m is the (2x2) input matrix, u_m is the (2x1) input vector and the subscript m holds for motor. As it can be seen from Equation (2-5), the dc motor is modeled

with two inputs such that armature voltage V_a and load torque T_L are inputs. On the other hand, rotor speed w and the armature current i_a can be defined as the outputs giving the following equation

$$\begin{bmatrix} w(t) \\ i_a(t) \end{bmatrix} = \begin{bmatrix} 0 & 1 \\ 1 & 0 \end{bmatrix} \cdot \begin{bmatrix} i_a(t) \\ w(t) \end{bmatrix} \quad (2-7)$$

or in the compact form

$$y_m = C_m \cdot x_m \quad (2-8)$$

As a consequence of the Equations (2-5) and (2-7), the dc motor has been modelled as a 2-input, 2-output system, in other words as a multi-input, multi-output (MIMO) system.

2.3 Modeling of Chopper

Chopper is a nonlinear power electronics circuit which controls the power flow from a constant input supply voltage and produces a chopped output voltage. It is widely used for the control of the dc motors in the servo system and traction applications because they have a number of advantages such as high efficiency, flexibility in control, light weight, small size and fast response (Dubey, 1989; Sen, 1991).

In this thesis, class-C two quadrant chopper is used to drive the dc motor. This type of chopper is used especially in applications where a smooth transition from motoring to braking and vice versa is required. Class-C two quadrant chopper circuit and its output voltage waveform is given in Figure 2 . 2. The output waveform is called pulsewidth modulated waveform (PWM) because the chopping frequency (and hence the chopping period T) is kept constant and the on-time t_{on} in which load is

connected to input voltage is varied. As it can be observed from the output waveform in Figure 2 . 2, the amplitude of the output is constant at the level of K_{pwm} . However, the time t_{on} or the ratio t_{on}/T which is known duty cycle (δ) can be changed via control signals E_c . Thus, the average output voltage changes.

In the modeling of chopper, the average value modeling (Wester & Middlebrook, 1973) and real time simulation usually have been used. In the average value modeling, it is assumed that the average value of the PWM signal is applied to the armature of the motor. Despite the system response has ripples due to pulsewidth modulation, these ripples are not taken into account when the average value model is used. The real time simulation can be used to simulate the chopper with the help of a digital computer by integrating the differential equations governing the system dynamics.

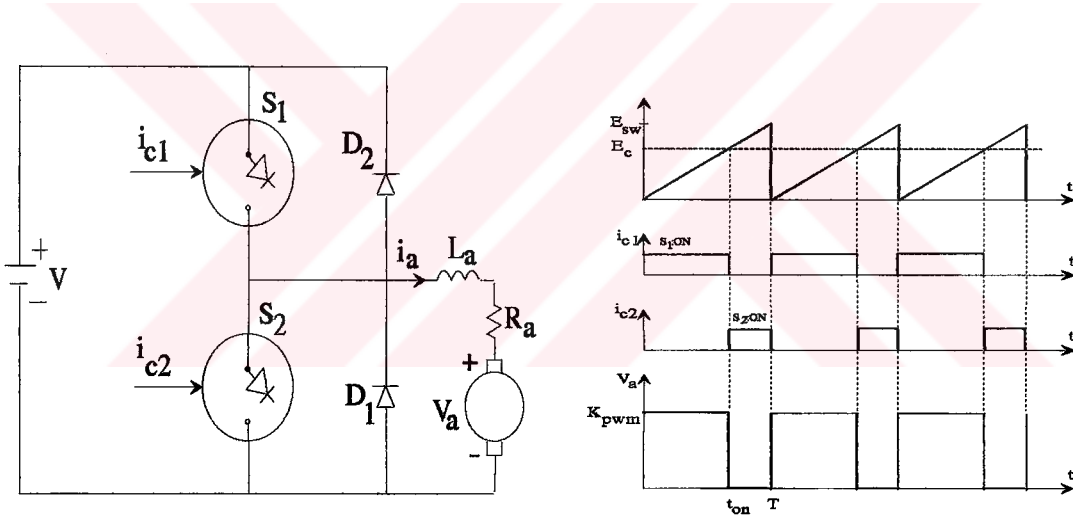


Figure 2 . 2 Class-C chopper circuit and related waveforms

Since, in the closed-loop system, i_{c1} and i_{c2} are related to current controller output signal (E_c) and the peak value of sawtooth signal (E_{sw}) as being observed in Figure 2 . 2, the following equations can be written

$$t_{on} = \frac{T}{E_{sw}} E_c \quad \text{for } 0 \leq E_c \leq E_{sw} \quad (2-9)$$

$$t_{on} = T \quad \text{for } E_c > E_{sw} \quad (2-10)$$

As it is clearly seen from Equation (2-9) and Equation (2-10) the chopper has a nonlinear characteristic and this nonlinear relation between input E_c and output t_{on} is illustrated with Figure 2 . 3.

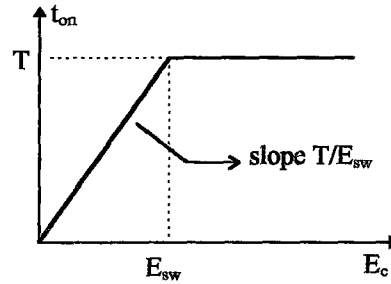


Figure 2 . 3 Input-output characteristic of chopper

In this thesis, it is assumed that the current controller's output voltage (E_c) is limited to the peak value of the sawtooth signal (E_{sw}) providing linearity. Thus, under this assumption, the transfer function of the chopper can be taken as a pure gain, T/E_{sw} .

2.4. Modeling of DC Motor with Chopper Drive

The variable $V_a(t)$ in Equation (2-5) represents the amplitude of the voltage applied to armature. The output voltage of the chopper is a function t_{on} and the amplitude of the voltage K_{pwm} . Since the amplitude of voltage is kept constant, t_{on} is the only variable in the formulation. Therefore, the input variable in the motor model will be related to t_{on} . Hence, the output of the controllers will be connected to the input of the motor via this parameter. The chopper output voltage is sampled as it arises from zero level to its magnitude. This sampling information enables to identify the duty cycle as well as the modeling of controllers and motor in z-domain.

The general solution of Equation (2-6) is given below(Chen, 1984)

$$\mathbf{x}_m(t) = e^{A_m(t-t_0)}\mathbf{x}_m(t_0) + \int_{t_0}^t e^{A_m(t-\lambda)}\mathbf{B}_m\mathbf{u}_m(\lambda)d\lambda \quad (2-11)$$

where $\exp(A_m t)$ is the matrix exponential. In Equation (2-11), the first element of the input vector \mathbf{u}_m is the PWM signal which is the constant K_{pwm} (volts) for the fraction t_{on}/T of each period, and zero for the remainder of each period. This is shown in Figure 2 . 4. The sampling period is equal to the pulse period of the PWM signal and it is assumed that PWM signal is sampled at the instants of nT , $(n+1)T$, $(n+2)T$, etc. Let's divide the sampling period, from $t_0=nT$ to $t=(n+1)T$, into two intervals: first interval is from $t_0=nT$ to $t=nT+t_{on}(nT)$, second interval is from $t_0=nT+t_{on}(nT)$ to $t=(n+1)T$. In the first interval, pulsewidth $t_{on}(nT)$ can vary from sampling period to sampling period and pulse height is constant whereas in the second interval input is zero. Then, the solution in the first interval of one period of the PWM signal can be written as follows (Muir & Neuman, 1985)

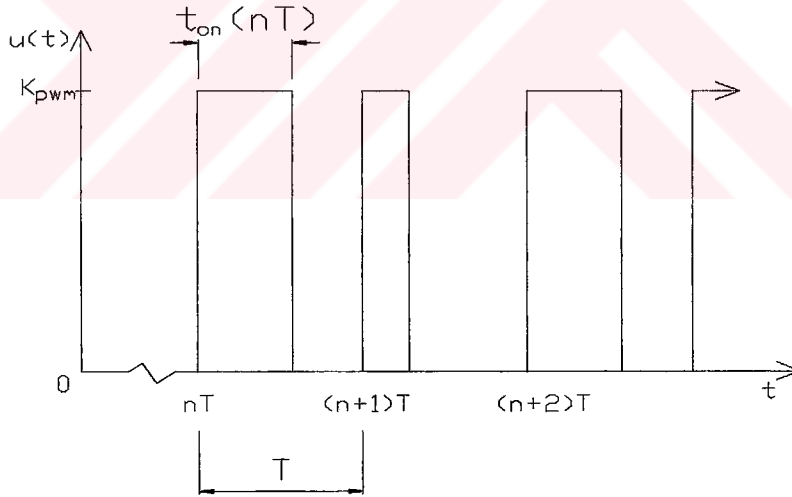


Figure 2 . 4 Pulsewidth modulated signal

$$\mathbf{x}_m[nT + t_{on}(nT)] = e^{A_m(nT+t_{on}(nT)-nT)}\mathbf{x}_m(nT) + \int_{nT}^{nT+t_{on}(nT)} e^{A_m(nT+t_{on}(nT)-\lambda)}\mathbf{B}_m\mathbf{u}_m(\lambda)d\lambda \quad \dots(2-12)$$

By substituting B_m and u_m described in Equation (2-6) into Equation (2-12) the following equation can be written

$$x_m[nT + t_{on}(nT)] = e^{A_m t_{on}(nT)} x_m(nT) + \int_{nT}^{nT+t_{on}(nT)} e^{A_m(nT+t_{on}(nT)-\lambda)} \begin{bmatrix} 1/L_a & 0 \\ 0 & -1/J \end{bmatrix} \cdot \begin{bmatrix} V_a(\lambda) \\ T_L \end{bmatrix} d\lambda \quad \dots(2-13)$$

Since $V_a(\lambda)$ is equal to K_{pwm} in this interval, the following equation can be written

$$x_m[nT + t_{on}(nT)] = e^{A_m t_{on}(nT)} x_m(nT) + \int_{nT}^{nT+t_{on}(nT)} e^{A_m(nT+t_{on}(nT)-\lambda)} \begin{bmatrix} K_{pwm}/L_a \\ -T_L/J \end{bmatrix} d\lambda \quad (2-14)$$

If the integral variable λ is changed to ϑ , so that $nT + t_{on}(nT) - \lambda = \vartheta$, then $d\vartheta = -d\lambda$. In this case, for $\lambda = nT$, $\vartheta = t_{on}(nT)$ and for $\lambda = nT + t_{on}(nT)$, $\vartheta = 0$. Thus Equation (2-14) can be written as below

$$x_m[nT + t_{on}(nT)] = e^{A_m t_{on}(nT)} x_m(nT) + \int_{t_{on}(nT)}^0 e^{A_m \vartheta} \begin{bmatrix} K_{pwm}/L_a \\ -T_L/J \end{bmatrix} (-d\vartheta) \quad (2-15)$$

Furthermore, the integral boundaries can be changed in order to eliminate the negative sign. Hence, it is obtained that

$$x_m[nT + t_{on}(nT)] = e^{A_m t_{on}(nT)} x_m(nT) + \int_0^{t_{on}(nT)} e^{A_m \lambda} d\lambda \begin{bmatrix} K_{pwm}/L_a \\ -T_L/J \end{bmatrix} \quad (2-16)$$

In the second interval, that is the interval between $[nT + t_{on}(nT)]$ and $(n+1)T$, the solution according to Equation (2-11) is

$$x_m[(n+1)T] = e^{A_m((n+1)T - (nT + t_{on}(nT)))} x_m(nT + t_{on}(nT))$$

$$+ \int_{nT+t_{on}(nT)}^{(n+1)T} e^{A_m((n+1)T-\lambda)} \begin{bmatrix} 1/L_a & 0 \\ 0 & -1/J \end{bmatrix} \cdot \begin{bmatrix} V_a(\lambda) \\ T_L \end{bmatrix} d\lambda \quad (2-17)$$

Since $V_a(\lambda)=0$ in this interval

$$x_m[(n+1)T] = e^{A_m(T-t_{on}(nT))} x_m(nT + t_{on}(nT)) + \int_{nT+t_{on}(nT)}^{(n+1)T} e^{A_m((n+1)T-\lambda)} \begin{bmatrix} 0 \\ -T_L / J \end{bmatrix} d\lambda \quad \dots(2-18)$$

After taking the term independent of λ out of the integral, the following equation is obtained

$$x_m[(n+1)T] = e^{A_m(T-t_{on}(nT))} x_m(nT + t_{on}(nT)) + e^{A_m(n+1)T} \int_{nT+t_{on}(nT)}^{(n+1)T} e^{-A_m\lambda} d\lambda \begin{bmatrix} 0 \\ -T_L / J \end{bmatrix} \quad \dots(2-19)$$

Substituting $x_m[nT+t_{on}(nT)]$ in Equation (2-16) into Equation (2-19)

$$x_m[(n+1)T] = e^{A_m(T-t_{on}(nT))} \left\{ e^{A_m t_{on}(nT)} x_m(nT) + \int_0^{t_{on}(nT)} e^{A_m\lambda} d\lambda \begin{bmatrix} K_{pwm} / L_a \\ -T_L / J \end{bmatrix} \right\} + e^{A_m(n+1)T} \int_{nT+t_{on}(nT)}^{(n+1)T} e^{-A_m\lambda} d\lambda \begin{bmatrix} 0 \\ -T_L / J \end{bmatrix} \quad (2-20)$$

or equivalently

$$x_m[(n+1)T] = e^{A_m T} x_m(nT) + e^{A_m(T-t_{on}(nT))} \int_0^{t_{on}(nT)} e^{A_m\lambda} d\lambda \begin{bmatrix} K_{pwm} / L_a \\ -T_L / J \end{bmatrix}$$

$$+ e^{A_m(n+1)T} \int_{nT+t_{on}(nT)}^{(n+1)T} e^{-A_m\lambda} d\lambda \begin{bmatrix} 0 \\ -T_L / J \end{bmatrix} \quad (2-21)$$

After taking the integral operation, it is obtained that

$$\begin{aligned} x_m[(n+1)T] = & e^{A_m T} x_m(nT) + e^{A_m(T-t_{on}(nT))} \left\{ \frac{e^{A_m t_{on}(nT)} - e^0}{A_m} \right\} \begin{bmatrix} K_{pwm} / L_a \\ -T_L / J \end{bmatrix} \\ & + e^{A_m(n+1)T} \left\{ \frac{e^{-A_m(n+1)T} - e^{-A_m(nT+t_{on}(nT))}}{-A_m} \right\} \begin{bmatrix} 0 \\ -T_L / J \end{bmatrix} \end{aligned} \quad (2-22)$$

or equivalently

$$\begin{aligned} x_m[(n+1)T] = & e^{A_m T} x_m(nT) + \left\{ \frac{e^{A_m T} - e^{A_m(T-t_{on}(nT))}}{A_m} \right\} \begin{bmatrix} K_{pwm} / L_a \\ -T_L / J \end{bmatrix} \\ & + \left\{ \frac{e^0 - e^{A_m(T-t_{on}(nT))}}{-A_m} \right\} \begin{bmatrix} 0 \\ -T_L / J \end{bmatrix} \end{aligned} \quad (2-23)$$

Under the assumption that the sampling period is much smaller than the time-constants of the system, matrix exponentials can be approximated by their first-order series expansion, i.e. $\exp(AT) \cong I + AT$. By using this approximation

$$x_m[(n+1)T] = [I + A_m T] x_m(nT) + t_{on}(nT) \begin{bmatrix} K_{pwm} / L_a \\ -T_L / J \end{bmatrix} + (T - t_{on}(nT)) \begin{bmatrix} 0 \\ -T_L / J \end{bmatrix} \quad (2-24)$$

rewriting

$$\mathbf{x}_m[(n+1)T] = [\mathbf{I} + \mathbf{A}_m T] \mathbf{x}_m(nT) + \begin{bmatrix} \frac{K_{pwm}}{L_a} t_{on}(nT) \\ -\frac{T_L}{J} t_{on}(nT) - \frac{T \cdot T_L}{J} + \frac{T_L}{J} t_{on}(nT) \end{bmatrix} \quad (2-25)$$

or equivalently

$$\mathbf{x}_m[(n+1)T] = [\mathbf{I} + \mathbf{A}_m T] \mathbf{x}_m(nT) + \begin{bmatrix} K_{pwm} / L_a & 0 \\ 0 & -T / J \end{bmatrix} \begin{bmatrix} t_{on}(nT) \\ T_L \end{bmatrix} \quad (2-26)$$

Finally, by substituting the state vector and motor matrix, and dropping T , discrete-time state equation of the PWM driven DC motor is obtained as given below

$$\begin{bmatrix} i_a \\ w \end{bmatrix}_{n+1} = \begin{bmatrix} (L_a - R_a) / L_a & -K_a \phi T / L_a \\ K_a \phi T / J & (J - B_v T) / J \end{bmatrix} \begin{bmatrix} i_a \\ w \end{bmatrix}_n + \begin{bmatrix} K_{pwm} / L_a & 0 \\ 0 & -T / J \end{bmatrix} \begin{bmatrix} t_{on} \\ T_L \end{bmatrix}_n \quad \dots(2-27)$$

The open loop chopper drive has been modeled in discrete time in above relations. The advantage of this model to average value modeling in continuous time is that the variation of PWM signal in time is properly represented here.

2.5 Modeling of Controllers

As it is obviously seen from the block diagram of the closed loop system (see Figure 2 . 1), there are two controllers; one for speed and one for current control. For both of the speed and current controllers, proportional-integral (PI) control is selected because it stabilizes the drive, adjusts the damping ratio at the desired value, makes the steady-state speed-error close to zero by integral action, and filters out noise again due to the integral action (Dubey, 1989).

The backward and forward difference or trapezoidal integration technique can be employed to integrate the error signal in digital controllers. Mapping from s-plane to z-plane according to backward difference, forward difference and trapezoidal integration rule is as depicted in Figure 2 . 5 (Phillips & Nagle, 1984). As it is seen from the Figure 2 . 5-b, according to backward difference, stable analog filters will always result in stable digital equivalents and also some unstable analog filters give stable ones. However, this mapping has a major disadvantage. The $j\omega$ -axis in the s-plane does not map to the unit circle in the z-plane, that is, frequency response may be different from the analog filter. In the forward difference mapping, shown in Figure 2 . 5-c, left-half plane in the s-domain maps to the region to the left of $z=1$. Thus, because the interior of the unit circle represent the stability region in the z-plane, some stable analog filters will give unstable digital ones. However, Figure 2 . 5-d represents the mapping from s-plane to z-plane according to the trapezoidal rule. This mapping eliminates the mentioned disadvantages above because the entire left-half of s-plane maps to the interior of the unit circle in the z-plane. Thus it is the reason why this method is commonly used in practice.

In this study, the transfer functions of both the current and speed controller are obtained by using the trapezoidal integration rule which is also called Tustin method or bilinear transformation (Franklin, Powell & Workman, 1990).

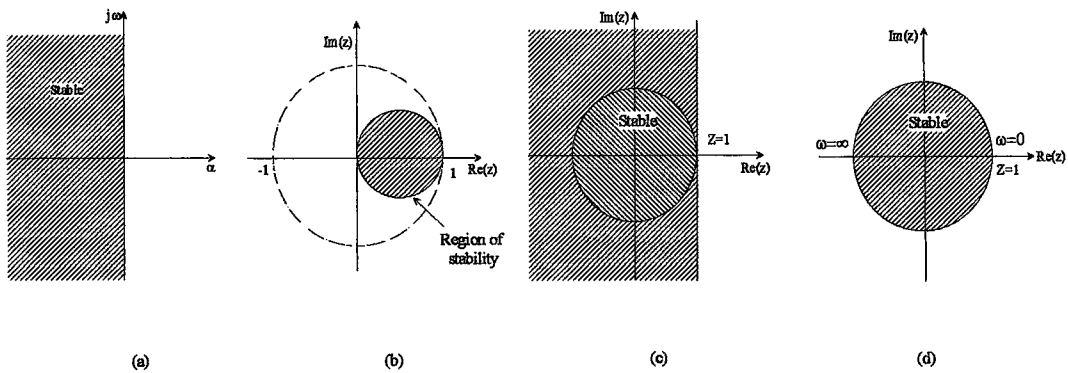


Figure 2 . 5 Mapping of the s-plane(a) according to backward difference(b), forward difference(c), and trapezoidal rule(d) to the z-plane

2.5.1 Modeling of Current Controller

A digital PI controller transfer function using the trapezoidal integration rule is given in the form of (Phillips & Nagle, 1984)

$$K_p + K_i \frac{T(z+1)}{2(z-1)} \quad (2-28)$$

where K_p is the proportional constant, K_i is the integral constant, and the T is the sampling period. In this work, a unit delay term is used to include all the computational and loop delays that may occur, and thus the current controller's transfer function, $G_{ci}(z)$, is taken as

$$G_{ci}(z) = \frac{K_{pi}}{z} + \frac{K_{ii}}{z} \frac{T(z+1)}{2(z-1)} \quad (2-29)$$

where K_{pi} is the proportional constant and K_{ii} is the integral constant of the current controller. Block diagram representation of this transfer function is depicted in Figure 2 . 6.

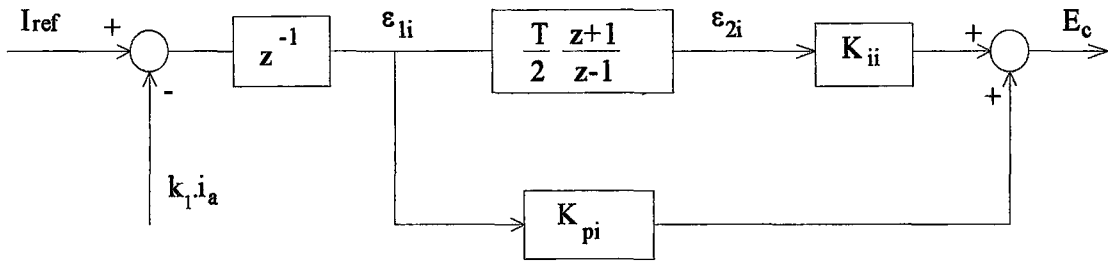


Figure 2 . 6 Block diagram of the current controller

From Figure 2 . 6, it can be written that

$$z\varepsilon_{li}(z) = I_{ref}(z) - k_1 \cdot i_a(z) \quad (2-30)$$

and

$$\varepsilon_{2i}(z) = \frac{T(z+1)}{2(z-1)}\varepsilon_{li}(z) \quad (2-31)$$

where ε_{li} and ε_{2i} are the state variables of the current controller, I_{ref} is the output of the speed controller and serves as current reference for current controller, and i_a is the actual current.

Since the time-shift property of the z-transform (for $n=1$) is

$$\mathfrak{Z}^{-1}\{zE(z)\}=e(n+1)$$

where $E(z)$ is the z-transform of $e(n)$, after taking the inverse z-transformation of the Equation (2-30) and Equation (2-31) it is obtained that

$$\varepsilon_{li}(n+1) = I_{ref}(n) - k_1 \cdot i_a(n) \quad (2-32)$$

and

$$2\varepsilon_{2i}(n+1) - 2\varepsilon_{2i}(n) = T\varepsilon_{li}(n+1) + T\varepsilon_{li}(n) \quad (2-33)$$

respectively. Substituting Equation (2-32) into Equation (2-33)

$$\varepsilon_{2i}(n+1) = \varepsilon_{2i}(n) + \frac{T}{2}I_{ref}(n) - k_1 \cdot \frac{T}{2}i_a(n) + \frac{T}{2}\varepsilon_{li}(n) \quad (2-34)$$

Finally Equation (2-32) and Equation (2-34) are rearranged in the state-space form as given below

$$\begin{bmatrix} \epsilon_{1i} \\ \epsilon_{2i} \end{bmatrix}_{n+1} = \begin{bmatrix} 0 & 0 \\ T/2 & 1 \end{bmatrix} \cdot \begin{bmatrix} \epsilon_{1i} \\ \epsilon_{2i} \end{bmatrix}_n + \begin{bmatrix} 1 & -k_1 \\ \frac{T}{2} & -k_1 \cdot \frac{T}{2} \end{bmatrix} \cdot \begin{bmatrix} I_{ref} \\ i_a \end{bmatrix}_n \quad (2-35)$$

and, output equation is

$$E_c(n) = \begin{bmatrix} K_{pi} & K_{ii} \end{bmatrix} \cdot \begin{bmatrix} \epsilon_{1i} \\ \epsilon_{2i} \end{bmatrix}_n \quad (2-36)$$

The difference equation of the current controller given above can be written as given below in state-space form

$$\begin{aligned} E_c(n+2) = E_c(n+1) &+ \left\{ K_{pi} + K_{ii} \cdot \frac{T}{2} \right\} \cdot \{ I_{ref}(n+1) - k_1 \cdot i_a(n+1) \} \\ &+ \left\{ K_{ii} \cdot \frac{T}{2} - K_{pi} \right\} \cdot \{ I_{ref}(n) - k_1 \cdot i_a(n) \} \end{aligned} \quad (2-37)$$

2.5.2 Modeling of Speed Controller

Similar to that of current controller, speed controller transfer function, $G_{cs}(z)$, is taken as

$$G_{cs}(z) = \frac{K_{ps}}{z} + \frac{K_{is}}{z} \cdot \frac{T}{2} \frac{(z+1)}{(z-1)} \quad (2-38)$$

where K_{ps} is the proportional constant and K_{is} is the integral constant of the speed controller. Block diagram representation of this transfer function is depicted in Figure 2.7.

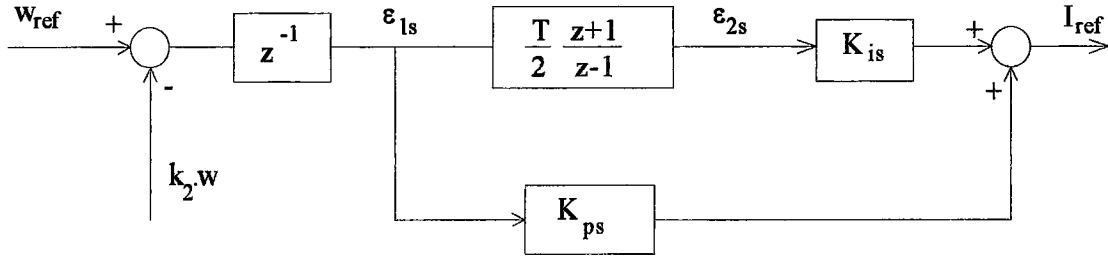


Figure 2 . 7 Block diagram of the speed controller

From Figure 2 . 7 it can be written that

$$z\epsilon_{1s}(z) = \omega_{ref}(z) - k_2 \cdot \omega(z) \quad (2-39)$$

and

$$\epsilon_{2s}(z) = \frac{T(z+1)}{2(z-1)} \epsilon_{1s}(z) \quad (2-40)$$

where ϵ_{1s} and ϵ_{2s} are the state variables of the speed controller, w_{ref} is the speed reference, ω is the actual speed and I_{ref} is the output of the speed controller.

By taking the inverse z-transformation of the Equation (2-39) and Equation (2-40) it is obtained that

$$\epsilon_{1s}(n+1) = \omega_{ref}(n) - k_2 \cdot \omega(n) \quad (2-41)$$

and

$$2\epsilon_{2s}(n+1) - 2\epsilon_{2s}(n) = T\epsilon_{1s}(n+1) + T\epsilon_{1s}(n) \quad (2-42)$$

respectively. Substituting Equation (2-41) into Equation (2-42)

$$\varepsilon_{2s}(n+1) = \varepsilon_{2s}(n) + \frac{T}{2} \omega_{\text{ref}}(n) - k_2 \cdot \frac{T}{2} \omega(n) + \frac{T}{2} \varepsilon_{1s}(n) \quad (2-43)$$

Finally, rearranging the Equation (2-41) and Equation (2-43) the state-space model of the speed controller can be obtained as given below

$$\begin{bmatrix} \varepsilon_{1s} \\ \varepsilon_{2s} \end{bmatrix}_{n+1} = \begin{bmatrix} 0 & 0 \\ T/2 & 1 \end{bmatrix} \cdot \begin{bmatrix} \varepsilon_{1s} \\ \varepsilon_{2s} \end{bmatrix}_n + \begin{bmatrix} 1 & -k_2 \\ \frac{T}{2} & -k_2 \cdot \frac{T}{2} \end{bmatrix} \cdot \begin{bmatrix} \omega_{\text{ref}} \\ \omega \end{bmatrix}_n \quad (2-44)$$

and output equation is

$$I_{\text{ref}}(n) = \begin{bmatrix} K_{ps} & K_{is} \end{bmatrix} \cdot \begin{bmatrix} \varepsilon_{1s} \\ \varepsilon_{2s} \end{bmatrix}_n \quad (2-45)$$

The difference equation of the speed controller is as given below

$$\begin{aligned} I_{\text{ref}}(n+2) = I_{\text{ref}}(n+1) + \left\{ K_{ps} + K_{is} \cdot \frac{T}{2} \right\} \cdot \{ w_{\text{ref}}(n+1) - k_2 \cdot w(n+1) \} \\ + \left\{ K_{is} \cdot \frac{T}{2} - K_{ps} \right\} \cdot \{ w_{\text{ref}}(n) - k_2 \cdot w(n) \} \end{aligned} \quad (2-46)$$

CHAPTER THREE

OPTIMAL CONTROLLER DESIGN WITH OUTPUT FEEDBACK

3.1. Introduction

Classical control theory is not easy to apply on MIMO or multiloop systems, such as the system in this thesis having 2-inputs and 2-outputs and also 2 loops. In order to apply the classical control theory in MIMO systems, it is required a painstaking effort using the approach of closing one loop at a time by graphical techniques. This is a trial-and-error procedure, and it does not guarantee good results, or even closed-loop stability (Lewis, 1992).

Modern control techniques, on the other hand, can eliminate many of the limitations of the classical control for multivariable feedback control systems. In pole-assignment technique which is termed modern technique it is assumed that the pole locations that yield the best control system are known. However, the designer may not really know the desirable closed-loop pole locations. In such case pole assignment technique can not be applied, therefore, the other modern control techniques, namely optimal control methods, are required. An optimal control system is the system whose performance is optimal in terms of some predefined performance criterion (Houpis & Lamont, 1987). The performance criterion or performance index is selected to give the best trade-off between performance and cost of control. In addition performance index must always be a positive number or zero because then the best system may be defined as the system that minimizes this index (Saadat, 1993; Dorf, 1992). Therefore,

the suitable performance index widely used in optimal control systems is the quadratic performance index. It is a linear combination of the quadratics of the states and the inputs of the system. Therefore it is called the Linear Quadratic (LQ) approach.

Modern design techniques are fundamentally time-domain techniques since they use state-space model, whereas classical control design is a frequency-domain technique. In fact, the power of modern control is due to fact that state-space model can represent a MIMO system as well as a single-input single-output (SISO) system. However, in real design problems only some of the states are available because some state components may be too expensive to obtain or even impossible to measure. Therefore state-feedback is usually impossible to implement in practice and the measured outputs should be used for feedback purposes, which is called output feedback. In addition, output feedback design provides the flexibility in choosing the controllers any desired structures (Lewis, 1992; Umanand & Bhat, 1996). The output feedback problem is a new era and is still the focus of research. One disadvantage of the output feedback problem is being nonlinear whereas the state feedback is linear. According to Huang & Li (Huang & Li, 1989) the fundamental problems on optimal output feedback have not been answered and still occupy control system theorists.

There are two basic techniques on control system design using the available outputs. In one technique, a state feedback controller whose control law is $u = -Kx$ is first designed. Then, the measured output $y(t)$ is used to estimate the nonavailable states. Finally, the state estimate $\hat{x}(t)$ is used in the state variable feedback controller as if it were exactly equal to $x(t)$; that is, it is set to $u = -K\hat{x}$. In order to estimate the state from $y(t)$, observer is used. However the estimation of the nonavailable states will depend on the accuracy with which the system parameters are known. The other technique for output-feedback design is to deal only with the available outputs and to develop the related formulations depending on them. In this technique, control law is $u = -Ky$ (Lewis, 1992; Umanand & Bhat, 1996). In this study, the output feedback is chosen to design the controller parameters.

In the following sections, first the LQ tracker with output feedback formulation of the entire system will be given. Then SIMPLEX algorithm which is used for the minimization of the performance index will be outlined. Later, finding the optimum controller gains using the SIMPLEX method in MATLAB (MathWorks, 1993) will be given. Finally, the analysis of the model for optimal gains will be presented.

3.2. Formulation of the Entire System as a Linear Quadratic (LQ) Tracker with Output Feedback

In Chapter 2, state-space model of each block of the system was given. If the model of each block is examined, it can be observed that the entire system has 6 states. These are i_a , ω , ε_{1i} , ε_{2i} , ε_{1s} , and ε_{2s} . In addition the system has two external inputs. Therefore the entire system can be represented in state-space form with 6 states and 2 inputs. Let's define the state vector of the entire system as

$$\mathbf{x}(n) = [i_a \quad \omega \quad \varepsilon_{1i} \quad \varepsilon_{2i} \quad \varepsilon_{1s} \quad \varepsilon_{2s}]^T$$

and the external inputs as

$$\mathbf{r}(n) = [\omega_{ref} \quad T_L]^T$$

where superscript T denotes the matrix transpose. On the other hand, since the system is closed-loop it has some internal inputs or variables. For example, E_c which is the output of current controller is the input to the chopper at the same time. Thus the variable E_c appears in the models of both current controller and chopper driven DC motor. Therefore by linking the internal variables like E_c in the models of blocks, state space form of the entire system can be obtained in terms of $\mathbf{x}(n)$ and $\mathbf{r}(n)$ only. The model of the closed-loop system obtained in this way is given below

$$\begin{bmatrix} i_a \\ \omega \\ \varepsilon_{li} \\ \varepsilon_{2i} \\ \varepsilon_{ls} \\ \varepsilon_{2s} \end{bmatrix}_{n+1} = \begin{bmatrix} (L_a - R_a T)/L_a & -K_a \phi T/L_a & \frac{K_{pwm}}{L_a} \frac{T}{E_{sw}} K_{pi} & \frac{K_{pwm}}{L_a} \frac{T}{E_{sw}} K_{ii} & 0 & 0 \\ K_a \phi T/J & (J - B_v T)/J & 0 & 0 & 0 & 0 \\ -k_1 & 0 & 0 & 0 & K_{ps} & K_{is} \\ -k_1 \cdot T/2 & 0 & T/2 & 1 & \frac{T}{2} K_{ps} & \frac{T}{2} K_{is} \\ 0 & -k_2 & 0 & 0 & 0 & 0 \\ 0 & -k_2 \cdot T/2 & 0 & 0 & T/2 & 1 \end{bmatrix} \cdot \begin{bmatrix} i_a \\ \omega \\ \varepsilon_{li} \\ \varepsilon_{2i} \\ \varepsilon_{ls} \\ \varepsilon_{2s} \end{bmatrix}_n$$

$$+ \begin{bmatrix} 0 & 0 \\ 0 & -T/J \\ 0 & 0 \\ 0 & 0 \\ 1 & 0 \\ T/2 & 0 \end{bmatrix} \cdot \begin{bmatrix} \omega_{ref} \\ T_L \end{bmatrix}_n \quad (3-1)$$

In the case of output feedback, since the control law is $u = -K \cdot y$ where y is the available outputs, the controller gains that will be optimized should be available as a separate matrix K . For this purpose, the first term in the right-hand side of the Equation (3-1) can be partitioned into two parts giving the following equation

$$\begin{bmatrix} i_a \\ \omega \\ \varepsilon_{li} \\ \varepsilon_{2i} \\ \varepsilon_{ls} \\ \varepsilon_{2s} \end{bmatrix}_{n+1} = \begin{bmatrix} (L_a - R_a T)/L_a & -K_a \phi T/L_a & 0 & 0 & 0 & 0 \\ K_a \phi T/J & (J - B_v T)/J & 0 & 0 & 0 & 0 \\ -k_1 & 0 & 0 & 0 & 0 & 0 \\ -k_1 \cdot T/2 & 0 & T/2 & 1 & 0 & 0 \\ 0 & -k_2 & 0 & 0 & 0 & 0 \\ 0 & -k_2 \cdot T/2 & 0 & 0 & T/2 & 1 \end{bmatrix} \cdot \begin{bmatrix} i_a \\ \omega \\ \varepsilon_{li} \\ \varepsilon_{2i} \\ \varepsilon_{ls} \\ \varepsilon_{2s} \end{bmatrix}_n$$

$$+ \begin{bmatrix} 0 & 0 & \frac{K_{pwm}}{L_a} \frac{T}{E_{sw}} K_{pi} & \frac{K_{pwm}}{L_a} \frac{T}{E_{sw}} K_{ii} & 0 & 0 \\ 0 & 0 & 0 & 0 & 0 & 0 \\ 0 & 0 & 0 & 0 & K_{ps} & K_{is} \\ 0 & 0 & 0 & 0 & \frac{T}{2} K_{ps} & \frac{T}{2} K_{is} \\ 0 & 0 & 0 & 0 & 0 & 0 \\ 0 & 0 & 0 & 0 & 0 & 0 \end{bmatrix} \cdot \begin{bmatrix} i_a \\ \omega \\ \varepsilon_{li} \\ \varepsilon_{2i} \\ \varepsilon_{ls} \\ \varepsilon_{2s} \end{bmatrix}_n$$

$$+ \begin{bmatrix} 0 & 0 \\ 0 & -T/J \\ 0 & 0 \\ 0 & 0 \\ 1 & 0 \\ T/2 & 0 \end{bmatrix} \cdot \begin{bmatrix} \omega_{ref} \\ T_L \end{bmatrix}_n \quad (3-2)$$

Rewriting Equation (3-2)

$$\begin{bmatrix} i_a \\ \omega \\ \varepsilon_{li} \\ \varepsilon_{2i} \\ \varepsilon_{ls} \\ \varepsilon_{2s} \end{bmatrix}_{n+1} = \begin{bmatrix} (L_a - R_a T)/L_a & -K_a \phi T/L_a & 0 & 0 & 0 & 0 \\ K_a \phi T/J & (J - B_v T)/J & 0 & 0 & 0 & 0 \\ -k_1 & 0 & 0 & 0 & 0 & 0 \\ -k_1 \cdot T/2 & 0 & T/2 & 1 & 0 & 0 \\ 0 & -k_2 & 0 & 0 & 0 & 0 \\ 0 & -k_2 \cdot T/2 & 0 & 0 & T/2 & 1 \end{bmatrix} \cdot \begin{bmatrix} i_a \\ \omega \\ \varepsilon_{li} \\ \varepsilon_{2i} \\ \varepsilon_{ls} \\ \varepsilon_{2s} \end{bmatrix}_n + \begin{bmatrix} \frac{K_{pwm}}{L_a} \cdot \frac{T}{E_{sw}} \cdot \{K_{pi} \varepsilon_{li} + K_{ii} \varepsilon_{2i}\} \\ 0 \\ K_{ps} \varepsilon_{ls} + K_{is} \varepsilon_{2s} \\ \frac{T}{2} \cdot \{K_{ps} \varepsilon_{ls} + K_{is} \varepsilon_{2s}\} \\ 0 \\ 0 \end{bmatrix} + \begin{bmatrix} 0 & 0 \\ 0 & -T/J \\ 0 & 0 \\ 0 & 0 \\ 1 & 0 \\ T/2 & 0 \end{bmatrix} \cdot \begin{bmatrix} \omega_{ref} \\ T_L \end{bmatrix}_n \quad (3-3)$$

By substituting Equations (2-36) and (2-45) into Equation (3-3), the following form of the model for closed loop system, which is proper for LQ tracker design with output feedback, is obtained.

$$\begin{bmatrix} i_a \\ \omega \\ \varepsilon_{1i} \\ \varepsilon_{2i} \\ \varepsilon_{1s} \\ \varepsilon_{2s} \end{bmatrix}_{n+1} = \begin{bmatrix} (L_a - R_a T) / L_a & -K_a \phi T / L_a & 0 & 0 & 0 & 0 \\ K_a \phi T / J & (J - B_v T) / J & 0 & 0 & 0 & 0 \\ -k_1 & 0 & 0 & 0 & 0 & 0 \\ -k_1 \cdot T / 2 & 0 & T / 2 & 1 & 0 & 0 \\ 0 & -k_2 & 0 & 0 & 0 & 0 \\ 0 & -k_2 \cdot T / 2 & 0 & 0 & T / 2 & 1 \end{bmatrix} \cdot \begin{bmatrix} i_a \\ \omega \\ \varepsilon_{1i} \\ \varepsilon_{2i} \\ \varepsilon_{1s} \\ \varepsilon_{2s} \end{bmatrix}_n$$

$$+ \begin{bmatrix} 0 & \frac{K_{pwm} T}{L_a E_{sw}} \\ 0 & 0 \\ 1 & 0 \\ T / 2 & 0 \\ 0 & 0 \\ 0 & 0 \end{bmatrix} \cdot \begin{bmatrix} I_{ref} \\ E_c \end{bmatrix}_n + \begin{bmatrix} 0 & 0 \\ 0 & -T / J \\ 0 & 0 \\ 0 & 0 \\ 1 & 0 \\ T / 2 & 0 \end{bmatrix} \cdot \begin{bmatrix} \omega_{ref} \\ T_L \end{bmatrix}_n \quad (3-4)$$

or in the compact form

$$x(n+1) = Ax(n) + Bu(n) + Er(n) \quad (3-5)$$

where x is the (6x1) state vector, A is the (6x6) system matrix, B is the (6x2) control matrix, u is the (2x1) control input, E is the (6x2) input matrix, and r is the (2x1) external or reference input.

From the Equation (3-4) and Equation (3-5), control input is defined as

$$u(n) = \begin{bmatrix} I_{ref} \\ E_c \end{bmatrix}_n \quad (3-6)$$

Since the control law for the output feedback is of the form

$$u(n) = -K \cdot y(n) \quad (3-7)$$

the linear gains which are the relation between $u(n)$ and $y(n)$ can be obtained from Equation (2-36) and Equation(2-45) as follows

$$\begin{bmatrix} I_{ref} \\ E_c \end{bmatrix}_n = - \begin{bmatrix} 0 & 0 & -K_{ps} & -K_{is} \\ -K_{pi} & -K_{ii} & 0 & 0 \end{bmatrix} \cdot \begin{bmatrix} \epsilon_{1i} \\ \epsilon_{2i} \\ \epsilon_{1s} \\ \epsilon_{2s} \end{bmatrix}_n \quad (3-8)$$

where

$$K = \begin{bmatrix} 0 & 0 & -K_{ps} & -K_{is} \\ -K_{pi} & -K_{ii} & 0 & 0 \end{bmatrix} \quad (3-9)$$

This formulation also provides the content of output vector $y(n)$

$$y(n) = \begin{bmatrix} \epsilon_{1i} \\ \epsilon_{2i} \\ \epsilon_{1s} \\ \epsilon_{2s} \end{bmatrix}_n \quad (3-10)$$

The relation between state variables and the output variables can be defined as follows

$$\begin{bmatrix} \epsilon_{1i} \\ \epsilon_{2i} \\ \epsilon_{1s} \\ \epsilon_{2s} \end{bmatrix}_n = \begin{bmatrix} 0 & 0 & 1 & 0 & 0 & 0 \\ 0 & 0 & 0 & 1 & 0 & 0 \\ 0 & 0 & 0 & 0 & 1 & 0 \\ 0 & 0 & 0 & 0 & 0 & 1 \end{bmatrix} \cdot \begin{bmatrix} i_a \\ \omega \\ \epsilon_{1i} \\ \epsilon_{2i} \\ \epsilon_{1s} \\ \epsilon_{2s} \end{bmatrix}_n \quad (3-11)$$

In compact form

$$y(n) = C \cdot x(n) \quad (3-12)$$

The performance output of the system, z_n is selected as

$$z_n = \begin{bmatrix} \omega \\ i_a \end{bmatrix}_n \quad (3-13)$$

and the relation between the state variables and performance output of the system is defined below

$$\begin{bmatrix} \omega \\ i_a \end{bmatrix}_n = \begin{bmatrix} 0 & 1 & 0 & 0 & 0 & 0 \\ 1 & 0 & 0 & 0 & 0 & 0 \end{bmatrix} \cdot \begin{bmatrix} i_a \\ \omega \\ \epsilon_{1i} \\ \epsilon_{2i} \\ \epsilon_{1s} \\ \epsilon_{2s} \end{bmatrix}_n \quad (3-14)$$

or in compact form

$$z(n) = Hx(n). \quad (3-15)$$

The difference between reference input and performance output is defined as the tracking error, e_n , that is

$$e(n) = r(n) - z(n) \quad (3-16)$$

Finally, block diagram representation of the LQ tracker model of the system with output feedback is as shown in Fig (3-1).

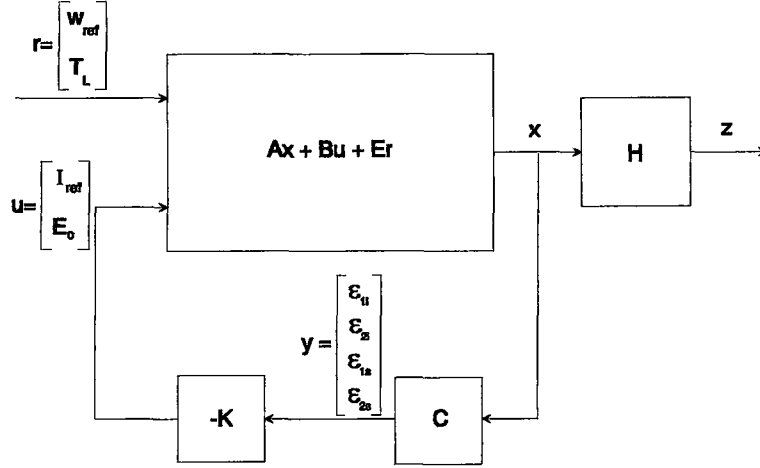


Figure 3 . 1 Block diagram representation of the system as an LQ tracker with output feedback

3.3. The Performance Index and Optimal Cost

In Section 3.2, DC motor control system has been formulated as an LQ tracker problem with output feedback. The objective now is to determine the gain matrix K which minimizes a specified performance index. In this thesis, in order to minimize the tracking error e_n , a quadratic performance index is chosen as given below

$$J_c = \frac{1}{2} \sum_{n=0}^{\infty} (\tilde{e}_n^T \tilde{e}_n + \tilde{u}_n^T R \tilde{u}_n) + \frac{1}{2} \bar{e}^T V \bar{e} + \frac{1}{2} \sum_i \sum_j g_{ij} k_{ij}^2 \quad (3-17)$$

where \bar{e} denotes the steady-state error while \tilde{e}_n denotes the error deviation and $e_n = \tilde{e}_n + \bar{e}$. Note that performance index weights both \tilde{e}_n and \bar{e} but separately. This is suboptimal in the sense that minimizing J_c does not minimize a quadratic function of the total error e_n but it does generally result in excellent tracker designs (Lewis, 1992).

From the definition of error in terms of steady-state error and error deviation and in terms of reference input and performance output as given in Equation (3-16), the

error deviation can be related to the state deviation \tilde{x}_n by using the Equation (3-15) as given below

$$\begin{aligned}
 \tilde{e}_n &= e_n - \bar{e} \\
 &= (r - H \cdot x_n) - (r - H \cdot \bar{x}) \\
 &= r - H \cdot x_n - r + H \cdot \bar{x} \\
 &= -H(x_n - \bar{x}) \\
 &= -H\tilde{x}_n
 \end{aligned} \tag{3-18}$$

After substituting Equation (3-18) into Equation (3-17) the following equation can be obtained

$$J_c = \frac{1}{2} \sum_{n=0}^{\infty} (\tilde{x}_n^T Q \tilde{x}_n + \tilde{u}_n^T R \tilde{u}_n) + \frac{1}{2} \bar{e}^T V \bar{e} + \frac{1}{2} \sum_i \sum_j g_{ij} k_{ij}^2 \tag{3-19}$$

where $Q = H^T H$ and Q and R are the symmetric state and input weighting matrices, respectively, to be selected by the designer but the selection of Q and R is only weakly connected to the performance specifications (Franklin et al; Egami, Wang & Tsuchiya, 1985). Therefore, a certain amount of trial and error is usually required with an interactive computer program before a satisfactory design results. However, some hints can be given for the choice which is based on the relative importance of the various states and controls because Q and R affect the time-domain response. If the elements of Q is chosen as a large value, the resulting gain K leads to a faster response of the system and vice versa. Similarly, the larger elements of R provides the slower system response. On the other hand, some weight will almost always be selected for the control in order that the components of the control vector will be limited in magnitude such that the design is physically realizable.

In Equation (3-19), V is the steady-state error weighting matrix. Since the PI controllers are used in both speed and current loop, steady-state error will be zero. Thus, V can be set to zero in performance index.

The last term in the performance index covers the weighting of the k_{ij} elements of the control gain matrix K . Since some of the terms in the gain matrix K given in Equation (3-9) are zero, minimization without a weight on zero elements may give neither very small nor zero elements at the end of optimization. In order to obtain zero or very small values on those elements after completing the minimization, these zero elements can be weighted with a very large value of g_{ij} . Thus, minimization will result very small values of k_{ij} and they can be set to zero during the implementation stage.

As it can be observed from Figure 3 . 1, the control deviation can be written in terms of the state deviation as given below

$$\tilde{u}_n = -K\tilde{x}_n \quad (3-20)$$

The cost in the following formulation can be obtained after the substitution of Equation (3-20) into Equation (3-19)

$$J_c = \frac{1}{2} \sum_{n=0}^{\infty} \tilde{x}_n^T (Q + C^T K^T R K C) \tilde{x}_n + \frac{1}{2} \tilde{e}^T V \tilde{e} + \frac{1}{2} \sum_i \sum_j g_{ij} k_{ij}^2 \quad (3-21)$$

subject to the closed-loop dynamics of the deviation given in the following equation as

$$\tilde{x}_{n+1} = A_c \tilde{x}_n \quad (3-22)$$

where A_c is the closed-loop matrix and it is the (6x6) matrix in Equation (3-1).

Now, suppose that it can be found a constant positive definite matrix P such that

$$\tilde{x}_{n+1}^T \cdot P \cdot \tilde{x}_{n+1} - \tilde{x}_n^T \cdot P \cdot \tilde{x}_n = -\tilde{x}_n^T (Q + C^T K^T R K C) \tilde{x}_n \quad (3-23)$$

Then

$$J_c = -\frac{1}{2} \sum_{n=0}^{\infty} (\tilde{x}_{n+1}^T \cdot P \cdot \tilde{x}_{n+1} - \tilde{x}_n^T \cdot P \cdot \tilde{x}_n) + \frac{1}{2} \bar{e}^T V \bar{e} + \frac{1}{2} \sum_i \sum_j g_{ij} k_{ij}^2 \quad (3-24)$$

or equivalently

$$J_c = \frac{1}{2} \tilde{x}_0^T \cdot P \cdot \tilde{x}_0 + \tilde{x}_{\infty}^T \cdot P \cdot \tilde{x}_{\infty} + \frac{1}{2} \bar{e}^T V \bar{e} + \frac{1}{2} \sum_i \sum_j g_{ij} k_{ij}^2 \quad (3-25)$$

By substituting the Equation (3-22) into the Equation (3-23) the following result will be obtained

$$\tilde{x}_n^T (A_c^T P A_c - P + Q + C^T K^T R K C) \tilde{x}_n = 0 \quad (3-26)$$

Since this must hold for all initial conditions, the following equation known as discrete Lyapunov equation must be satisfied

$$A_c^T P A_c - P + Q + C^T K^T R K C = 0 \quad (3-27)$$

If the closed-loop system is asymptotically stable, then the \tilde{x}_n goes to zero with n . In addition, when the plant starts at rest, the initial value of the state deviation is as follows

$$\tilde{x}_0 = -\bar{x} = (A_c - I)^{-1} \cdot E \cdot r \quad (3-28)$$

Thus the cost given in Equation (3-25) can be written as given below

$$J_c = \frac{1}{2} \bar{\mathbf{x}}^T \cdot \mathbf{P} \cdot \bar{\mathbf{x}} + \frac{1}{2} \bar{\mathbf{e}}^T \mathbf{V} \bar{\mathbf{e}} + \frac{1}{2} \sum_i \sum_j g_{ij} k_{ij}^2 \quad (3-29)$$

or

$$J_c = \frac{1}{2} \text{trace}(\mathbf{P}\mathbf{X}) + \frac{1}{2} \bar{\mathbf{e}}^T \mathbf{V} \bar{\mathbf{e}} + \frac{1}{2} \sum_i \sum_j g_{ij} k_{ij}^2 \quad (3-30)$$

where

$$\mathbf{X} = \bar{\mathbf{x}} \cdot \bar{\mathbf{x}}^T$$

$$\bar{\mathbf{x}} = -(\mathbf{A}_c - \mathbf{I})^{-1} \mathbf{E} \mathbf{r}$$

$$\mathbf{A}_c = \mathbf{A} - \mathbf{B}\mathbf{K}\mathbf{C}$$

and \mathbf{P} is a positive definite matrix.

For any fixed gain matrix \mathbf{K} if there exists a positive definite \mathbf{P} that satisfies the Lyapunov equation, then the cost J_c for the closed loop system is given in terms of \mathbf{P} by the Equation (3-30). Therefore LQ tracker design with output feedback is the determination of the optimal feedback gain \mathbf{K} by minimizing the optimal cost function in Equation (3-30) subject to the algebraic constraint given in Equation (3-27).

In order to find suitable gains \mathbf{K} for closed-loop stable system it is necessary for $(\sqrt{\mathbf{Q}}, \mathbf{A})$ to be detectable and (\mathbf{A}, \mathbf{B}) to be controllable (Lewis, 1992). The determination of observability is preferred to the determination of detectability since observability is easier to check than detectability and the detectability of $(\sqrt{\mathbf{Q}}, \mathbf{A})$ is guaranteed by its observability. For the pair (\mathbf{A}, \mathbf{B}) to be controllable, the rank of the following matrix must be equal to 6 for the system given in Equations (3-4), (3-8) and (3-11).

$$[B \ AB \ A^2B \ \dots \ A^{k-1}B]$$

For the pair (\sqrt{Q}, A) to be observable, the rank of the matrix given below must be equal to 6 again for the system.

$$\begin{bmatrix} A \\ A\sqrt{Q} \\ A(\sqrt{Q})^2 \\ \vdots \\ \vdots \\ \vdots \end{bmatrix}$$

3.4. LQ Tracker Design with Output Feedback

In the preceding two sections the necessary formulation related to the LQ tracker design was given. It is shown that the LQ tracker design is the minimization of Equation (3-30) under the constraint in Equation (3-27). This section covers the solution method of the problem. Since SIMPLEX method is used as the minimization method, first of all, simplex optimization algorithm will be outlined then the usage of the simplex algorithm for the constrained optimization problem will be given. Finally the optimum controller gains obtained by using the simplex method will be presented.

3.4.1 Simplex Algorithm for Optimization

Simplex method, which is also called downhill simplex method (Press, Flannery, Teukolsky & Vetterling, 1992), is an unconstrained nonlinear optimization method. This method should not be confused with the simplex method for linear programming problems (Luenberger, 1973). The method requires only function evaluations not derivatives for the minimization of a function, and has been found to work particularly

well if the number of variables does not exceed five or six (Walsh, 1979). In this study, the number of variables estimated by using the optimization program is four.

Simplex which gives the name to the method is a geometrical figure formed by a set of $n+1$ points (or vertices), in n dimensional space, and all their interconnecting line segments, polygonal faces etc. Thus, simplex is a triangle in two dimensions and it is a tetrahedron in three dimensions. Simplex method is based on the idea of comparing the values of the objective function at the $n+1$ vertices of a general simplex and moving this simplex gradually towards the optimum point during the iterative process (Rao, 1984). Reflection, contraction and expansion are the three operations used for this movement. Graphical representations of them are given in Figure 3 . 2.

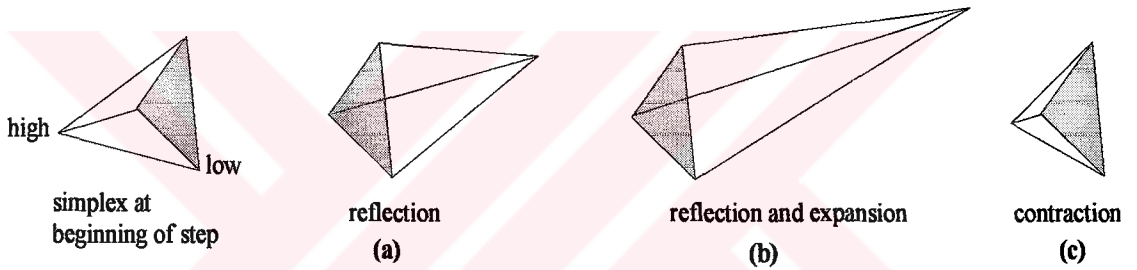


Figure 3 . 2 Possible outcomes in the simplex method

In the current simplex, let

x_h be the vertex with the highest function value,

x_l be the vertex with the lowest function value,

x_o be the centroid of all the vertices except x_h , i.e.

$$x_o = \frac{1}{n} \sum_{i=1, i \neq h}^{n+1} x_i . \quad (3-31)$$

Also let x_r , x_e and x_c are the points obtained from the reflection, expansion and contraction operations.

It is expected the point x_r obtained by reflecting the point x_h in the opposite face to have the smallest value. If this is the case, it can be constructed a new simplex by rejecting the point x_h from the simplex and including the new point x_r . This is the reflection operation. Mathematically the reflected point x_r is given by

$$x_r = (1 + \alpha)x_o - \alpha x_h \quad (3-32)$$

where $\alpha > 0$ is the reflection coefficient.

If a reflection process gives a point x_r for which the function has the value smaller than the $f(x_h)$, generally it can be expected to decrease the function value further by moving along the direction x_o to x_r . Thus x_r is expanded to x_e by the relation

$$x_e = \gamma \cdot x_r + (1 - \gamma)x_o \quad (3-33)$$

where $\gamma > 1$ is the expansion constant.

If the reflection process gives a point x_r for which $f(x_r) > f(x_h)$, then contraction is made as follows

$$x_c = \beta \cdot x_h + (1 - \beta)x_o \quad (3-34)$$

where β is the contraction constant and $0 \leq \beta \leq 1$. $\alpha=1$, $\beta=0.5$ and $\gamma=2$ are the values suggested for the reflection, contraction and expansion factors, respectively.

Using the reflection, expansion and contraction operations outlined above, simplex algorithm starts with an initial simplex and searches the minimum (local, at least) until a convergence criterion satisfy.

Convergence criterion is that the calculations terminate whenever the standard deviation of the function at the $n+1$ vertices of the current simplex is less than some prescribed small quantity (Rao, 1984; Walsh, 1979).

The flowchart of the simplex algorithm (Nelder & Mead, 1965) for the minimization of unconstrained nonlinear function of $f(x)$ is given in Figure 3 . 3.

3.4.2 Using the Simplex Algorithm for Constrained Optimization

Simplex algorithm which is outlined in Section 3.4.1 and available in Matlab Optimization Toolbox (Grace, 1992) is for the optimization of unconstrained problems. The Lyapunov equation which is a constraint function can be easily solved with the 'dlyap' function of Matlab Control System Toolbox (MathWorks, 1993). The simplex algorithm in Matlab Optimization Toolbox is modified in order to solve the constrained optimization problem having the Lyapunov equation as a constraint function.

Optimal cost is a function of the positive definite matrix P and the controller gain matrix K in which the parameters will be optimized. Positive definite matrix P can be obtained from the solution of Lyapunov equation at the specified value of K . Thus at the beginning for any initial K , Lyapunov equation is solved for P . Then cost is evaluated for these P and K . This cost is saved. After that, according to the simplex algorithm given in Figure 3 . 3, optimum K is searched. Also during this search process, Lyapunov equation is solved for the matrix P before the every cost evaluation operation at every step of simplex algorithm. Process is terminated in the same manner mentioned in Section 3.4.1. The controller gain matrix K obtained in this way minimizes the cost function and satisfies the Lyapunov equation as a constraint. The flowchart of the nonlinear optimization with constraint (Lyapunov equation) using the simplex algorithm is given in Figure 3 . 4.

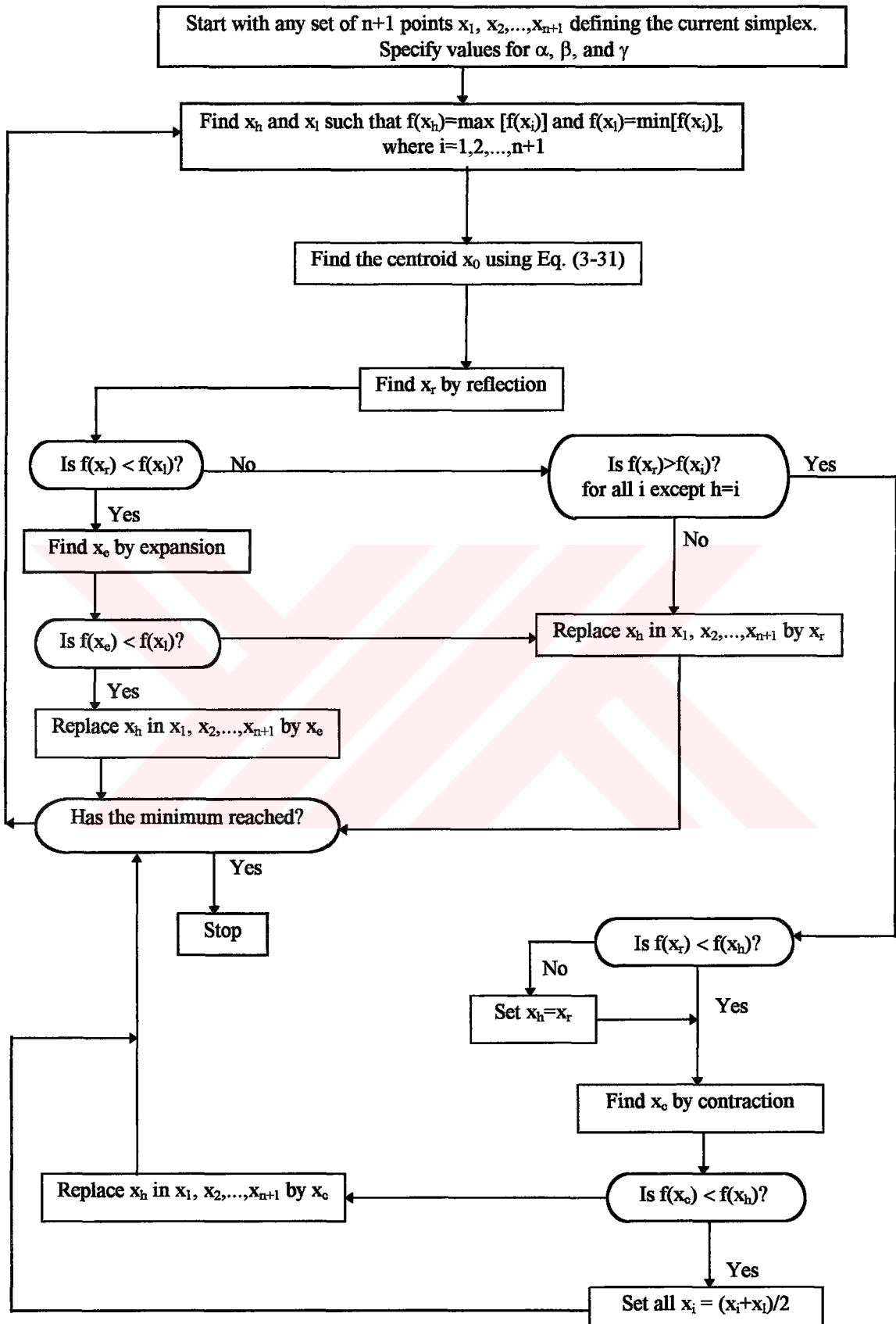
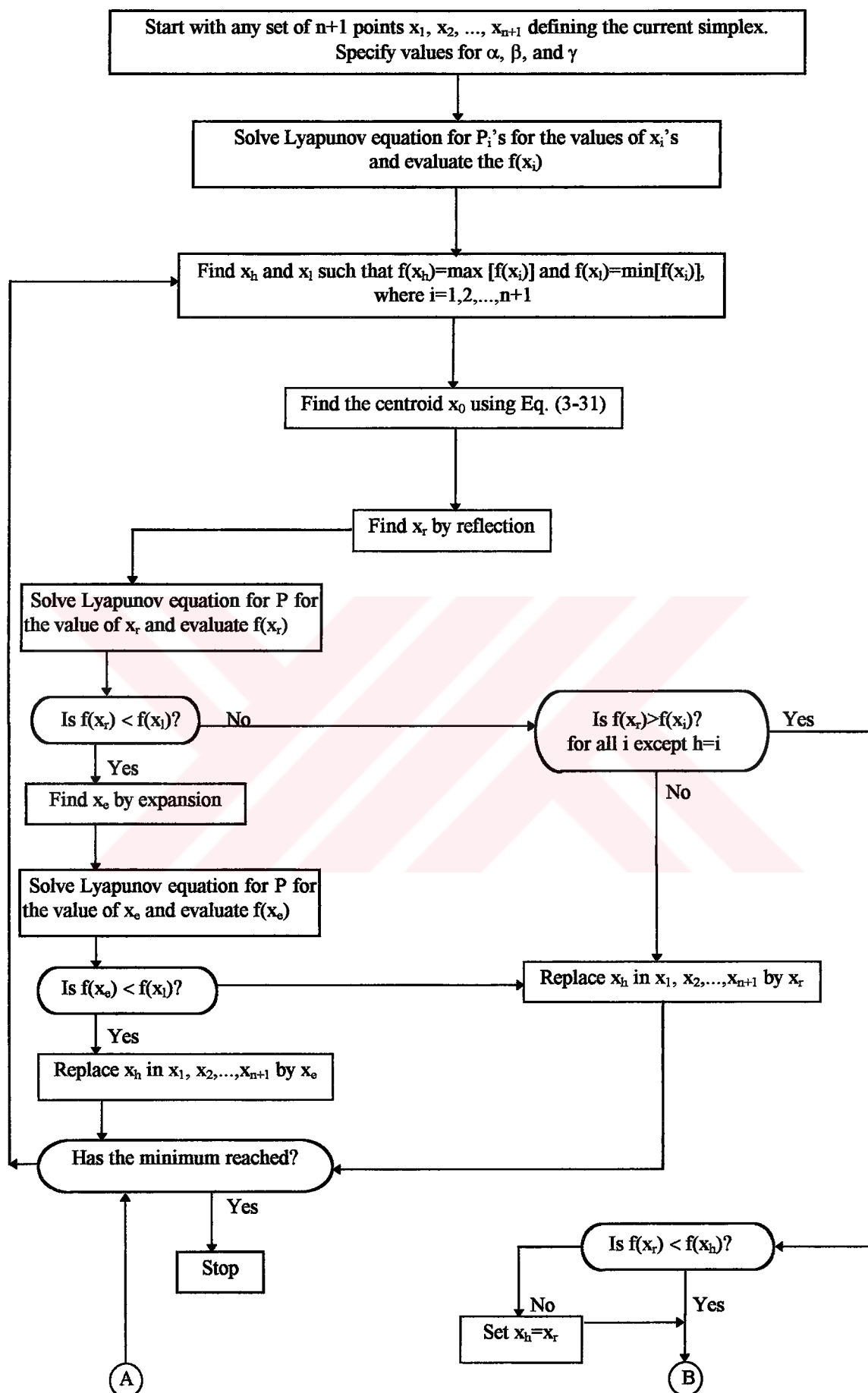


Figure 3 . 3 Flowchart of the simplex optimization algorithm



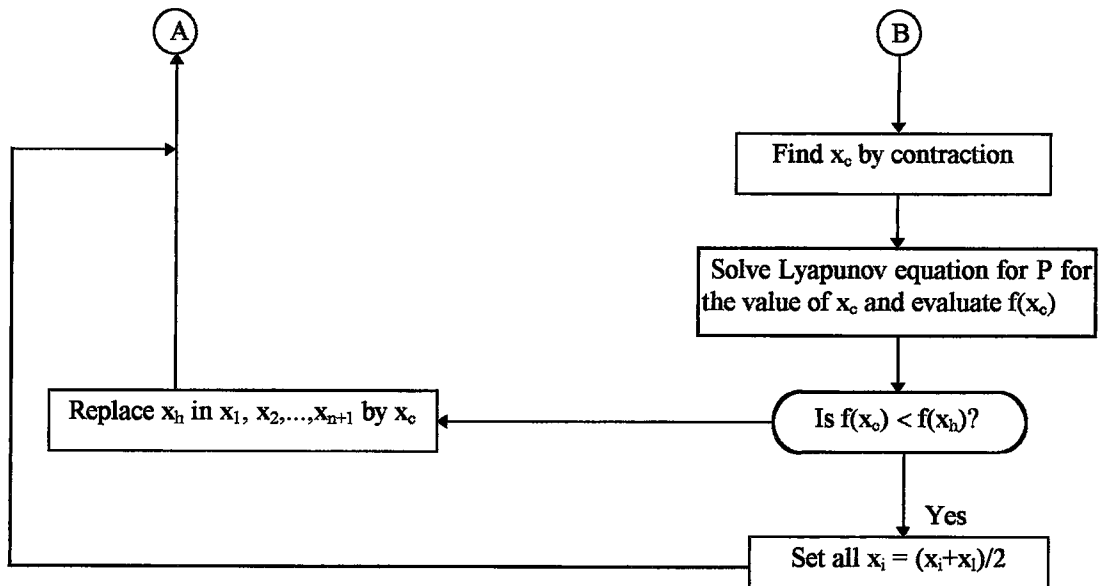


Figure 3 . 4 Flowchart of the simplex algorithm for Lyapunov constrained functions

3.4.3 The Initial Values of Variables

Like any other minimization algorithm, SIMPLEX method also require an initial value of variables. Finding an initial gain K_{initial} that stabilizes the system to start the search procedure is a major problem. One way to find a stabilizing gain is to use discrete root-locus techniques by closing one loop at a time in the control system while this is a trial-and-error procedure (Lewis, 1992).

Let's first consider the current loop given in Figure 3 . 5 below

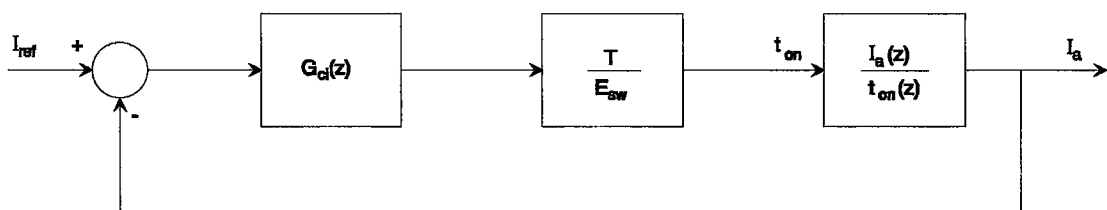


Figure 3 . 5 Inner current loop of the system

Open loop function of the inner loop, i.e. $G_{ai}(z)$, is

$$G_{ai}(z) = G_{ci}(z) \cdot \frac{T}{E_{sw}} \cdot \frac{I_a(z)}{t_{on}(z)} \quad (3-35)$$

where $G_{ci}(z)$ is given in explicit form in Equation (2-29). The transfer function $I_a(z)/t_{on}(z)$ is obtained from the state space model of the motor given in Equation (2-27) after substituting the parameters defined in Section 3.4.4.

$$\frac{I_a(z)}{t_{on}(z)} = \frac{2391z - 2391}{z^2 - 1.998z + 0.998}$$

Thus open loop function of the inner loop $G_{ai}(z)$ is obtained as

$$G_{ai}(z) = \left\{ \frac{(2K_{pi} + K_{ii}T)z + K_{ii}T - 2K_{pi}}{2z(z-1)} \right\} \cdot \frac{T}{E_{sw}} \cdot \left\{ \frac{2391(z-1)}{z^2 - 1.998z + 0.998} \right\} \quad (3-36)$$

Since the loop has two controller parameters, one of them should be chosen, then the other will be searched by root-locus technique for stable operation. The proportional constant of the current controller K_{pi} is chosen as the value of 10. Thus the characteristic equation of this loop is

$$1 + G_{ai}(z) = 0$$

After rearranging

$$1 + K_{ii} \cdot \frac{1.9925 \cdot 10^{-6}(z+1)}{2z^3 - 3.996z^2 + 2.3941z - 0.3985} = 0 \quad (3-37)$$

or in the compact form

$$1 + K_{ii} \frac{\text{numi}(z)}{\text{deni}(z)} = 0$$

When the commands given below are entered into the Matlab, root locations corresponding to the different values of K_{ii} are obtained and given in Table 3. 1.

```
numi=1.9925e-6*[1 1];
deni=[2 -3.996 (1.9956+0.3985i) -0.3985i];
[R,Kii]=rlocus(numi,deni);
```

Table 3. 1 Root locations of the inner loop for different values of K_{ii}

Root1	Root2	Root3	Kii
1.0010	0.7209	0.2761	0
1.0010	0.7209	0.2761	7.5024e-002
0.9934	0.7314	0.2732	7.5024e+002
0.9661	0.7671	0.2648	3.0147e+003
0.9639	0.7698	0.2643	3.1671e+003
0.9616	0.7727	0.2637	3.3273e+003
0.9590	0.7759	0.2631	3.4955e+003
0.9563	0.7792	0.2625	3.6723e+003
0.9533	0.7829	0.2618	3.8580e+003
0.9500	0.7869	0.2612	4.0531e+003
0.9464	0.7912	0.2604	4.2580e+003
0.9423	0.7960	0.2597	4.4733e+003
0.9378	0.8013	0.2589	4.6995e+003
0.9326	0.8073	0.2581	4.9372e+003
0.9266	0.8141	0.2573	5.1868e+003
0.9194	0.8222	0.2564	5.4491e+003
0.9103	0.8322	0.2555	5.7247e+003
0.8971	0.8463	0.2545	6.0141e+003
0.8722 + 0.0165i	0.8722 - 0.0165i	0.2535	6.3183e+003
0.8728 + 0.0351i	0.8728 - 0.0351i	0.2525	6.6378e+003
0.8733 + 0.0473i	0.8733 - 0.0473i	0.2514	6.9734e+003
0.8739 + 0.0574i	0.8739 - 0.0574i	0.2503	7.3260e+003
0.8744 + 0.0663i	0.8744 - 0.0663i	0.2491	7.6965e+003
0.8750 + 0.0744i	0.8750 - 0.0744i	0.2479	8.0857e+003
0.8757 + 0.0821i	0.8757 - 0.0821i	0.2466	8.4945e+003
0.8763 + 0.0895i	0.8763 - 0.0895i	0.2453	8.9241e+003
0.8770 + 0.0965i	0.8770 - 0.0965i	0.2439	9.3753e+003
0.8777 + 0.1034i	0.8777 - 0.1034i	0.2425	9.8494e+003
0.8783 + 0.1086i	0.8783 - 0.1086i	0.2414	1.0229e+004
0.8800 + 0.1228i	0.8800 - 0.1228i	0.2380	1.1374e+004

0.8847 + 0.1569i	0.8847 - 0.1569i	0.2286	1.4779e+004
0.8962 + 0.2219i	0.8962 - 0.2219i	0.2057	2.4027e+004
0.9172 + 0.3175i	0.9172 - 0.3175i	0.1636	4.5307e+004
0.9495 + 0.4449i	0.9495 - 0.4449i	0.0990	9.0748e+004
0.9974 + 0.6252i	0.9974 - 0.6252i	0.0031	1.9565e+005
1.0700 + 0.9145i	1.0700 - 0.9145i	-0.1419	4.8225e+005
1.1619 + 1.3579i	1.1619 - 1.3579i	-0.3258	1.2445e+006
1.2484 + 1.9265i	1.2484 - 1.9265i	-0.4987	2.8381e+006
1.3207 + 2.6340i	1.3207 - 2.6340i	-0.6434	5.8072e+006
1.3805 + 3.5891i	1.3805 - 3.5891i	-0.7631	1.1527e+007
1.4280 + 5.0030i	1.4280 - 5.0030i	-0.8579	2.3510e+007
1.4616 + 7.2544i	1.4616 - 7.2544i	-0.9251	5.1053e+007
1.4819 + 11.0546i	1.4819 - 11.0546i	-0.9658	1.2079e+008
1.4921 + 17.7122i	1.4921 - 17.7122i	-0.9863	3.1298e+008

From the root locations in Table 3. 1, it is observed that K_{ii} must be chosen approximately greater than 0.075 and less than 90748 for stable operation. In order to identify the lower limit precisely, the interval of K_{ii} between 0 and 750 is expanded with the step length of 10 by the following commands

```
Kii=0:10:750;  
R=rlocus(numi,deni,Kii);  
[abs(R) Kii']
```

The absolute values of root locations are presented in Table 3. 2.

Table 3. 2 The absolute values of roots of the inner loop for K_{ii} in the range (0-750)

<u> Root1 </u>	<u> Root2 </u>	<u> Root3 </u>	<u>K_{ii}</u>
1.0010	0.7209	0.2761	0
1.0009	0.7210	0.2761	10.0000
1.0008	0.7212	0.2760	20.0000
1.0007	0.7213	0.2760	30.0000
1.0006	0.7214	0.2760	40.0000
1.0005	0.7216	0.2759	50.0000
1.0004	0.7217	0.2759	60.0000
1.0003	0.7219	0.2758	70.0000
1.0002	0.7220	0.2758	80.0000
1.0001	0.7221	0.2758	90.0000
1.0000	0.7223	0.2757	100.0000

0.9999	0.7224	0.2757	110.0000
0.9998	0.7225	0.2756	120.0000
0.9997	0.7227	0.2756	130.0000
0.9996	0.7228	0.2756	140.0000
0.9995	0.7230	0.2755	150.0000
0.9994	0.7231	0.2755	160.0000
0.9993	0.7232	0.2755	170.0000
0.9992	0.7234	0.2754	180.0000
0.9991	0.7235	0.2754	190.0000
0.9990	0.7237	0.2753	200.0000
0.9989	0.7238	0.2753	210.0000
0.9988	0.7239	0.2753	220.0000
0.9987	0.7241	0.2752	230.0000
0.9986	0.7242	0.2752	240.0000
0.9985	0.7244	0.2751	250.0000
0.9984	0.7245	0.2751	260.0000
0.9983	0.7246	0.2751	270.0000
0.9982	0.7248	0.2750	280.0000
0.9981	0.7249	0.2750	290.0000
0.9980	0.7251	0.2749	300.0000
0.9979	0.7252	0.2749	310.0000
0.9978	0.7253	0.2749	320.0000
0.9977	0.7255	0.2748	330.0000
0.9976	0.7256	0.2748	340.0000
0.9975	0.7258	0.2747	350.0000
0.9974	0.7259	0.2747	360.0000
0.9973	0.7260	0.2747	370.0000
0.9972	0.7262	0.2746	380.0000
0.9971	0.7263	0.2746	390.0000
0.9970	0.7265	0.2746	400.0000
0.9969	0.7266	0.2745	410.0000
0.9968	0.7267	0.2745	420.0000
0.9967	0.7269	0.2744	430.0000
0.9966	0.7270	0.2744	440.0000
0.9965	0.7272	0.2744	450.0000
0.9964	0.7273	0.2743	460.0000
0.9963	0.7274	0.2743	470.0000
0.9962	0.7276	0.2742	480.0000
0.9961	0.7277	0.2742	490.0000
0.9960	0.7279	0.2742	500.0000
0.9959	0.7280	0.2741	510.0000
0.9958	0.7281	0.2741	520.0000
0.9957	0.7283	0.2741	530.0000
0.9956	0.7284	0.2740	540.0000
0.9955	0.7286	0.2740	550.0000
0.9954	0.7287	0.2739	560.0000
0.9952	0.7289	0.2739	570.0000
0.9951	0.7290	0.2739	580.0000
0.9950	0.7291	0.2738	590.0000

0.9949	0.7293	0.2738	600.0000
0.9948	0.7294	0.2737	610.0000
0.9947	0.7296	0.2737	620.0000
0.9946	0.7297	0.2737	630.0000
0.9945	0.7299	0.2736	640.0000
0.9944	0.7300	0.2736	650.0000
0.9943	0.7301	0.2735	660.0000
0.9942	0.7303	0.2735	670.0000
0.9941	0.7304	0.2735	680.0000
0.9940	0.7306	0.2734	690.0000
0.9939	0.7307	0.2734	700.0000
0.9938	0.7309	0.2734	710.0000
0.9937	0.7310	0.2733	720.0000
0.9936	0.7311	0.2733	730.0000
0.9935	0.7313	0.2732	740.0000
0.9934	0.7314	0.2732	750.0000

As it can be clearly recognize from the list of the magnitudes of root locations given in Table 3. 2, K_{ii} can be selected greater than 110 in order to keep the system stable.

Similarly, the following commands are entered into the Matlab in order to expand the interval between 45000 and 90000 with the step length of 1000 to find the upper limit precisely.

```
Kii=45000:1000:90000;
R=rlocus(numi,deni,Kii);
[abs(R) (Kii*1e-4)']
```

The absolute values of roots are given in Table 3. 3.

Table 3. 3 The absolute values of roots of the inner loop for K_{ii} in the range (45000-90000)

<u> Root1 </u>	<u> Root2 </u>	<u> Root3 </u>	<u>$K_{ii} \cdot 10^4$</u>
0.9700	0.9700	0.1641	4.5000
0.9720	0.9720	0.1624	4.6000
0.9740	0.9740	0.1607	4.7000
0.9760	0.9760	0.1590	4.8000
0.9779	0.9779	0.1573	4.9000

0.9798	0.9798	0.1556	5.0000
0.9818	0.9818	0.1540	5.1000
0.9837	0.9837	0.1524	5.2000
0.9856	0.9856	0.1508	5.3000
0.9874	0.9874	0.1492	5.4000
0.9893	0.9893	0.1476	5.5000
0.9912	0.9912	0.1460	5.6000
0.9930	0.9930	0.1445	5.7000
0.9948	0.9948	0.1429	5.8000
0.9966	0.9966	0.1414	5.9000
0.9984	0.9984	0.1399	6.0000
1.0002	1.0002	0.1384	6.1000
1.0020	1.0020	0.1369	6.2000
1.0037	1.0037	0.1355	6.3000
1.0055	1.0055	0.1340	6.4000
1.0072	1.0072	0.1326	6.5000
1.0090	1.0090	0.1311	6.6000
1.0107	1.0107	0.1297	6.7000
1.0124	1.0124	0.1283	6.8000
1.0141	1.0141	0.1269	6.9000
1.0157	1.0157	0.1255	7.0000
1.0174	1.0174	0.1242	7.1000
1.0191	1.0191	0.1228	7.2000
1.0207	1.0207	0.1214	7.3000
1.0224	1.0224	0.1201	7.4000
1.0240	1.0240	0.1188	7.5000
1.0256	1.0256	0.1174	7.6000
1.0272	1.0272	0.1161	7.7000
1.0288	1.0288	0.1148	7.8000
1.0304	1.0304	0.1135	7.9000
1.0320	1.0320	0.1122	8.0000
1.0336	1.0336	0.1110	8.1000
1.0352	1.0352	0.1097	8.2000
1.0367	1.0367	0.1084	8.3000
1.0383	1.0383	0.1072	8.4000
1.0398	1.0398	0.1060	8.5000
1.0414	1.0414	0.1047	8.6000
1.0429	1.0429	0.1035	8.7000
1.0444	1.0444	0.1023	8.8000
1.0459	1.0459	0.1011	8.9000
1.0474	1.0474	0.0999	9.0000

According to the data collected in Table 3. 2 and Table 3. 3, K_{ii} can be selected in the range between 110 and 60000 for the stable operation of the inner loop, and it is chosen as 500 in this study.

When the speed loop is closed one parameter of the speed controller should be kept constant. For this reason K_{ps} is chosen at the value of 1. Now, the characteristic polynomial including K_{is} as varying parameter can be obtained as given in Equation (3-38) from Mathcad (MathSoft, 1994) via the program kinitia1 given in Appendix 1.

$$\begin{aligned} & (2.94627551815 \cdot 10^{-11} \cdot z - 5.87781965872 \cdot 10^{-9} + 5.9072824139 \cdot 10^{-9} \cdot z^2) \cdot K_{is} \dots \\ & + z^6 - 3.99781748481 \cdot z^5 + 6.19322673095 \cdot z^4 - 4.59177646291 \cdot z^3 \dots \\ & + 1.59526082642 \cdot z^2 - 0.199011166043 \cdot z + 1.17556393174 \cdot 10^{-4} \end{aligned} \quad (3-38)$$

After rearranging the Equation (3-38) it is obtained in the form of

$$1 + K_{is} \frac{\text{nums}(z)}{\text{dens}(z)} = 0$$

where

$$\begin{aligned} \text{nums}(z) &= 5.9072824139 \cdot 10^{-9} \cdot z^2 + 2.94627551815 \cdot 10^{-11} \cdot z - 5.87781965872 \cdot 10^{-9} \\ \text{dens}(z) &= z^6 - 3.99781748481 \cdot z^5 + 6.19322673095 \cdot z^4 - 4.59177646291 \cdot z^3 \\ &+ 1.59526082642 \cdot z^2 - 0.199011166043 \cdot z + 1.17556393174 \cdot 10^{-4} \end{aligned}$$

The following commands written in Matlab provides the root locations with respect to the values of K_{is} denoted in the last column in Table 3. 4.

```
nums=[0 0 0 0 5.9072824139e-9 2.94627551815e-11 -5.87781965872e-9];
dens=[1 -3.99781748481 6.19322673095 -4.59177646291...
      1.59526082642 -0.199011166043 1.17556393174e-4];
[R,Kis]=rlocus(nums,dens);
```

Table 3. 4 Root locations of the system for different values of K_{is}

Root1	Root2	Root3	Root4	Root5	Root6	K_{is}
1.0000	0.9994	0.9949	0.7300	0.2729	0.0006	0
1.0000	0.9994	0.9949	0.7300	0.2729	0.0006	9.9940e-003
1.0000	0.9994	0.9949	0.7300	0.2729	0.0006	1.6228e-002

1.0000	0.9994	0.9949	0.7300	0.2729	0.0006	2.6351e-002
1.0000	0.9994	0.9949	0.7300	0.2729	0.0006	4.2788e-002
1.0000	0.9994	0.9949	0.7300	0.2729	0.0006	6.9478e-002
1.0000	0.9994	0.9949	0.7300	0.2729	0.0006	1.1282e-001
1.0000	0.9994	0.9949	0.7300	0.2729	0.0006	1.8319e-001
1.0000	0.9994	0.9949	0.7300	0.2729	0.0006	2.9746e-001
0.9999	0.9995	0.9949	0.7300	0.2729	0.0006	4.8300e-001
0.9999	0.9995	0.9949	0.7300	0.2729	0.0006	7.8429e-001
0.9998	0.9996	0.9949	0.7300	0.2729	0.0006	1.2735e+000
0.9997 + 0.0002i	0.9997 - 0.0002i	0.9949	0.7300	0.2729	0.0006	2.0679e+000
0.9997 + 0.0003i	0.9997 - 0.0003i	0.9949	0.7300	0.2729	0.0006	3.3578e+000
0.9997 + 0.0005i	0.9997 - 0.0005i	0.9949	0.7300	0.2729	0.0006	5.4523e+000
0.9997 + 0.0007i	0.9997 - 0.0007i	0.9949	0.7300	0.2729	0.0006	8.8534e+000
0.9997 + 0.0009i	0.9997 - 0.0009i	0.9949	0.7300	0.2729	0.0006	1.4376e+001
0.9997 + 0.0011i	0.9997 - 0.0011i	0.9949	0.7300	0.2729	0.0006	2.3343e+001
0.9997 + 0.0015i	0.9997 - 0.0015i	0.9949	0.7300	0.2729	0.0006	3.7904e+001
0.9997 + 0.0019i	0.9997 - 0.0019i	0.9949	0.7300	0.2729	0.0006	6.1548e+001
0.9997 + 0.0024i	0.9997 - 0.0024i	0.9949	0.7300	0.2729	0.0006	9.9940e+001
0.9997 + 0.0025i	0.9997 - 0.0025i	0.9949	0.7300	0.2729	0.0006	1.0763e+002
0.9997 + 0.0028i	0.9997 - 0.0028i	0.9949	0.7300	0.2729	0.0006	1.3083e+002
0.9997 + 0.0034i	0.9997 - 0.0034i	0.9950	0.7300	0.2729	0.0006	2.0086e+002
0.9997 + 0.0050i	0.9997 - 0.0050i	0.9950	0.7299	0.2729	0.0006	4.1222e+002
0.9998 + 0.0079i	0.9998 - 0.0079i	0.9950	0.7296	0.2730	0.0006	1.0501e+003
1.0002 + 0.0133i	1.0002 - 0.0133i	0.9950	0.7288	0.2732	0.0005	2.9730e+003
1.0011 + 0.0228i	1.0011 - 0.0228i	0.9950	0.7264	0.2739	0.0003	8.7369e+003
1.0037 + 0.0384i	1.0037 - 0.0384i	0.9950	0.7197	0.2758	-0.0002	2.5569e+004
1.0099 + 0.0615i	1.0099 - 0.0615i	0.9950	0.7035	0.2810	-0.0015	7.0167e+004
1.0208 + 0.0897i	1.0208 - 0.0897i	0.9950	0.6726	0.2928	-0.0042	1.6691e+005
1.0363 + 0.1208i	1.0363 - 0.1208i	0.9950	0.6215	0.3177	-0.0091	3.5062e+005
1.0579 + 0.1565i	1.0579 - 0.1565i	0.9950	0.5116	0.3931	-0.0177	7.1091e+005
1.0589 + 0.1579i	1.0589 - 0.1579i	0.9950	0.5027	0.4005	-0.0182	7.3002e+005
1.0599 + 0.1594i	1.0599 - 0.1594i	0.9950	0.4920	0.4097	-0.0186	7.4965e+005
1.0608 + 0.1609i	1.0608 - 0.1609i	0.9950	0.4776	0.4226	-0.0191	7.6980e+005
1.0618 + 0.1624i	1.0618 - 0.1624i	0.9950	0.4493 - 0.0137i	0.4493 + 0.0137i	-0.0195	7.9049e+005
1.0628 + 0.1639i	1.0628 - 0.1639i	0.9950	0.4486 - 0.0339i	0.4486 + 0.0339i	-0.0200	8.1174e+005
1.0638 + 0.1654i	1.0638 - 0.1654i	0.9950	0.4478 - 0.0461i	0.4478 + 0.0461i	-0.0205	8.3356e+005
1.0649 + 0.1669i	1.0649 - 0.1669i	0.9950	0.4470 - 0.0558i	0.4470 + 0.0558i	-0.0209	8.5596e+005
1.0659 + 0.1684i	1.0659 - 0.1684i	0.9950	0.4462 - 0.0641i	0.4462 + 0.0641i	-0.0214	8.7897e+005
1.0670 + 0.1700i	1.0670 - 0.1700i	0.9950	0.4454 - 0.0716i	0.4454 + 0.0716i	-0.0219	9.0260e+005
1.0680 + 0.1715i	1.0680 - 0.1715i	0.9950	0.4446 - 0.0785i	0.4446 + 0.0785i	-0.0225	9.2686e+005
1.0691 + 0.1731i	1.0691 - 0.1731i	0.9950	0.4438 - 0.0849i	0.4438 + 0.0849i	-0.0230	9.5177e+005
1.0702 + 0.1746i	1.0702 - 0.1746i	0.9950	0.4430 - 0.0910i	0.4430 + 0.0910i	-0.0235	9.7735e+005
1.0713 + 0.1762i	1.0713 - 0.1762i	0.9950	0.4422 - 0.0967i	0.4422 + 0.0967i	-0.0241	1.0036e+006
1.0724 + 0.1778i	1.0724 - 0.1778i	0.9950	0.4413 - 0.1022i	0.4413 + 0.1022i	-0.0246	1.0306e+006
1.0735 + 0.1794i	1.0735 - 0.1794i	0.9950	0.4405 - 0.1075i	0.4405 + 0.1075i	-0.0252	1.0583e+006
1.0746 + 0.1810i	1.0746 - 0.1810i	0.9950	0.4397 - 0.1126i	0.4397 + 0.1126i	-0.0258	1.0868e+006
1.0758 + 0.1826i	1.0758 - 0.1826i	0.9950	0.4388 - 0.1176i	0.4388 + 0.1176i	-0.0263	1.1160e+006
1.0769 + 0.1842i	1.0769 - 0.1842i	0.9950	0.4380 - 0.1224i	0.4380 + 0.1224i	-0.0269	1.1460e+006
1.0781 + 0.1858i	1.0781 - 0.1858i	0.9950	0.4371 - 0.1271i	0.4371 + 0.1271i	-0.0276	1.1768e+006

1.0793 + 0.1875i	1.0793 - 0.1875i	0.9950	0.4362 - 0.1317i	0.4362 + 0.1317i	-0.0282
1.0805 + 0.1891i	1.0805 - 0.1891i	0.9950	0.4353 - 0.1362i	0.4353 + 0.1362i	-0.0288
1.0817 + 0.1908i	1.0817 - 0.1908i	0.9950	0.4345 - 0.1406i	0.4345 + 0.1406i	-0.0295
1.0829 + 0.1924i	1.0829 - 0.1924i	0.9950	0.4336 - 0.1450i	0.4336 + 0.1450i	-0.0301
1.0841 + 0.1941i	1.0841 - 0.1941i	0.9950	0.4327 - 0.1493i	0.4327 + 0.1493i	-0.0308
1.0853 + 0.1958i	1.0853 - 0.1958i	0.9950	0.4318 - 0.1535i	0.4318 + 0.1535i	-0.0314
1.0866 + 0.1975i	1.0866 - 0.1975i	0.9950	0.4309 - 0.1576i	0.4309 + 0.1576i	-0.0321
1.0879 + 0.1992i	1.0879 - 0.1992i	0.9950	0.4300 - 0.1617i	0.4300 + 0.1617i	-0.0328
1.0891 + 0.2009i	1.0891 - 0.2009i	0.9950	0.4290 - 0.1658i	0.4290 + 0.1658i	-0.0336
1.0904 + 0.2026i	1.0904 - 0.2026i	0.9950	0.4281 - 0.1698i	0.4281 + 0.1698i	-0.0343
1.0916 + 0.2041i	1.0916 - 0.2041i	0.9950	0.4273 - 0.1733i	0.4273 + 0.1733i	-0.0349
1.0949 + 0.2085i	1.0949 - 0.2085i	0.9950	0.4249 - 0.1831i	0.4249 + 0.1831i	-0.0368
1.1041 + 0.2205i	1.1041 - 0.2205i	0.9950	0.4184 - 0.2083i	0.4184 + 0.2083i	-0.0423
1.1259 + 0.2478i	1.1259 - 0.2478i	0.9950	0.4035 - 0.2601i	0.4035 + 0.2601i	-0.0560
1.1653 + 0.2943i	1.1653 - 0.2943i	0.9950	0.3776 - 0.3382i	0.3776 + 0.3382i	-0.0831
1.2233 + 0.3587i	1.2233 - 0.3587i	0.9950	0.3411 - 0.4349i	0.3411 + 0.4349i	-0.1260
1.3013 + 0.4409i	1.3013 - 0.4409i	0.9950	0.2930 - 0.5468i	0.2930 + 0.5468i	-0.1858
1.4011 + 0.5421i	1.4011 - 0.5421i	0.9950	0.2312 - 0.6736i	0.2312 + 0.6736i	-0.2617
1.5243 + 0.6639i	1.5243 - 0.6639i	0.9950	0.1528 - 0.8154i	0.1528 + 0.8154i	-0.3514
1.6733 + 0.8087i	1.6733 - 0.8087i	0.9950	0.0537 - 0.9734i	0.0537 + 0.9734i	-0.4511
1.8514 + 0.9806i	1.8514 - 0.9806i	0.9950	-0.0718 - 1.1502i	-0.0718 + 1.1502i	-0.5564
2.0640 + 1.1853i	2.0640 - 1.1853i	0.9950	-0.2316 - 1.3509i	-0.2316 + 1.3509i	-0.6620
2.3193 + 1.4315i	2.3193 - 1.4315i	0.9950	-0.4373 - 1.5837i	-0.4373 + 1.5837i	-0.7613
2.6318 + 1.7339i	2.6318 - 1.7339i	0.9950	-0.7068 - 1.8643i	-0.7068 + 1.8643i	-0.8473
3.0275 + 2.1187i	3.0275 - 2.1187i	0.9950	-1.0692 - 2.2214i	-1.0692 + 2.2214i	-0.9139
3.5519 + 2.6314i	3.5519 - 2.6314i	0.9950	-1.5714 - 2.7051i	-1.5714 + 2.7051i	-0.9583
4.2759 + 3.3431i	4.2759 - 3.3431i	0.9950	-2.2831 - 3.3912i	-2.2831 + 3.3912i	-0.9828

The stable operation can be performed by choosing K_{is} in the range given below

$$0.483 \leq K_{is} \leq 1050$$

and that value is chosen 5 in this study.

Finally, the initial values are collected in the matrix given below which is a proper form for the optimization

$$K_{\text{initial}} = \begin{bmatrix} 0 & 0 & -1 & -5 \\ -10 & -500 & 0 & 0 \end{bmatrix}$$

3.4.4 MATLAB Solution of the Optimization

In this study, 110V, 2.5 hp, 1800 rpm a separately excited DC motor having the following parameters is used:

$$R_a=1 \text{ ohm}$$

$$L_a=46 \text{ mH}$$

$$J=0.093 \text{ kgm}^2$$

$$B_v=0.008 \text{ Nt-m/rd/sec}$$

$$K_\phi=0.55 \text{ V/rad/sec.}$$

The other parameters related to the system are given below;

Sampling period, $T=0.0001 \text{ sec}$

Amplitude of PWM signal, $K_{pwm}=110 \text{ V}$

Peak value of the sawtooth waveform, $E_{sw}=12 \text{ V}$

Reference speed, $w_{ref}=80 \text{ rad/sec}$

Load torque, $T_L=0$

In addition, the linear gains of current and speed transducers (k_1 and k_2) have been chosen unity.

Finally, the optimization parameters used in simplex algorithm are given below

Reflection coefficient, $\alpha=0.75$

Contraction coefficient, $\beta=0.5$

Expansion constant, $\gamma=1.6$.

In this section, numerical solution of the minimization problem given in Equation (3-30) subject to the constraint in Equation (3-27) will be given. For the solution of the minimization problem, simplex algorithm has been used. When the simplex

algorithm is used, the zero elements of the gain matrix can be set to zero, and the optimal values for the non-zero elements of the gain matrix K can be obtained by minimizing the performance index. In other words, g_{ij} weightings in Equation (3-30) are not used with the Simplex method. Furthermore, V can also be set to zero in Equation (3-30) because the error at the output of PI controller is zero at steady-state. As a consequence, the problem becomes to the minimizing of the

$$J_c = \frac{1}{2} \text{trace}(PX) \quad (3-39)$$

subject to the constraint

$$A_c^T P A_c - P + Q + C^T K^T R K C = 0 \quad (3-40)$$

Solution of the optimization problem is obtained by a number of programs or routines written in Matlab. The list of these routines is given in Appendix 1. Using these routines with different state weighting matrices given below, the optimal controller gain matrices are obtained. In the state weighting matrix Q_1 , the error deviations on current and speed responses are equally weighted.

$$Q_1 = \begin{bmatrix} 1 & 0 & 0 & 0 & 0 & 0 \\ 0 & 1 & 0 & 0 & 0 & 0 \\ 0 & 0 & 0 & 0.1 & 0 & 0 \\ 0 & 0 & 0.1 & 0 & 0 & 0 \\ 0 & 0 & 0 & 0 & 0 & 0.1 \\ 0 & 0 & 0 & 0 & 0.1 & 0 \end{bmatrix}, \quad R = \begin{bmatrix} 0.1 & 0 \\ 0 & 0.1 \end{bmatrix}$$

The controller gains are computed from the optimization routine and given below

$$K_{opt1} = \begin{bmatrix} 0 & 0 & -0.95744 & -3.6026 \\ -10.137 & -525.24 & 0 & 0 \end{bmatrix}$$

Optimum cost J_{e1} is 7.5013×10^6 whereas initial cost is 8.1397×10^6 .

In the state weighting matrix Q_2 given below, the error deviation of speed is dominantly weighted against the error deviation of current.

$$Q_2 = \begin{bmatrix} 1 & 0 & 0 & 0 & 0 & 0 \\ 0 & 10 & 0 & 0 & 0 & 0 \\ 0 & 0 & 0 & 0.1 & 0 & 0 \\ 0 & 0 & 0.1 & 0 & 0 & 0 \\ 0 & 0 & 0 & 0 & 0 & 0.1 \\ 0 & 0 & 0 & 0 & 0.1 & 0 \end{bmatrix}, \quad R = \begin{bmatrix} 0.1 & 0 \\ 0 & 0.1 \end{bmatrix}$$

initial cost is 3.2260×10^7 .

The controller gains for this weighting matrix are

$$K_{opt2} = \begin{bmatrix} 0 & 0 & -1.2172 & -4.8778 \\ -10.668 & -500.93 & 0 & 0 \end{bmatrix}$$

and optimum cost J_{e2} is 2.7767×10^7 .

3.5. Results of Analysis

In this section, the model developed for the closed-loop control of dc drive is used to analyze the system. The set of equation in discrete time domain given in Equation (3-4), (3-6) and (3-15) are solved altogether. The relation between duty cycle and the control voltage is depicted in Figure 2.3. The duty cycle is limited by the PI controller. This limitation is not included in the model developed in Chapter 3. Because this linearized model will be used to design the optimal controllers and to analyze the stability. Therefore the analysis of the system here will be obtained in the case of linear relation defined between duty cycle and control signal (unlimited duty cycle),

and nonlinear relation as a result of including the limitation on duty cycle (limited duty cycle). The results are divided into two sections. Both sections will cover the result of the analysis obtained by using the initial value of controller parameters, K_{initial} and two local optimal values (K_{opt1} and K_{opt2}) estimated by the simplex algorithm for nonlinear optimization.

3.5.1. Results of Analysis with Unlimited Duty Cycle

Figure 3 . 6, Figure 3 . 7 and Figure 3 . 8 show the rotor speed, armature current and reference current with respect to time for the initial value of PI parameters given in Section 3.4.3. In the analysis of the model, the duty cycle is not limited.

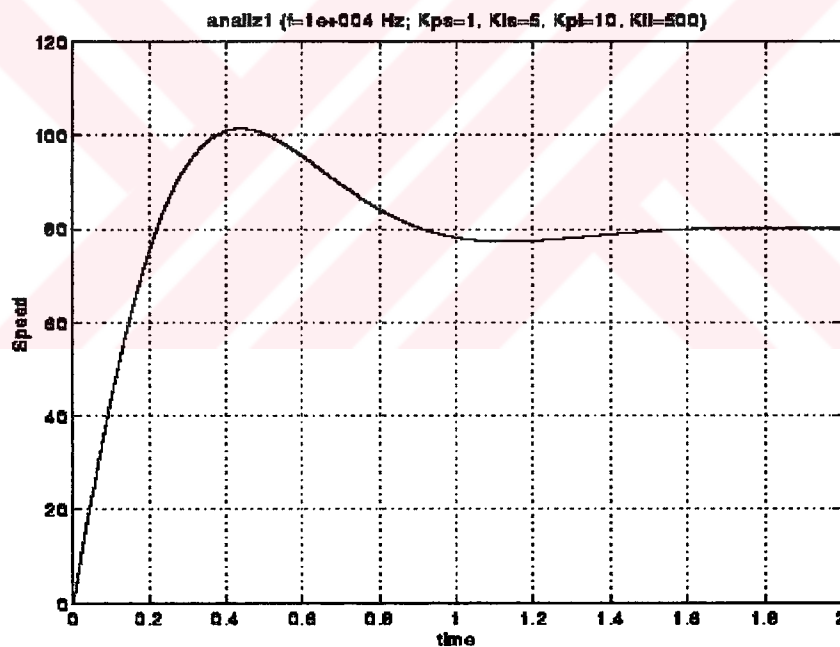


Figure 3 . 6 Speed response for K_{initial} with unlimited duty cycle

Figure 3 . 6 presents the rotor speed in terms of rad/sec with respect to time in terms of second. In closed loop system the reference speed is set to 80 rad/sec and load torque is assumed to be zero. The motor is started from standstill by means of controllers. The rotor accelerates in 0.4 seconds to reach at its maximum speed. After

taking an overshoot around 20 rad/sec over the setting value, it slows and settles down 80 rad/sec at steady state.

Figure 3 . 7 shows the motor armature current with respect to time. Since the back emf is zero at the stanstill, the motor demands high starting current as it is seen in Figure 3 . 7. As the rotor accelerates the back emf given in Equation (2-2) increases and the armature current decreases. The maximum value of starting current is limited only by the armature resistance since the output of speed controller is not limited. That is the reason why the armature current given in this figure arises to its maximum with a sharp rise time. The settling time of the response follows that value in the response of rotor speed. The armature current settles down around 1 A at steady state because of inclusion of damping coefficient into the model in Equation (2-3).

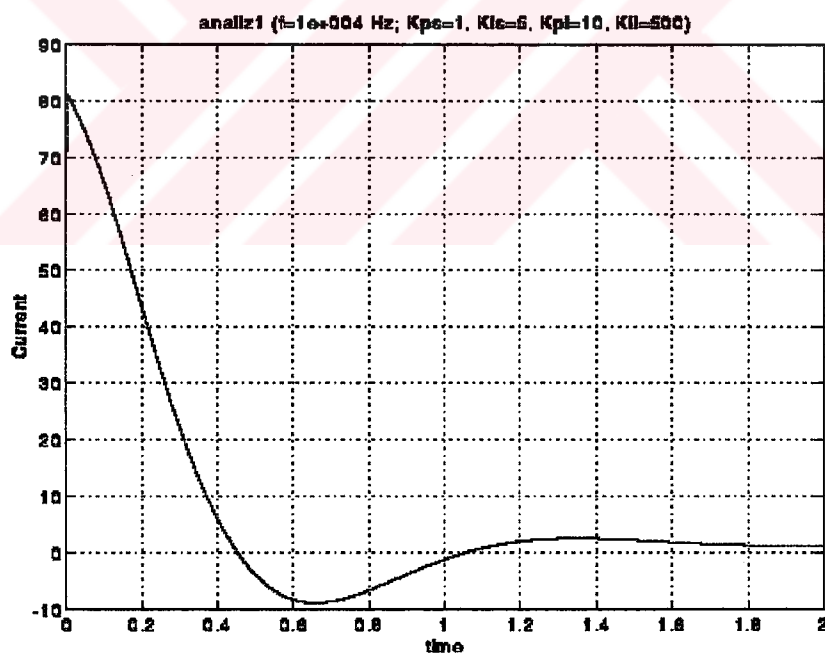


Figure 3 . 7 Armature current variation for $K_{initial}$ with unlimited duty cycle

It can be clearly shown that the actual current in Figure 3 . 7 follows the reference current in Figure 3 . 8 dictated by the speed controller.

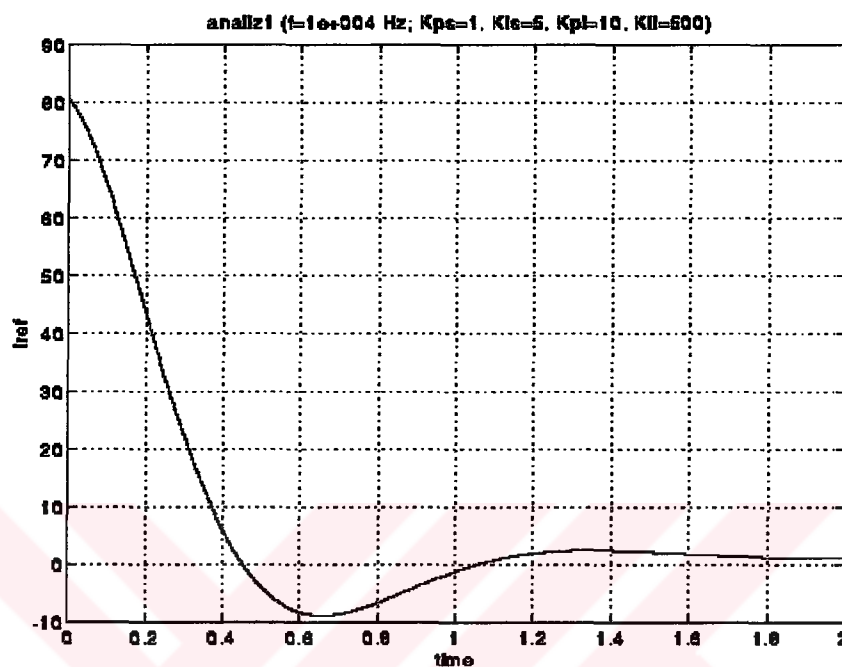


Figure 3 . 8 Reference current variation for $K_{initial}$ with unlimited duty cycle

In this part of results, the analysis will be carried out for two local optimum value of cost function. The optimal values of controllers are given in Section 3.4.4. These two local optimum values are obtained because two different state weighting matrices are used through the optimization. If these weighting matrices given in Section 3.4.4 are treated, it can be recognized that the error estimated over the area between the actual speed and reference speed is more minimized in the case of K_{opt2} . Figure 3 . 9 and Figure 3 . 12 show the rotor speed in terms of rad/sec with respect to time for optimal value of K_{opt1} and K_{opt2} respectively. The results in Figure 3 . 9 and Figure 3 . 12 clearly present that the area between actual and reference speed in Figure 3 . 12 is lower. The peak time in Figure 3 . 9 is greater than that of Figure 3 . 12. The overshoot of rotor speed in the case of K_{opt1} is greater than that value given in Figure 3 . 12.

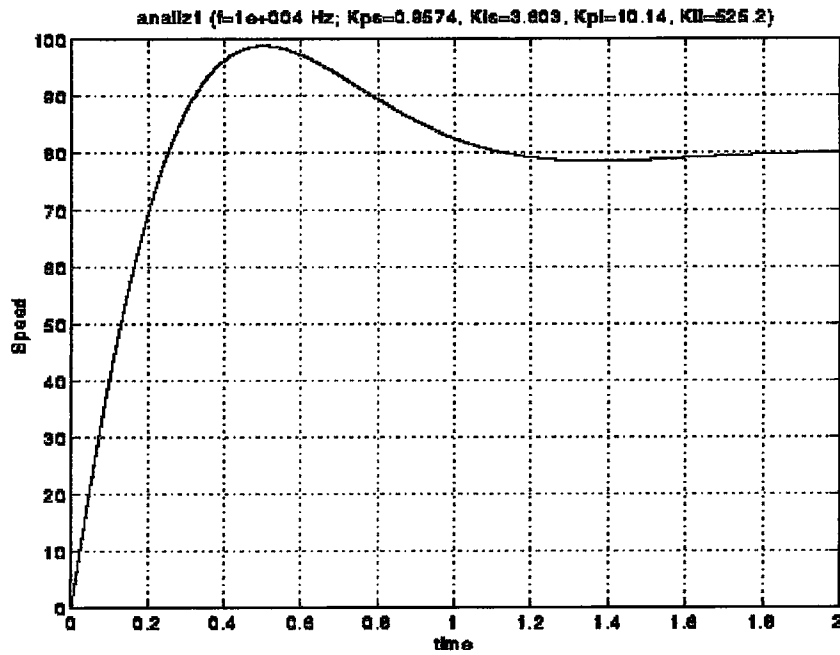


Figure 3 . 9 Speed response for K_{opt1} with unlimited duty cycle

Figure 3 . 10 and Figure 3 . 13 show the motor armature current for K_{opt1} and K_{opt2} respectively. As it can be clearly observed from the state weighting matrices given in Section 3.4.4, the error estimated over the area between the actual current and reference current is calculated through the optimization by keeping the weighting coefficient constant. The reference currents for K_{opt1} and K_{opt2} are given in Figure 3 . 11 and Figure 3 . 14 respectively. The actual currents are following the reference currents as it is expected.

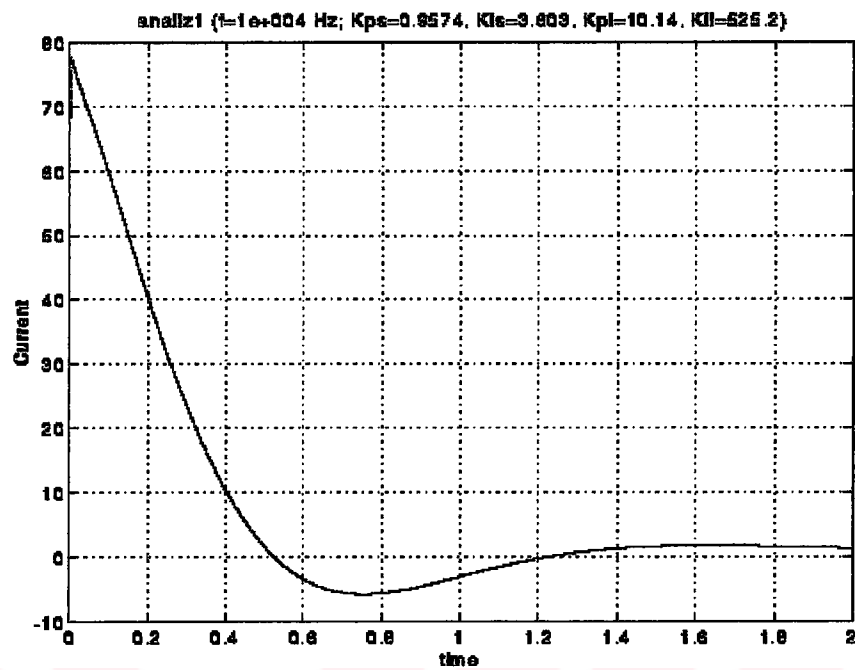


Figure 3 . 10 Armature current variation for K_{opt1} with unlimited duty cycle

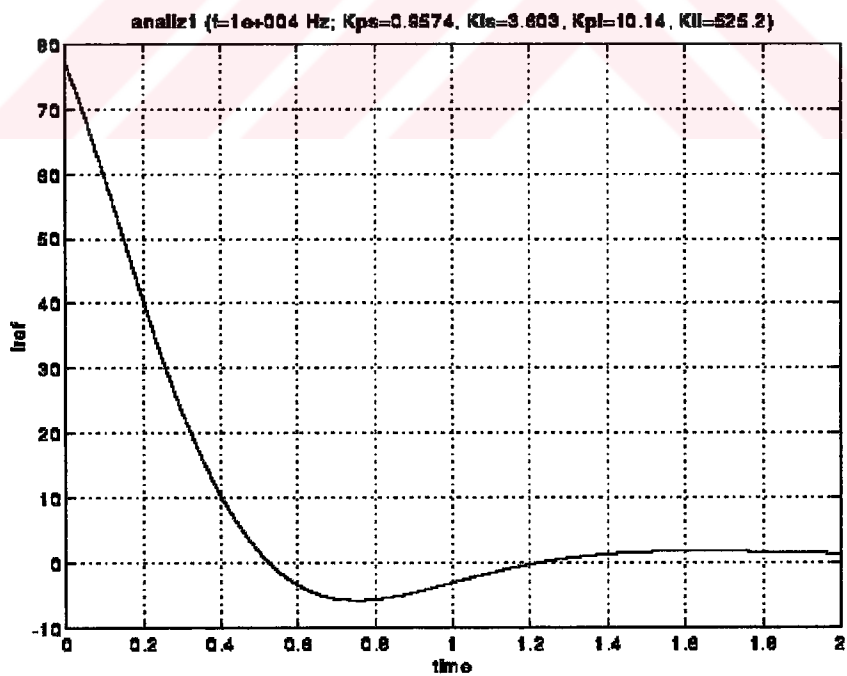


Figure 3 . 11 Reference current variation for K_{opt1} with unlimited duty cycle

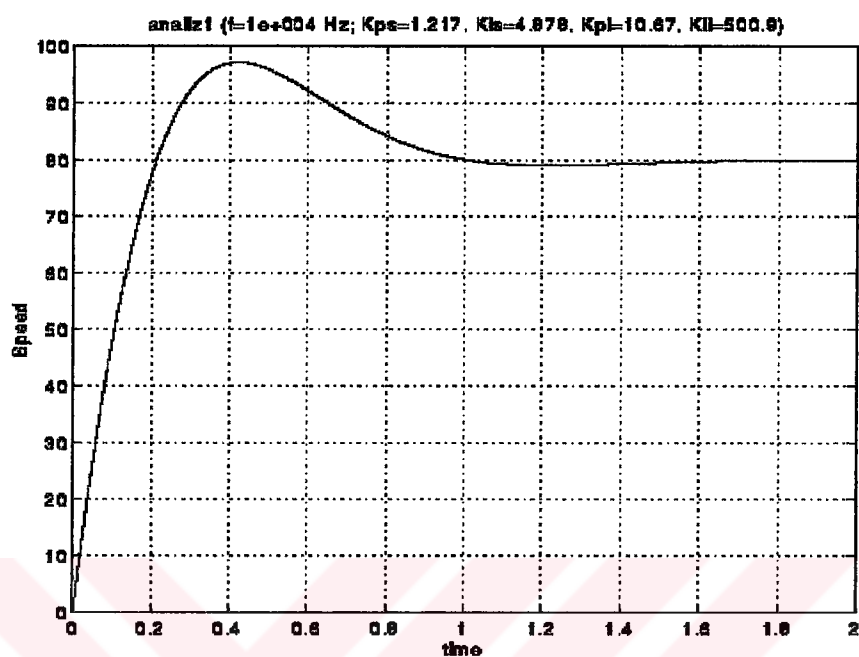


Figure 3 . 12 Speed response for K_{opt2} with unlimited duty cycle

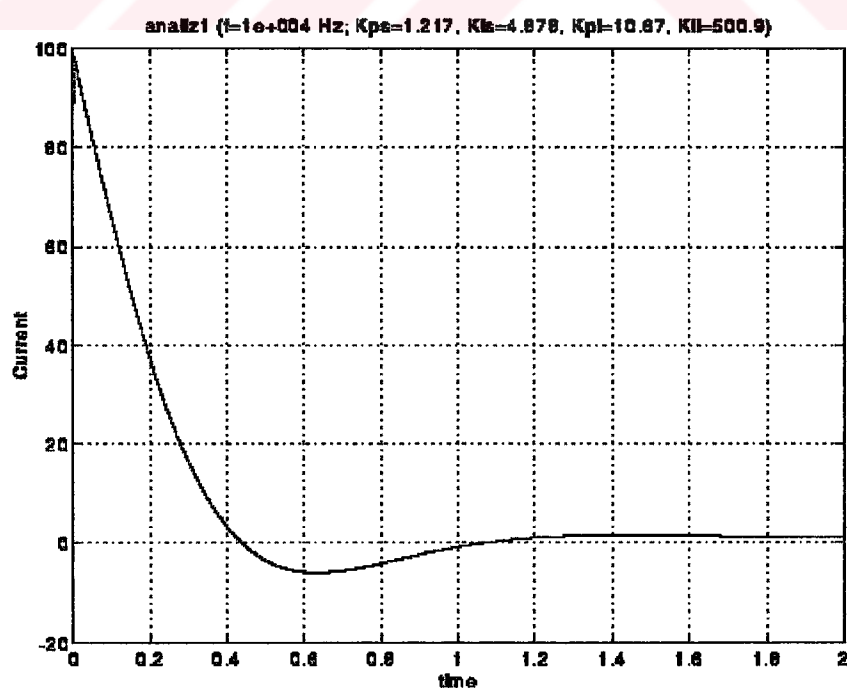


Figure 3 . 13 Armature current variation for K_{opt2} with unlimited duty cycle

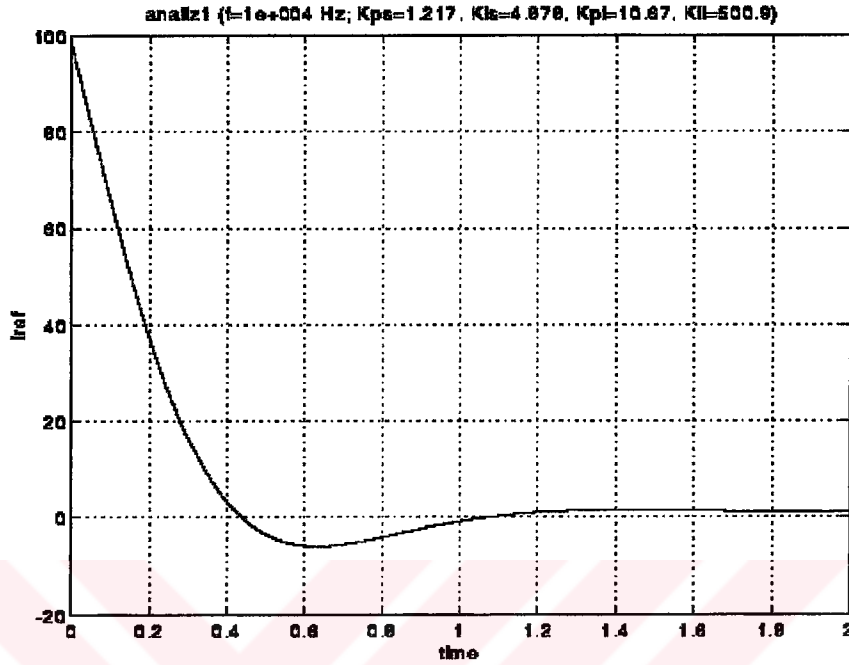


Figure 3 . 14 Reference current variation for K_{opt2} with unlimited duty cycle

3.5.2 Results of Analysis with Limited Duty Cycle

In this analysis, the duty cycle is limited to 0.9 at maximum value. The results will be presented for $K_{initial}$, K_{opt1} and K_{opt2} , and they will be compared with the results obtained from the real time simulation given in Chapter 5. This comparison has been performed in order to identify the validity of the model developed in Section 3.2.

Figure 3 . 15 to Figure 3 . 18 show the variation of rotor speed, armature current, reference current and duty cycle in time for $K_{initial}$. The duty cycle stays at 0.9 level for a while to accelerate the rotor from standstill to the steady-state as it is shown in Figure 3 . 18. After getting a low level on E_c , the duty cycle decreases to a level around 0.2. During this period the rotor accelerates and armature current decreases to reach at the steady-state values.

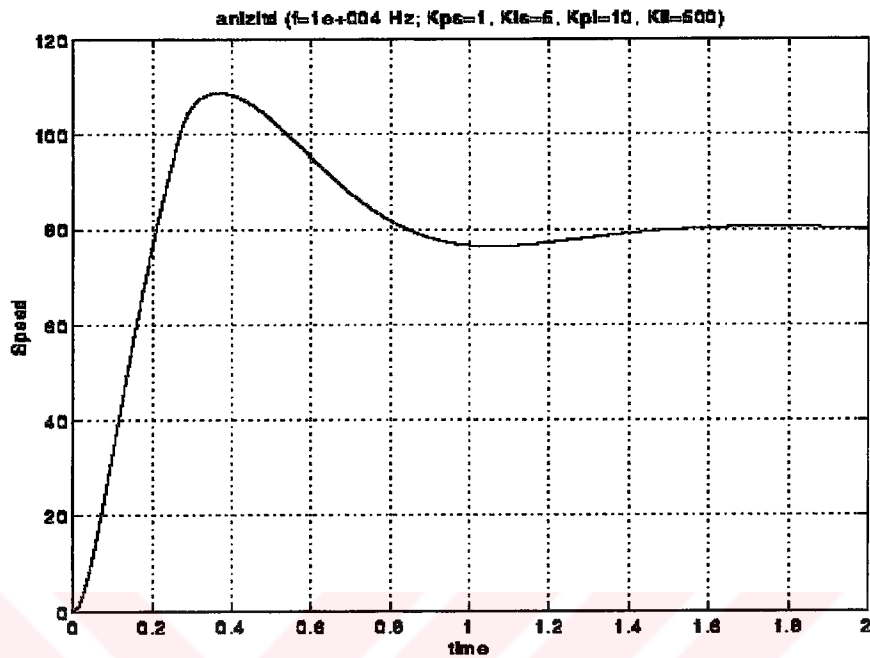


Figure 3 . 15 Speed response for $K_{initial}$ with limited duty cycle

When the envelope of speed obtained from the model developed in this thesis is compared with the envelope of speed obtained from the real time simulation given in Chapter 5, it is observed that the figures are similar to each other. The maximum value of speed from real time simulation is 106.8 rad/sec whereas the maximum value of speed from model is 108.6 rad/sec. In other words the percentage error is less than 2. This result proves the validity of the model developed in this thesis.

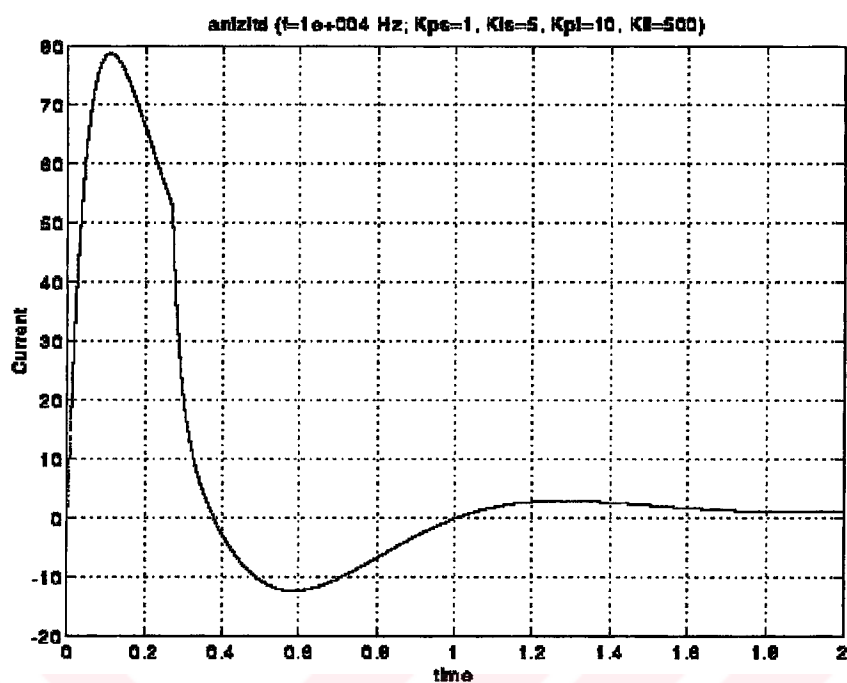


Figure 3 . 16 Armature current variation for $K_{initial}$ with limited duty cycle

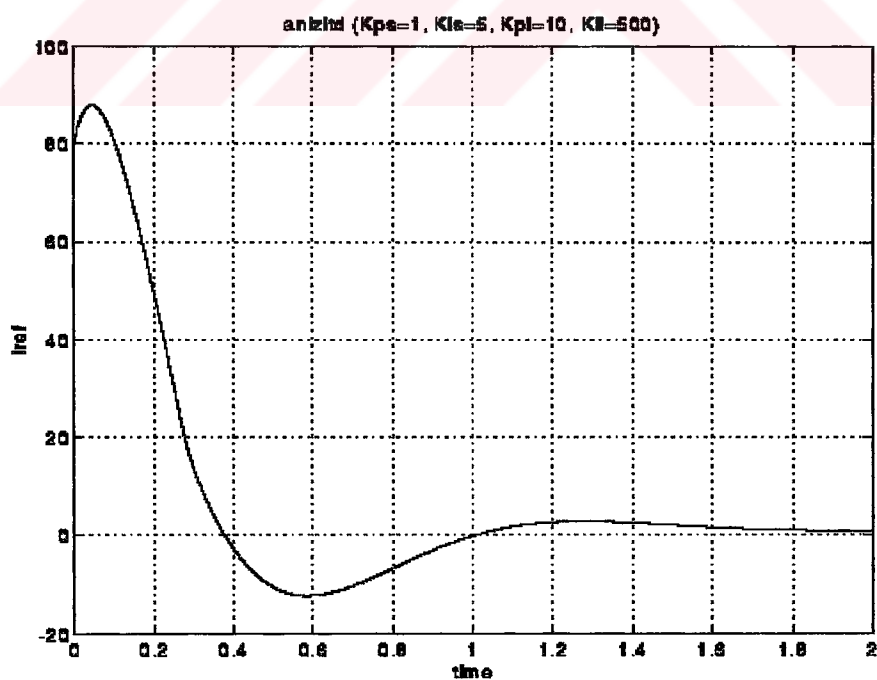


Figure 3 . 17 Reference current variation for $K_{initial}$ with limited duty cycle

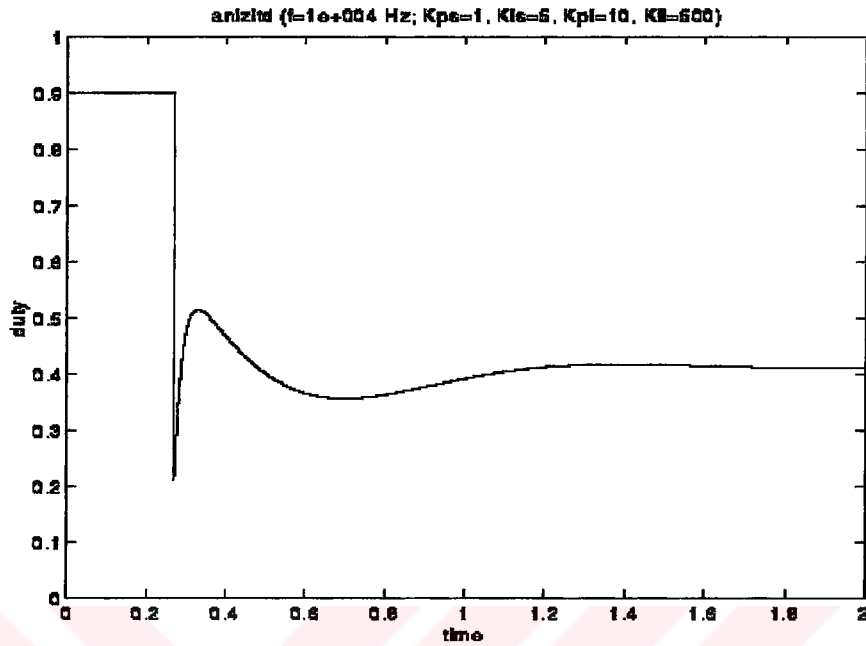


Figure 3 . 18 Duty cycle variation for $K_{initial}$

Figure 3 . 19 to Figure 3 . 22 presents the variation of rotor speed, armature current, reference current and duty cycle in time for K_{opt1} . Varying the optimal controller gains with the state weighting matrices do not change the maximum value of the armature current in the case of the analysis with limited duty cycle. However, in the case of the analysis with unlimited duty cycle, the maximum values of armature currents take place at different levels for $K_{initial}$, K_{opt1} and K_{opt2} as it is seen from Figure 3 . 7, Figure 3 . 10 and Figure 3 . 13.

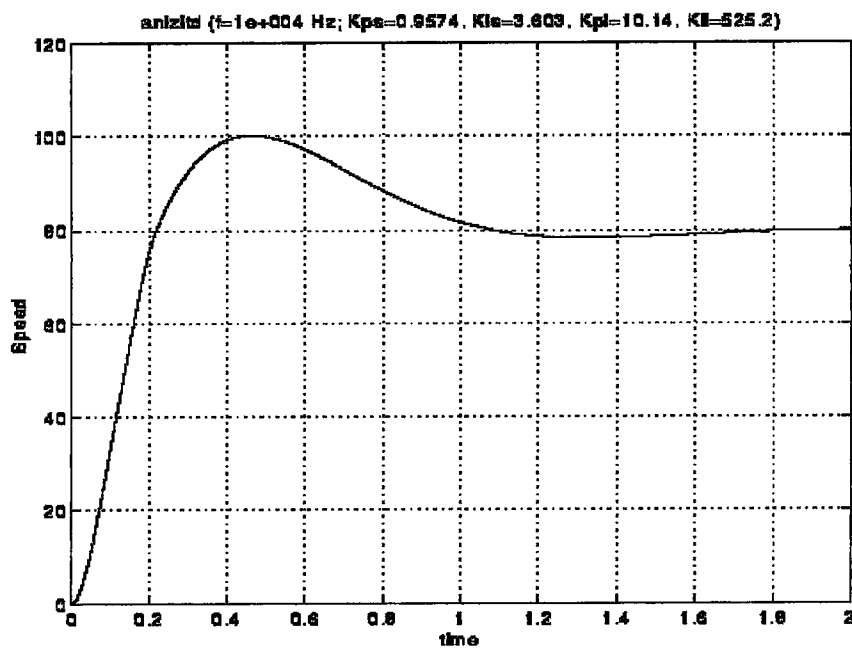


Figure 3 . 19 Speed response for K_{opt1} with limited duty cycle

Since the duty cycle is limited to 0.9, the voltage applied to the armature is limited too. This limitation on armature voltage provides the rise time of armature current during starting period higher than that value obtained from the unlimited duty cycle as it can be observed from Figure 3 . 20 and Figure 3 . 10.

The duty cycle is not allowed to take some values more than 0.9 in the simulation even if the E_c is greater than the peak value of sawtooth. Therefore the actual current follows the reference current with a time delay, as it can be seen from Figure 3 . 20 and Figure 3 . 21.

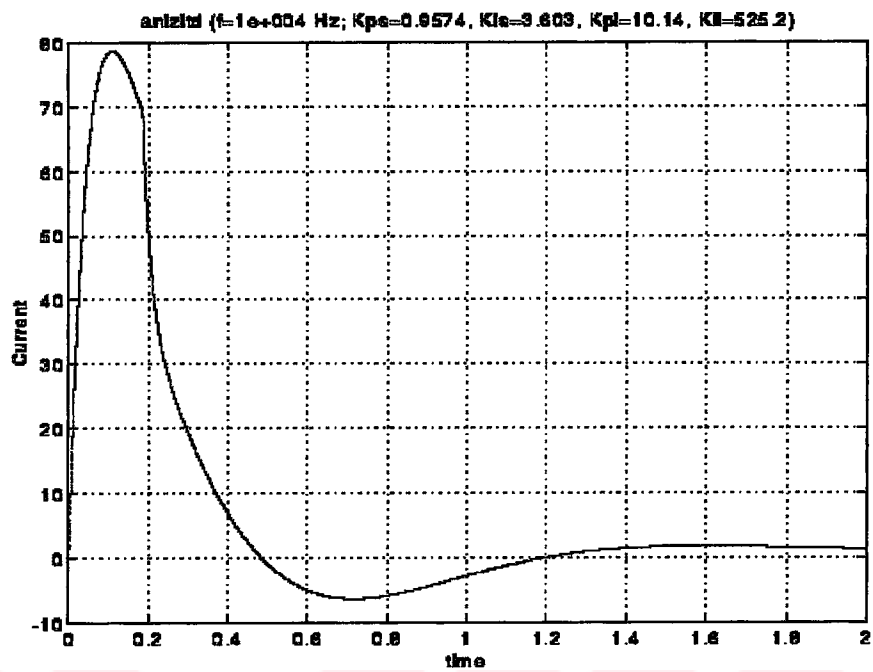


Figure 3 . 20 Armature current variation for K_{opt1} with limited duty cycle

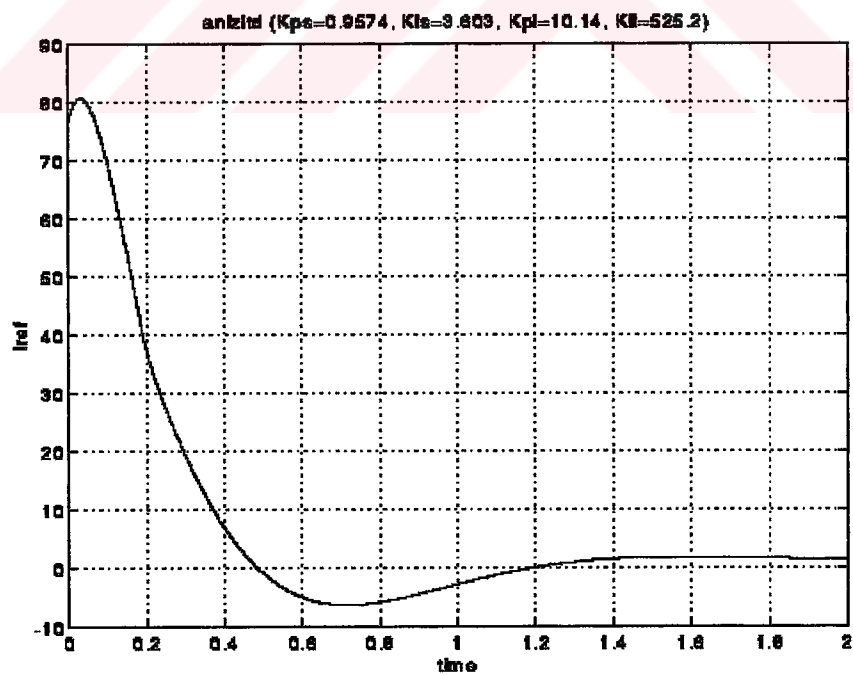


Figure 3 . 21 Reference current variation for K_{opt1} with limited duty cycle

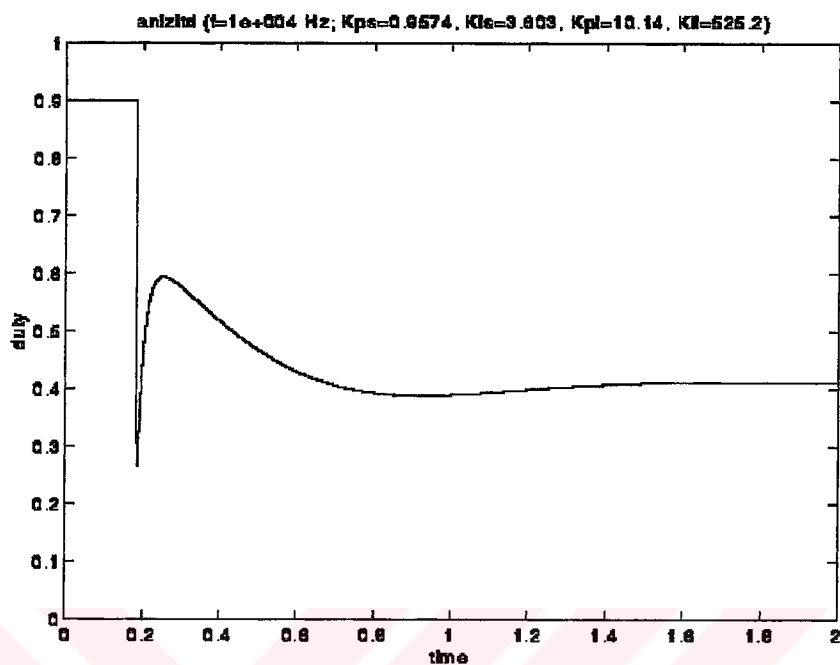


Figure 3 . 22 Duty cycle variation for K_{opt1}

Figure 3 . 23 to Figure 3 . 26 show the variation of rotor speed, armature current, reference current and duty cycle in time for K_{opt2} . As it can be recognized from Figure 3 . 23 and Figure 3 . 26, the rotor speed decelerates after the duty cycle jumps from 0.9 to 0.1.

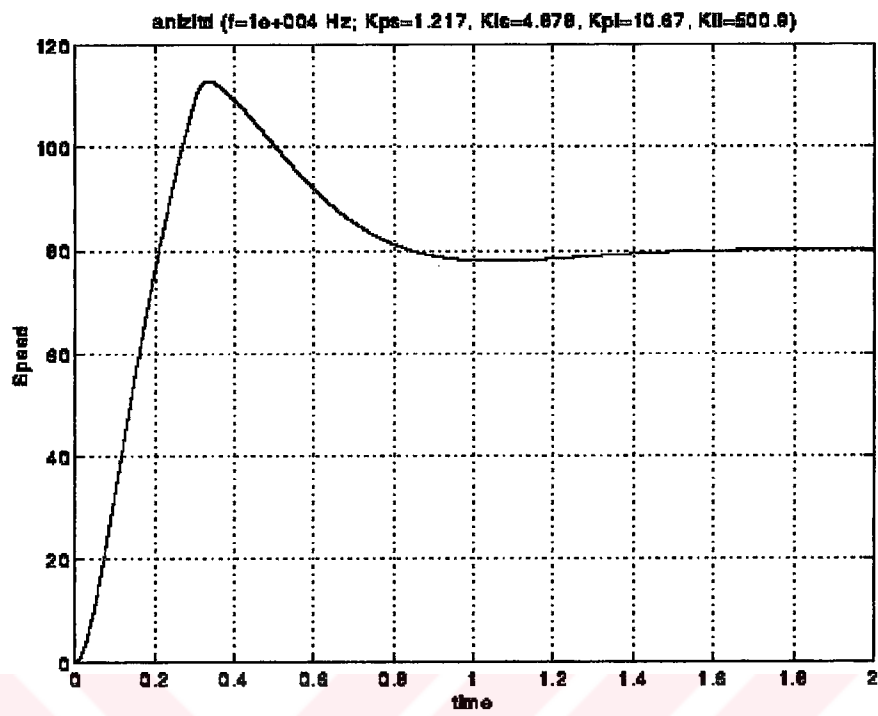


Figure 3 . 23 Speed response for K_{opt2} with limited duty cycle

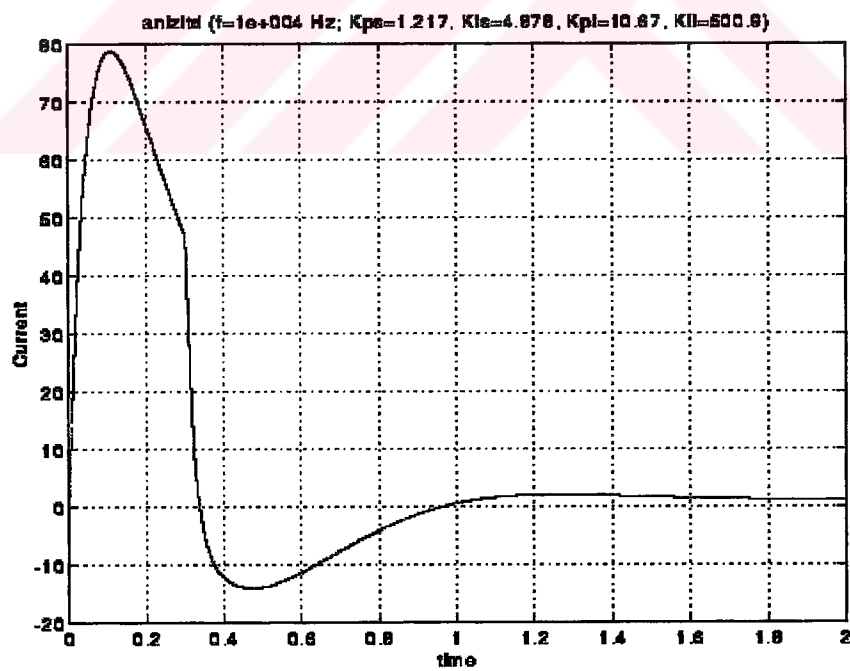


Figure 3 . 24 Armature current variation for K_{opt2} with limited duty cycle

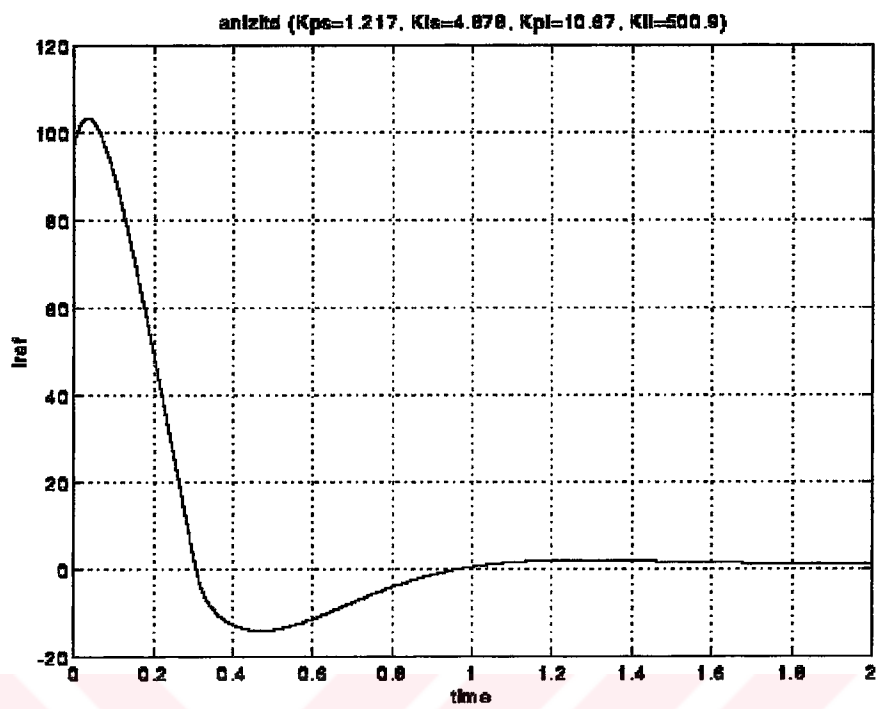


Figure 3 . 25 Reference current variation for K_{opt2} with limited duty cycle

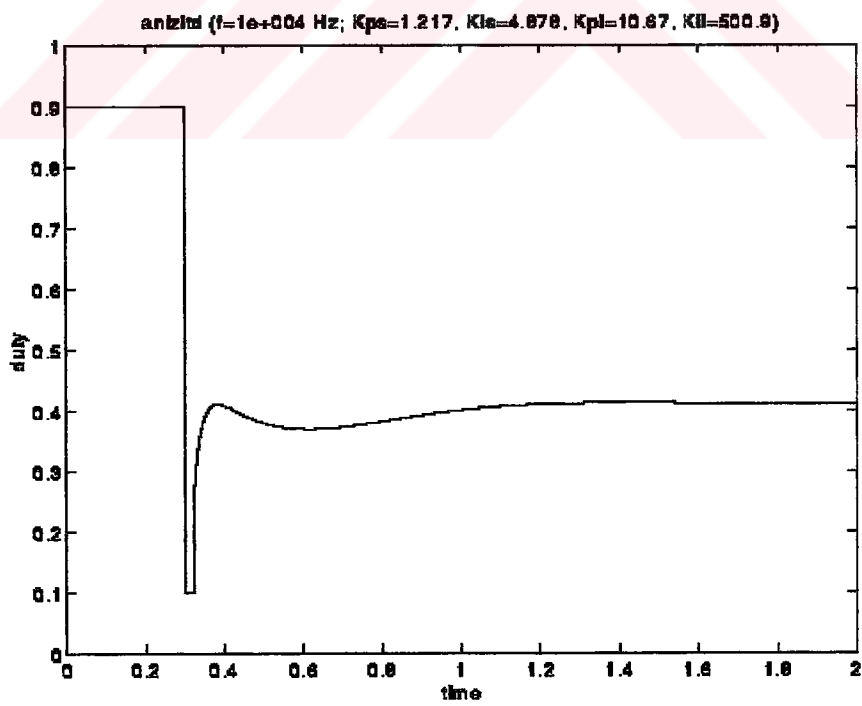


Figure 3 . 26 Duty cycle variation for K_{opt2}

CHAPTER FOUR

STABILITY ANALYSIS

4.1 Introduction

The stability analysis of discrete-time systems can be carried out by using two different techniques. One of them is the direct stability analysis in z-domain such as Jury test, Schur-Cohn criterion etc., whereas the other covers the techniques used for continuous-time systems after some certain modifications are made. The later includes the Routh-Hurwitz criterion, root-locus method and the frequency-response techniques.

During the design of the controller parameters using optimal control mentioned in previous chapter, the amplitude and the chopping period of PWM signal are considered at constant level. In this chapter, these two parameters are assumed to be varying and the effect of them on the stability of overall system will be investigated.

As it will be shown later in this chapter, characteristic equation of the system including K_{pwm} as a variable can be obtained as a linear function of K_{pwm} . However, the characteristic equation as a function of T can not be obtained as a linear function. Thus, the stability analysis of the system for the amplitude of PWM signal can be carried out by root-locus and it is investigated by both root-locus and jury test in this study. However, the stability analysis of the system for the varying chopping period is performed by only jury test.

In the following sections of this chapter, the stability analysis of the system will be given for the amplitude control of PWM signal by root-locus method and for the control of amplitude and chopping period of PWM signal by using Jury test. In addition the consistency of the results are being shown.

4.2 Stability Analysis for the Amplitude Control of PWM Signal by Root-Locus

In Chapter 3 the state equation of the system was obtained in the form of

$$x(n+1) = A \cdot x(n) + B \cdot u(n) + E \cdot r(n)$$

where $u(n) = -K \cdot y(n)$ and $y(n) = C \cdot x(n)$. Thus for the closed-loop system it can be written that

$$x(n+1) = A \cdot x(n) - BKC \cdot x(n) + E \cdot r(n)$$

$$x(n+1) = [A - BKC] \cdot x(n) + E \cdot r(n)$$

$$x(n+1) = A_c \cdot x(n) + E \cdot r(n)$$

The last equation is the compact form of the Equation (3-1). The characteristic equation of the system is

$$\det(zI - A_c) = 0 \quad (4-1)$$

The program `chrceq_k.mcd` of which list is given in Appendix 2 was written in Mathcad in order to obtain the characteristic equation as a function of K_{pwm} . In this program, 12 digits after decimal point is taken into consideration for precision. In this study, 3 and 7 digits after decimal point were considered but the results with these precisions were carrying enormous error in the calculation of characteristic equation. Therefore they have been kept out of the investigation.

As a consequence characteristic equation is obtained as

$$z^6 - 3.99781748481z^5 + 5.99345318022z^4 - 3.99345390603z^3 + 0.997818210612z^2 + K_{pwm}(1.81612318841 \cdot 10^{-3}z^4 - 5.43929597164 \cdot 10^{-3}z^3 + 5.43129677584 \cdot 10^{-3}z^2 - 1.80919241724 \cdot 10^{-3}z + 1.06842730978 \cdot 10^{-6}) \quad (4-2)$$

If Equation (4-2) is divided by the terms

$$z^6 - 3.99781748481z^5 + 5.99345318022z^4 - 3.99345390603z^3 + 0.997818210612z^2$$

the proper form of the equation for root-locus analysis can be obtained as follows

$$1 + K_{pwm} \frac{\text{num}(z)}{\text{den}(z)} = 0 \quad (4-3)$$

where

$$\begin{aligned} \text{num}(z) = & 1.81612318841 \cdot 10^{-3}z^4 - 5.43929597164 \cdot 10^{-3}z^3 \\ & + 5.43129677584 \cdot 10^{-3}z^2 - 1.80919241724 \cdot 10^{-3}z + 1.06842730978 \cdot 10^{-6} \end{aligned}$$

and

$$\begin{aligned} \text{den}(z) = & z^6 - 3.99781748481z^5 + 5.99345318022z^4 - 3.99345390603z^3 \\ & + 0.997818210612z^2 \end{aligned}$$

Now, it is possible to find the root-locus of the system as the K_{pwm} is a varying parameter. Various K_{pwm} and corresponding root locations can be obtained with the aid of rlocus function available in Matlab Control System Toolbox. The commands for this purpose in Matlab are given below:

$$\text{num}=[0 \ 0 \ 1.81612318841\text{e-}3 \ -5.43929597164\text{e-}3 \ 5.43129677584\text{e-}3 \ ...]$$

```

-1.80919241724e-3 1.06842730978e-6];
den=[1 -3.99781748481 5.99345318022 -3.99345390603 0.997818210612 0 0];
[R,Kpwm]=rlocus(num,den)

```

After these commands are entered into the Matlab, the root locations and the corresponding amplitude values of PWM signal are obtained as given Table 4. 1.

Table 4. 1 Absolute values of roots for K_{own}

[illegible]

0.0006	0.0093	0.9997 - 0.0002i	0.9942 + 0.0040i	0.9942 - 0.0040i	0.9997 + 0.0002i	0.0054
0.0006	0.0098	0.9997 - 0.0002i	0.9940 + 0.0039i	0.9940 - 0.0039i	0.9997 + 0.0002i	0.0057
0.0006	0.0103	0.9997 - 0.0002i	0.9938 + 0.0039i	0.9938 - 0.0039i	0.9997 + 0.0002i	0.0060
0.0006	0.0108	0.9997 - 0.0002i	0.9935 + 0.0038i	0.9935 - 0.0038i	0.9997 + 0.0002i	0.0062
0.0006	0.0113	0.9997 - 0.0003i	0.9933 + 0.0037i	0.9933 - 0.0037i	0.9997 + 0.0003i	0.0065
0.0006	0.0119	0.9997 - 0.0003i	0.9930 + 0.0035i	0.9930 - 0.0035i	0.9997 + 0.0003i	0.0068
0.0006	0.0125	0.9997 - 0.0003i	0.9927 + 0.0033i	0.9927 - 0.0033i	0.9997 + 0.0003i	0.0071
0.0006	0.0131	0.9997 - 0.0003i	0.9924 + 0.0031i	0.9924 - 0.0031i	0.9997 + 0.0003i	0.0075
0.0006	0.0137	0.9997 - 0.0003i	0.9921 + 0.0028i	0.9921 - 0.0028i	0.9997 + 0.0003i	0.0078
0.0006	0.0144	0.9997 - 0.0003i	0.9917 + 0.0024i	0.9917 - 0.0024i	0.9997 + 0.0003i	0.0082
0.0006	0.0151	0.9997 - 0.0003i	0.9914 + 0.0018i	0.9914 - 0.0018i	0.9997 + 0.0003i	0.0086
0.0006	0.0158	0.9997 - 0.0003i	0.9910 + 0.0007i	0.9910 - 0.0007i	0.9997 + 0.0003i	0.0089
0.0006	0.0166	0.9997 - 0.0003i	0.9889	0.9923	0.9997 + 0.0003i	0.0094
0.0006	0.0174	0.9997 - 0.0003i	0.9876	0.9928	0.9997 + 0.0003i	0.0098
0.0006	0.0183	0.9997 - 0.0003i	0.9865	0.9931	0.9997 + 0.0003i	0.0102
0.0006	0.0192	0.9997 - 0.0003i	0.9854	0.9933	0.9997 + 0.0003i	0.0107
0.0006	0.0201	0.9997 - 0.0004i	0.9843	0.9935	0.9997 + 0.0004i	0.0112
0.0006	0.0228	0.9997 - 0.0004i	0.9813	0.9938	0.9997 + 0.0004i	0.0126
0.0006	0.0310	0.9997 - 0.0004i	0.9725	0.9943	0.9997 + 0.0004i	0.0169
0.0006	0.0569	0.9997 - 0.0004i	0.9463	0.9947	0.9997 + 0.0004i	0.0300
0.0006	0.1462	0.9997 - 0.0004i	0.8567	0.9949	0.9997 + 0.0004i	0.0693
0.0006	0.1539	0.9997 - 0.0004i	0.8491	0.9949	0.9997 + 0.0004i	0.0723
0.0006	0.1620	0.9997 - 0.0004i	0.8410	0.9949	0.9997 + 0.0004i	0.0753
0.0006	0.1706	0.9997 - 0.0004i	0.8323	0.9949	0.9997 + 0.0004i	0.0785
0.0006	0.1799	0.9997 - 0.0004i	0.8230	0.9949	0.9997 + 0.0004i	0.0819
0.0006	0.1899	0.9997 - 0.0004i	0.8130	0.9949	0.9997 + 0.0004i	0.0853
0.0006	0.2006	0.9997 - 0.0004i	0.8023	0.9949	0.9997 + 0.0004i	0.0890
0.0006	0.2123	0.9997 - 0.0004i	0.7907	0.9949	0.9997 + 0.0004i	0.0927
0.0006	0.2249	0.9997 - 0.0004i	0.7780	0.9949	0.9997 + 0.0004i	0.0967
0.0006	0.2387	0.9997 - 0.0004i	0.7642	0.9949	0.9997 + 0.0004i	0.1008
0.0006	0.2540	0.9997 - 0.0004i	0.7489	0.9949	0.9997 + 0.0004i	0.1050
0.0006	0.2709	0.9997 - 0.0004i	0.7320	0.9949	0.9997 + 0.0004i	0.1095
0.0006	0.2900	0.9997 - 0.0004i	0.7129	0.9949	0.9997 + 0.0004i	0.1142
0.0006	0.3120	0.9997 - 0.0004i	0.6909	0.9949	0.9997 + 0.0004i	0.1190
0.0006	0.3380	0.9997 - 0.0004i	0.6649	0.9949	0.9997 + 0.0004i	0.1241
0.0006	0.3705	0.9997 - 0.0004i	0.6324	0.9949	0.9997 + 0.0004i	0.1293
0.0006	0.4168	0.9997 - 0.0004i	0.5861	0.9949	0.9997 + 0.0004i	0.1348
0.0006	0.5014 + 0.0568i	0.9997 - 0.0004i	0.5014 - 0.0568i	0.9949	0.9997 + 0.0004i	0.1405
0.0006	0.5014 + 0.1186i	0.9997 - 0.0004i	0.5014 - 0.1186i	0.9950	0.9997 + 0.0004i	0.1465
0.0006	0.5014 + 0.1593i	0.9997 - 0.0004i	0.5014 - 0.1593i	0.9950	0.9997 + 0.0004i	0.1527
0.0006	0.5014 + 0.1928i	0.9997 - 0.0004i	0.5014 - 0.1928i	0.9950	0.9997 + 0.0004i	0.1592
0.0006	0.5014 + 0.2223i	0.9997 - 0.0004i	0.5014 - 0.2223i	0.9950	0.9997 + 0.0004i	0.1660
0.0006	0.5014 + 0.2495i	0.9997 - 0.0004i	0.5014 - 0.2495i	0.9950	0.9997 + 0.0004i	0.1730
0.0006	0.5014 + 0.2749i	0.9997 - 0.0004i	0.5014 - 0.2749i	0.9950	0.9997 + 0.0004i	0.1804
0.0006	0.5014 + 0.2992i	0.9997 - 0.0004i	0.5014 - 0.2992i	0.9950	0.9997 + 0.0004i	0.1880
0.0006	0.5014 + 0.3186i	0.9997 - 0.0004i	0.5014 - 0.3186i	0.9950	0.9997 + 0.0004i	0.1946
0.0006	0.5014 + 0.3710i	0.9997 - 0.0004i	0.5014 - 0.3710i	0.9950	0.9997 + 0.0004i	0.2145
0.0006	0.5014 + 0.4968i	0.9997 - 0.0005i	0.5014 - 0.4968i	0.9950	0.9997 + 0.0005i	0.2746
0.0006	0.5014 + 0.7591i	0.9997 - 0.0005i	0.5014 - 0.7591i	0.9950	0.9997 + 0.0005i	0.4560
0.0006	0.5014 + 1.2531i	0.9997 - 0.0005i	0.5014 - 1.2531i	0.9950	0.9997 + 0.0005i	1.0034
0.0006	0.5014 + 2.1378i	0.9997 - 0.0005i	0.5014 - 2.1378i	0.9950	0.9997 + 0.0005i	2.6552
0.0006	0.5014 + 3.6911i	0.9997 - 0.0005i	0.5014 - 3.6911i	0.9950	0.9997 + 0.0005i	7.6406

If the list of the root locations given above is examined, it is seen that the system has a pole outside the unit circle when K_{pwm} is less than approximately 4.6 and greater than approximately 1003. However, in order to find the exact values of K_{pwm} which are the limit on the stability, the following command is entered to expand the interval of K_{pwm} between 1 and 5 with the step length of 0.5. The amplitude of the complex poles are obtained as follows in this interval.

$$K_{pwm}=1:0.5:5;$$

$R = \text{rlocus}(\text{num}, \text{den}, K_{\text{pwm}})$

$[\text{abs}(R) \ K_{\text{pwm}}']$

Table 4. 2 Absolute values of roots for K_{pwm} in the range (1-5)

<u>abs(Root1)</u>	<u>abs(Root2)</u>	<u>abs(Root3)</u>	<u>abs(Root4)</u>	<u>abs(Root5)</u>	<u>abs(Root6)</u>	<u>K_{pwm}</u>
0.9985	0.9985	1.0005	0.9986	0.0010	0.0010	1.0000
0.9979	0.9979	1.0003	0.9989	0.0009	0.0019	1.5000
0.9975	0.9975	1.0002	0.9991	0.0007	0.0029	2.0000
0.9970	0.9970	1.0001	0.9992	0.0007	0.0038	2.5000
0.9965	0.9965	1.0000	0.9993	0.0007	0.0048	3.0000
0.9961	0.9961	0.9999	0.9994	0.0007	0.0057	3.5000
0.9956	0.9956	0.9998	0.9995	0.0006	0.0066	4.0000
0.9951	0.9951	0.9997	0.9996	0.0006	0.0076	4.5000
0.9947	0.9947	0.9997	0.9997	0.0006	0.0085	5.0000

The third pole is not in the unit circle during $K_{\text{pwm}} \leq 3$. Therefore, in order to keep the system in the stable region, the amplitude of PWM signal should be chosen greater than 3.

The other command given below is expanding the range between 450 and 600 with the step size of 5 to find the exact value of maximum PWM amplitude keeping the system in stable region. This command also returns the amplitude of the complex poles in the first 6 columns and the last column shows the value of corresponding K_{pwm} .

$K_{\text{pwm}} = 450:5:600;$

$R = \text{rlocus}(\text{num}, \text{den}, K_{\text{pwm}})$

$[\text{abs}(R) \ K_{\text{pwm}}']$

Table 4. 3 Absolute values of roots for K_{pwm} in the range (450-600)

<u>abs(Root1)</u>	<u>abs(Root2)</u>	<u>abs(Root3)</u>	<u>abs(Root4)</u>	<u>abs(Root5)</u>	<u>abs(Root6)</u>	<u>K_{pwm}</u>
0.9037	0.9037	0.9997	0.9997	0.9950	0.0006	450.0000
0.9087	0.9087	0.9997	0.9997	0.9950	0.0006	455.0000
0.9137	0.9137	0.9997	0.9997	0.9950	0.0006	460.0000
0.9187	0.9187	0.9997	0.9997	0.9950	0.0006	465.0000
0.9236	0.9236	0.9997	0.9997	0.9950	0.0006	470.0000
0.9285	0.9285	0.9997	0.9997	0.9950	0.0006	475.0000
0.9334	0.9334	0.9997	0.9997	0.9950	0.0006	480.0000

0.9382	0.9382	0.9997	0.9997	0.9950	0.0006	485.0000
0.9430	0.9430	0.9997	0.9997	0.9950	0.0006	490.0000
0.9478	0.9478	0.9997	0.9997	0.9950	0.0006	495.0000
0.9526	0.9526	0.9997	0.9997	0.9950	0.0006	500.0000
0.9574	0.9574	0.9997	0.9997	0.9950	0.0006	505.0000
0.9621	0.9621	0.9997	0.9997	0.9950	0.0006	510.0000
0.9668	0.9668	0.9997	0.9997	0.9950	0.0006	515.0000
0.9715	0.9715	0.9997	0.9997	0.9950	0.0006	520.0000
0.9762	0.9762	0.9997	0.9997	0.9950	0.0006	525.0000
0.9808	0.9808	0.9997	0.9997	0.9950	0.0006	530.0000
0.9854	0.9854	0.9997	0.9997	0.9950	0.0006	535.0000
0.9900	0.9900	0.9997	0.9997	0.9950	0.0006	540.0000
0.9946	0.9946	0.9997	0.9997	0.9950	0.0006	545.0000
0.9991	0.9991	0.9997	0.9997	0.9950	0.0006	550.0000
1.0037	1.0037	0.9997	0.9997	0.9950	0.0006	555.0000
1.0082	1.0082	0.9997	0.9997	0.9950	0.0006	560.0000
1.0127	1.0127	0.9997	0.9997	0.9950	0.0006	565.0000
1.0172	1.0172	0.9997	0.9997	0.9950	0.0006	570.0000
1.0216	1.0216	0.9997	0.9997	0.9950	0.0006	575.0000
1.0260	1.0260	0.9997	0.9997	0.9950	0.0006	580.0000
1.0305	1.0305	0.9997	0.9997	0.9950	0.0006	585.0000
1.0349	1.0349	0.9997	0.9997	0.9950	0.0006	590.0000
1.0392	1.0392	0.9997	0.9997	0.9950	0.0006	595.0000
1.0436	1.0436	0.9997	0.9997	0.9950	0.0006	600.0000

For the value of K_{pwm} , greater than 550, the system has two poles which are outside the unit circle denoting instability. Thus it can be recognized that the upper limit of K_{pwm} will be 550 for the stable operation.

As a consequence of the stability analysis by root-locus, it can be concluded that K_{pwm} must be kept in the range given below:

$$3.0 < K_{pwm} < 550.$$

The analysis results of the system for $K_{pwm}=545$ in stable region and $K_{pwm}=555$ in the unstable region without any limit on duty cycle are presented in Figure 4 . 1, Figure 4 . 2, Figure 4 . 3 and Figure 4 . 4.

Figure 4 . 1 and Figure 4 . 2 give the speed and current response, respectively, for the amplitude value of 545 of PWM signal. In these figures both the speed and current responses settle down and this denotes the stable operation for that value of K_{pwm} .

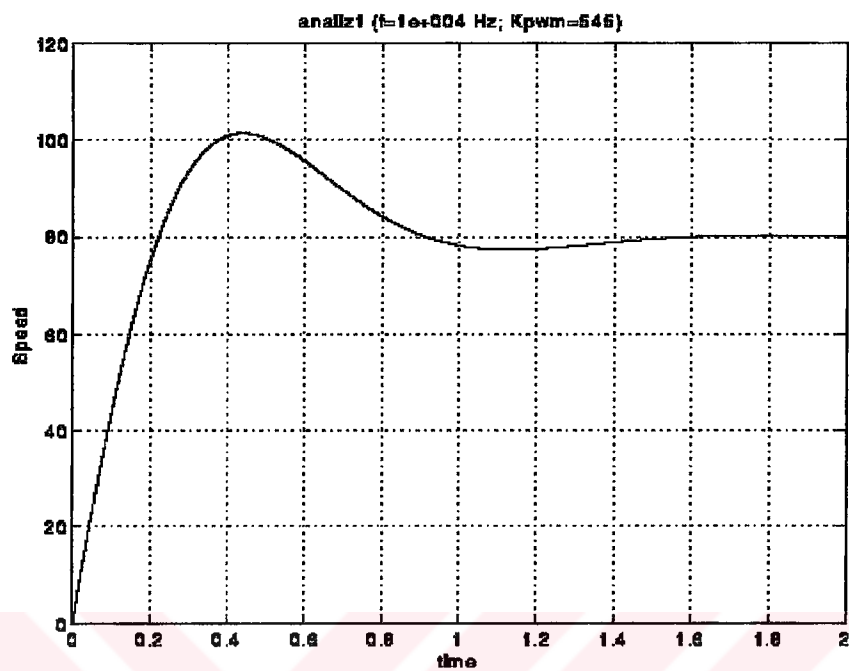


Figure 4 . 1 Rotor speed for $K_{pwm}=545$

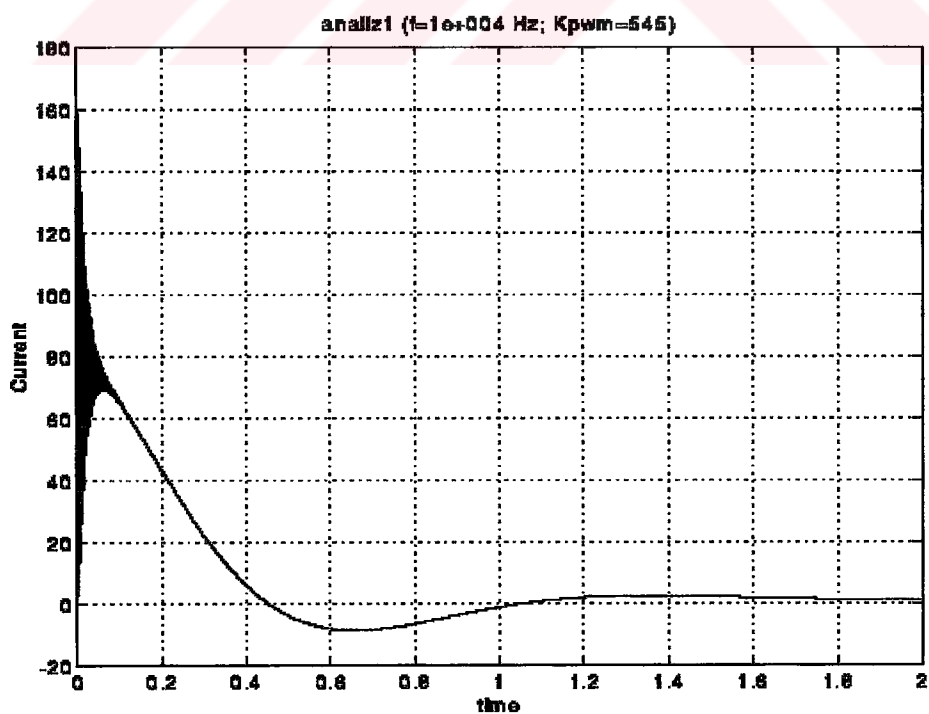


Figure 4 . 2 Armature current for $K_{pwm}=545$

Figure 4 . 3 and Figure 4 . 4 show the speed and current responses for the amplitude value of 555 of PWM signal respectively. As it is seen from these figures, both the speed and current responses are increasing in time and this shows the unstable operation.

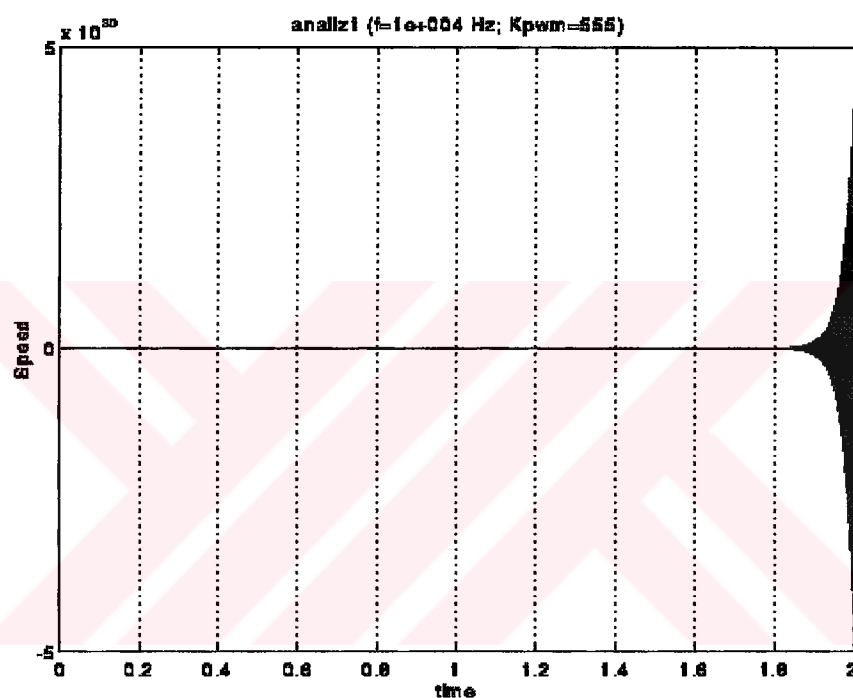


Figure 4 . 3 Rotor speed for $K_{pwm}=555$

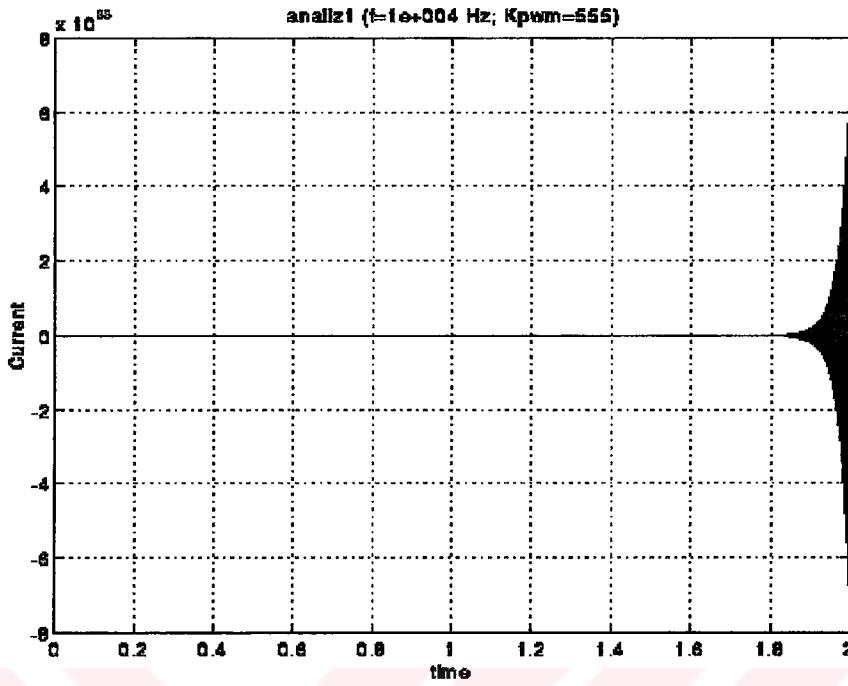


Figure 4 . 4 Armature current for $K_{pwm}=555$

4.3 Jury Stability Test

Jury stability test is a stability criterion for discrete-time systems that is similar to the Routh-Hurwitz criterion in continuous-time systems. It is applied to the characteristic equation written as a function of z . Since the system has 6 state-variables, sixth order characteristic equation of the system can be obtained in the form of

$$Q(z) = a_6 z^6 + a_5 z^5 + a_4 z^4 + a_3 z^3 + a_2 z^2 + a_1 z^1 + a_0 = 0 \quad (4-4)$$

where $a_6 > 0$. If this inequality is not satisfied, $Q(z)$ is multiplied by -1. Then the table below is formed.

Table 4. 4. Jury table for the 6th order system in thesis

z^0	z^1	z^2	z^3	z^4	z^5	z^6
a_0	a_1	a_2	a_3	a_4	a_5	a_6
a_6	a_5	a_4	a_3	a_2	a_1	a_0
b_0	b_1	b_2	b_3	b_4	b_5	
b_5	b_4	b_3	b_2	b_1	b_0	
c_0	c_1	c_2	c_3	c_4		
c_4	c_3	c_2	c_1	c_0		
d_0	d_1	d_2	d_3			
d_3	d_2	d_1	d_0			
e_0	e_1	e_2				

where

$$b_k = \begin{vmatrix} a_0 & a_{6-k} \\ a_6 & a_k \end{vmatrix}, \quad (4-5)$$

$$c_k = \begin{vmatrix} b_0 & b_{5-k} \\ b_5 & b_k \end{vmatrix}, \quad (4-6)$$

$$d_k = \begin{vmatrix} c_0 & c_{4-k} \\ c_4 & c_k \end{vmatrix}, \quad (4-7)$$

$$e_k = \begin{vmatrix} d_0 & d_{3-k} \\ d_3 & d_k \end{vmatrix}, \quad (4-8)$$

According to Jury's test, the following conditions must be satisfied for the stability

$$1) Q(1) > 0 \quad (4-9)$$

$$2) (-1)^6 Q(-1) > 0 \quad (4-10)$$

$$3) |a_0| < a_6 \quad (4-11)$$

$$4) |b_0| > |b_5| \quad (4-12)$$

$$5) |c_0| > |c_4| \quad (4-13)$$

$$6) |d_0| > |d_3| \quad (4-14)$$

$$7) |e_0| > |e_2| \quad (4-15)$$

Note that for the 6th-order system, there are total 7(6+1) constraints.

4.3.1 Stability Analysis for the Amplitude Control of PWM Signal

In Section 4.2, characteristic equation including K_{pwm} as a varying parameter was obtained and given in Equation (4-2). After rearranging Equation (4-2) in the form of Equation (4-4), the coefficients in Equation (4-4) can be obtained as given below

$$a_0 = 1.06842730978 \cdot 10^{-6} \cdot K_{pwm}$$

$$a_1 = -1.80919241724 \cdot 10^{-3} \cdot K_{pwm}$$

$$a_2 = 997818210612 + 5.43129677584 \cdot 10^{-3} \cdot K_{pwm}$$

$$a_3 = -3.99345390603 - 5.43929597164 \cdot 10^{-3} \cdot K_{pwm}$$

$$a_4 = 5.99345318022 + 1.81612318841 \cdot 10^{-3} \cdot K_{pwm}$$

$$a_5 = -3.99781748481$$

$$a_6 = 1,$$

Using these values, the other coefficients in Table 4. 4 are obtained by using Mathcad. The b_k 's ($k=0,1,...,5$) which are defined in Equation (4-5) are

$$b_0 := 1.14153691628 \cdot 10^{-12} \cdot K^2 - 1.$$

$$b_1 := -1.93299058723 \cdot 10^{-9} \cdot K^2 + 3.99781748481$$

$$b_2 := -1.81505709218 \cdot 10^{-3} \cdot K + 5.80294580283 \cdot 10^{-9} \cdot K^2 - 5.99345318022$$

$$b_3 := 5.43502925643 \cdot 10^{-3} \cdot K - 5.81149236208 \cdot 10^{-9} \cdot K^2 + 3.99345390603$$

$$b_4 := -5.42489320678 \cdot 10^{-3} \cdot K + 1.94039561242 \cdot 10^{-9} \cdot K^2 - .997818210612$$

$$b_5 := 1.80492103986 \cdot 10^{-3} \cdot K$$

where K is used instead of K_{pwm} hereafter until the end of this section in order to keep the coefficient equalities short.

The other coefficients c_k 's ($k=0,1,\dots,4$) in Equation (4-6) are

$$c_0 := 1.30310653123 \cdot 10^{-24} \cdot K^4 - 3.2577422432 \cdot 10^{-6} \cdot K^2 + 1.$$

$$c_1 := -2.20658011414 \cdot 10^{-21} \cdot K^4 + 9.79344144215 \cdot 10^{-6} \cdot K^2 - 3.99781748481 \dots \\ + \left[- \left(3.50226086651 \cdot 10^{-12} \cdot K^3 \right) \right] + 1.80098308229 \cdot 10^{-3} \cdot K$$

$$c_2 := 1.04872128826 \cdot 10^{-11} \cdot K^3 + 6.6242768571 \cdot 10^{-21} \cdot K^4 - 9.81560844474 \cdot 10^{-6} \cdot K^2 \dots \\ + \left[- \left(5.39281188452 \cdot 10^{-3} \cdot K \right) \right] + 5.99345318022$$

$$c_3 := -1.04676546862 \cdot 10^{-11} \cdot K^3 - 6.63403306999 \cdot 10^{-21} \cdot K^4 + 3.28185078526 \cdot 10^{-6} \cdot K^2 \dots \\ + 5.38268048996 \cdot 10^{-3} \cdot K - 3.99345390603$$

$$c_4 := 3.48270266488 \cdot 10^{-12} \cdot K^3 + 2.21503322377 \cdot 10^{-21} \cdot K^4 - 1.94153465874 \cdot 10^{-9} \cdot K^2 \dots \\ + \left[- \left(1.79085168507 \cdot 10^{-3} \cdot K \right) \right] + .997818210612$$

The d_k 's ($k=0,1,2,3$) in Equation (4-7) are as follows

$$d_0 := -4.90637048432 \cdot 10^{-42} \cdot K^8 - 1.21292177412 \cdot 10^{-23} \cdot K^6 + 1.0625354757 \cdot 10^{-11} \cdot K^4 \dots \\ + \left[- \left(9.71875964704 \cdot 10^{-6} \cdot K^2 \right) \right] + 4.35881857107 \cdot 10^{-3} + 3.57388884774 \cdot 10^{-3} \cdot K \dots \\ + \left(-1.39042095128 \cdot 10^{-11} \cdot K^3 - 1.54286042224 \cdot 10^{-32} \cdot K^7 + 1.35315094519 \cdot 10^{-20} \cdot K^5 \right)$$

$$d_1 := 1.46917282487 \cdot 10^{-41} \cdot K^8 + 3.64556478131 \cdot 10^{-23} \cdot K^6 - 3.19356283448 \cdot 10^{-11} \cdot K^4 \dots \\ + 4.62860037376 \cdot 10^{-32} \cdot K^7 - 4.05944194352 \cdot 10^{-20} \cdot K^5 + 2.91744388614 \cdot 10^{-5} \cdot K^2 \dots \\ + 4.14705713571 \cdot 10^{-11} \cdot K^3 - 1.30764541336 \cdot 10^{-2} - 1.07216371894 \cdot 10^{-2} \cdot K$$

$$d_2 := -4.62862456672 \cdot 10^{-32} \cdot K^7 - 1.46643611835 \cdot 10^{-41} \cdot K^8 - 3.65236824706 \cdot 10^{-23} \cdot K^6 \dots \\ + 4.059435545 \cdot 10^{-20} \cdot K^5 + 3.19952275191 \cdot 10^{-11} \cdot K^4 - 4.12287030728 \cdot 10^{-11} \cdot K^3 \dots \\ + \left[- \left(2.91926309518 \cdot 10^{-5} \cdot K^2 \right) \right] + 1.07216197474 \cdot 10^{-2} \cdot K + 1.30764525461 \cdot 10^{-2}$$

$$d3 := 1.54288461522 \cdot 10^{-32} \cdot K^7 + 4.87900341191 \cdot 10^{-42} \cdot K^8 + 1.2197252417 \cdot 10^{-23} \cdot K^6 \dots \\ + \left[\left(-1.3531445195 \cdot 10^{-20} \cdot K^5 \right) \right] - 1.0684953947 \cdot 10^{-11} \cdot K^4 + 1.36623411844 \cdot 10^{-11} \cdot K^3 \dots \\ + 9.73695174216 \cdot 10^{-6} \cdot K^2 - 3.57387140583 \cdot 10^{-3} \cdot K - 4.35881698352 \cdot 10^{-3}$$

Finally, the coefficients e_k 's ($k=0,1,2$) in Equation (4-8) are

$$e0 := 1.63399641547 \cdot 10^{-10} \cdot K + 1.29691281097 \cdot 10^{-10} \cdot K^3 + 2.8323175936 \cdot 10^{-10} \cdot K^2 \dots \\ + \left(-2.10526267157 \cdot 10^{-57} \cdot K^{13} \right) - 1.27007891017 \cdot 10^{-24} \cdot K^8 + 1.54723047165 \cdot 10^{-18} \cdot K^6 \dots \\ + \left(-3.51036769834 \cdot 10^{-24} \cdot K^7 \right) - 4.21424801861 \cdot 10^{-16} \cdot K^5 + 2.67797035977 \cdot 10^{-85} \cdot K^{16} \dots \\ + \left(-7.46580711026 \cdot 10^{-69} \cdot K^{14} \right) - 1.65504350601 \cdot 10^{-48} \cdot K^{12} + 2.89967787006 \cdot 10^{-36} \cdot K^{10} \dots \\ + \left(-1.60755308632 \cdot 10^{-33} \cdot K^9 \right) + 3.68389085167 \cdot 10^{-45} \cdot K^{11} + 8.4211070524 \cdot 10^{-76} \cdot K^{15} \dots \\ + \left(-3.56188980044 \cdot 10^{-13} \cdot K^4 \right) + 1.38396823247 \cdot 10^{-11}$$

$$e1 := -3.26799477921 \cdot 10^{-10} \cdot K - 2.59382328308 \cdot 10^{-10} \cdot K^3 - 5.66463612711 \cdot 10^{-10} \cdot K^2 \dots \\ + \left(-2.76791467211 \cdot 10^{-11} \right) + 4.21052158846 \cdot 10^{-57} \cdot K^{13} + 2.54015555968 \cdot 10^{-24} \cdot K^8 \dots \\ + \left(-3.09445818352 \cdot 10^{-18} \cdot K^6 \right) + 7.02073790107 \cdot 10^{-24} \cdot K^7 + 8.42848842034 \cdot 10^{-16} \cdot K^5 \dots \\ + \left(-5.35593595295 \cdot 10^{-85} \cdot K^{16} \right) + 1.49315970063 \cdot 10^{-68} \cdot K^{14} + 3.31008406154 \cdot 10^{-48} \cdot K^{12} \dots \\ + \left(-5.79935057485 \cdot 10^{-36} \cdot K^{10} \right) + 3.21510620078 \cdot 10^{-33} \cdot K^9 - 7.36777844956 \cdot 10^{-45} \cdot K^{11} \dots \\ + \left(-1.68421991224 \cdot 10^{-75} \cdot K^{15} \right) + 7.12377325693 \cdot 10^{-13} \cdot K^4$$

$$e2 := 1.63399409175 \cdot 10^{-10} \cdot K + 1.29691082699 \cdot 10^{-10} \cdot K^3 + 2.83231250227 \cdot 10^{-10} \cdot K^2 \dots \\ + \left(-2.10525948644 \cdot 10^{-57} \cdot K^{13} \right) - 1.27007698409 \cdot 10^{-24} \cdot K^8 + 1.54722811791 \cdot 10^{-18} \cdot K^6 \dots \\ + \left(-3.51037071474 \cdot 10^{-24} \cdot K^7 \right) - 4.21424153583 \cdot 10^{-16} \cdot K^5 + 2.6779662987 \cdot 10^{-85} \cdot K^{16} \dots \\ + \left(-7.46579974599 \cdot 10^{-69} \cdot K^{14} \right) - 1.65504100072 \cdot 10^{-48} \cdot K^{12} + 2.8996734767 \cdot 10^{-36} \cdot K^{10} \dots \\ + \left(-1.60754774877 \cdot 10^{-33} \cdot K^9 \right) + 3.68388197237 \cdot 10^{-45} \cdot K^{11} + 8.42109427529 \cdot 10^{-76} \cdot K^{15} \dots \\ + \left(-3.56188437929 \cdot 10^{-13} \cdot K^4 \right) + 1.38399002782 \cdot 10^{-11}$$

Stability condition 1 given in Equation (4-9), i.e. the value of characteristic equation at $z=1$, gives the polynomial

$$Q(1) = -8 \cdot 10^{-12} + 2.67978 \cdot 10^{-12} \cdot K$$

It is clear that $Q(1)$ is positive if K_{pwm} is greater than 2.9853.

Stability condition 2 given in Equation (4-10) gives the polynomial below

$$Q(-1) = 15.9829001449 + 1.44969767804 \cdot 10^{-2} \cdot K$$

and if K_{pwm} is greater than -1102.5, $Q(-1)$ takes positive values.

Stability condition 3 requires the following inequality

$$|1.06842730978 \cdot 10^{-6} K_{pwm}| < 1$$

The solution of this inequality yields that

$$K_{pwm} < 935955$$

and

$$K_{pwm} < -935955.$$

Having the coefficients in Jury table, the K_{pwm} ranges which provide the stability conditions 4 to 7 in Section 4.3 has been computed by using a dedicated program written in Matlab. This program is named in the juryk.m and given in Appendix 2. The logic used to find the solution of inequality, for example $|b_0| > |b_5|$, is as follows: First, the roots of $b_0 + b_5 = 0$ and $b_0 - b_5 = 0$ are found. Then the only real ones of these roots are considered since K_{pwm} is real. Later, these real roots are sorted in ascending order and a region between two neighbour roots is selected. If the inequality is verified at a trial point in the selected region, then this region is a solution region of the inequality.

According to the result of juryk.m, the stability condition 4 in Equation (4-12) gives the solution regions for K_{pwm} as follows

$$K_{pwm} < -1.581e+009,$$

$$-554 < K_{pwm} < 554,$$

and

$$K_{pwm} > 1.581e+009$$

The stability condition 5 in Equation (4-13) is satisfied in the following regions for K_{pwm} .

$$-1.572e+009 < K_{pwm} < -1.572e+009,$$

$$-9.36e+005 < K_{pwm} < -1103,$$

$$-1.216 < K_{pwm} < 550.9,$$

and

$$555.1 < K_{pwm} < 9.36e+005$$

The stability condition 6 in Equation (4-14) requires the following regions for K_{pwm} .

$$K_{pwm} < -1.581e+009,$$

$$-1.572e+009 < K_{pwm} < -1.572e+009,$$

$$-9.36e+005 < K_{pwm} < -9.36e+005,$$

$$-1102 < K_{pwm} < -554,$$

$$-1.216 < K_{pwm} < -0.8569,$$

$$-0.1018 < K_{pwm} < 550.9,$$

$$550.9 < K_{pwm} < 554,$$

$$9.36e+005 < K_{pwm} < 9.36e+005,$$

and

$$K_{pwm} > 1.581e+009$$

Finally, the stability condition 7 in Equation (4-15) is satisfied in the following regions for K_{pwm} .

$$K_{pwm} < -1.581e+009,$$

$$-1.567e+009 < K_{pwm} < -9.369e+005,$$

$$-9.352e+005 < K_{pwm} < -1103,$$

$$-1102 < K_{pwm} < -554,$$

$$-553.6 < K_{pwm} < -1.216,$$

$$-0.8569 < K_{pwm} < -0.1018,$$

$$0.4403 < K_{pwm} < 549.7,$$

$$550.9 < K_{pwm} < 550.9,$$

$$554 < K_{pwm} < 9.356e+005,$$

$$9.379e+005 < K_{pwm} < 1.579e+009,$$

and

$$K_{pwm} > 1.581e+009$$

The solution region that satisfies the all stability conditions from 1 to 7 is obtained by taking the intersection of the solution regions of each stability condition. Meanwhile, since stability condition 1 requires $K_{pwm} > 2.9853$, we may interested in only positive regions of solution intervals in the results. Therefore, from the intersection of the all solution intervals, for the stability of closed-loop system K_{pwm} must be in the region

$$2.9853 < K_{pwm} < 549.7.$$

Note that the results of the jury's stability test are consistent with the results of the stability analysis obtained from the root-locus method.

4.3.2 Stability Analysis for the Chopping Period Control

In order to make the stability analysis for the chopping period (T) by jury test, the characteristic equation including T as a varying parameter must be obtained. This is accomplished in Mathcad by the file chrceq_t.mcd presented in Appendix 2.

From the file chrceq_t.mcd, characteristic polynomial with respect to T is as follows

$$\begin{aligned}
& z^6 + (21.8251519T - 4.0) \cdot z^5 + (6.0 + 1927.27816T + 49891.4212T^2) \cdot z^4 \dots \\
& + (-5912.7854T - 49792.5822T^2 - 4.0 + 4285.49167T^3) \cdot z^3 \dots \\
& + (5956.43571T + 736568.879T^4 + 1.0 + 324090.307T^3 - 38303.9972T^2) \cdot z^2 \dots \\
& + (-1992.75362T + 1473137.76T^4 + 26420.0562T^2 - 4285.49167T^3) \cdot z \dots \\
& + (-324090.307T^3 + 11785.102T^2 + 736568.879T^4)
\end{aligned} \tag{4-16}$$

As it is clearly observed from Equation (4-16), the characteristic equation of the system is not in the proper form for the stability analysis that would be carried out by root-locus technique.

After the characteristic equation is rearranged in the form of Equation (4-4) the polynomial coefficients a_k 's ($k=0,1,2,\dots,6$) are obtained as follows;

$$\begin{aligned}
a_0 &= -324090.307 \cdot T^3 + 11785.102 \cdot T^2 + 736568.879 \cdot T^4 \\
a_1 &= -1992.75362 \cdot T + 1473137.76 \cdot T^4 + 26420.0562 \cdot T^2 - 4285.49167 \cdot T^3 \\
a_2 &= 5956.43571 \cdot T + 736568.879 \cdot T^4 + 1.0 + 324090.307 \cdot T^3 - 38303.9972 \cdot T^2 \\
a_3 &= -5912.7854 \cdot T - 49792.5822 \cdot T^2 - 4.0 + 4285.49167 \cdot T^3 \\
a_4 &= 5.0 + 1927.27816 \cdot T + 49891.4212 \cdot T^2 \\
a_5 &= 21.8251519 \cdot T - 4.0 \\
a_6 &= 1
\end{aligned}$$

By using the coefficients a_k 's ($k=0,1,2,\dots,6$) given above, the other coefficients in Jury table are obtained via Mathcad again. They are given in below:

The b_k 's ($k=0,1,2,\dots,5$) defined in Equation (4-5) are

$$\begin{aligned}
b_0 &:= 542533714304 \cdot T^8 - 477429668588 \cdot T^7 + 122395605947 \cdot T^6 - 7638874697.4T^5 \dots \\
&+ 138888630.862T^4 - 1.
\end{aligned}$$

$$\begin{aligned} b1 := & 1.0850674286110^{12} \cdot T^8 - 480586228381 \cdot T^7 + 38210156286.0 T^6 - 10080789352.8 T^5 \dots \\ & + (957195191.423 T^4 - 23484804.8548 T^3 - 21.8251519402 T) + 4. \end{aligned}$$

$$\begin{aligned} b2 := & 542533714304 \cdot T^8 - 124567519956 \cdot T^6 + 20620716741.4 T^5 - 2381103028.19 T^4 \dots \\ & + 69873112.6142 T^3 - 38106.3191523 T^2 - 6. - 1927.27816737 T \end{aligned}$$

$$\begin{aligned} b3 := & 3156559792.32 T^7 - 38064552791.6 T^6 + 11832624482.0 T^5 + 1326519500.7 T^4 \dots \\ & + (-68390703.8981 T^3) + 2652.1739131 T^2 + 5912.78541375 T + 4. \end{aligned}$$

$$\begin{aligned} b4 := & -32953836.8513 T^4 - 14749752901.0 T^5 + 36748468230.2 T^6 + 20444537.7758 T^3 \dots \\ & + 109014.609631 T^2 - 5956.43571763 T - 1. \end{aligned}$$

$$\begin{aligned} b5 := & 16075727.7103 T^5 - 11492733.4698 T^4 + 1557858.36302 T^3 - 73560.4643914 T^2 \dots \\ & + 1992.75362319 T \end{aligned}$$

The coefficients c_k 's ($k=0,1,\dots,4$) in Equation (4-6) are

$$\begin{aligned} c0 := & -11897774977.9 T^4 + 1.9106796379 \cdot 10^{16} \cdot T^8 - 4.42660544274 \cdot 10^{12} \cdot T^6 \dots \\ & + 3.91280372286 \cdot 10^{13} \cdot T^7 + 290275691199 \cdot T^5 + 2.94342831156 \cdot 10^{23} \cdot T^{16} \dots \\ & + (-5.18043382836 \cdot 10^{23} \cdot T^{15}) + 3.60746573866 \cdot 10^{23} \cdot T^{14} - 1.25159281293 \cdot 10^{23} \cdot T^{13} \dots \\ & + 2.2425438715 \cdot 10^{22} \cdot T^{12} - 2.00254850069 \cdot 10^{21} \cdot T^{11} + 9.23508644806 \cdot 10^{19} \cdot T^{10} \dots \\ & + ((-2.12153618799 \cdot 10^{18} \cdot T^9) + 1 + 293175763.879 T^3) - 3971067.00274 T^2 \end{aligned}$$

$$\begin{aligned} c1 := & -23855611622.2 T^4 + 3.37326386037 \cdot 10^{17} \cdot T^8 - 2.91444839979 \cdot 10^{12} \cdot T^6 \dots \\ & + (-4.13955359903 \cdot 10^{15} \cdot T^7) + 2014.57877513 T + 1.30780362222 \cdot 10^{12} \cdot T^5 \dots \\ & + (-630354772.611 T^3) + 11796148.3932 T^2 + 5.88685662314 \cdot 10^{23} \cdot T^{16} \dots \\ & + ((-7.78777614364 \cdot 10^{23} \cdot T^{15}) + 3.82983907176 \cdot 10^{23} \cdot T^{14}) - 9.08221671009 \cdot 10^{22} \cdot T^{13} \dots \\ & + (1.38307753237 \cdot 10^{22} \cdot T^{12} - 2.06280032036 \cdot 10^{21} \cdot T^{11}) + 2.11341124433 \cdot 10^{20} \cdot T^{10} \dots \\ & + (-1.18126840516 \cdot 10^{19} \cdot T^9) - 4. \end{aligned}$$

$$\begin{aligned}
c2 := & 128863378101 \cdot T^4 - 8.7310291952 \cdot 10^{17} \cdot T^8 + 1.89298239425 \cdot 10^{14} \cdot T^6 \dots \\
& + 7.85634290327 \cdot 10^{15} \cdot T^7 - 6043.73632539 T - 7.85298492196 \cdot 10^{12} \cdot T^5 \dots \\
& + (353557565.641 \cdot T^3 - 11450376.3797 \cdot T^2) + 2.94342831156 \cdot 10^{23} \cdot T^{16} \dots \\
& + (-2.59021691418 \cdot 10^{23} \cdot T^{15}) - 1.17833657445 \cdot 10^{21} \cdot T^{14} + 6.65153167521 \cdot 10^{22} \cdot T^{13} \dots \\
& + (-2.63079866955 \cdot 10^{22} \cdot T^{12}) + 6. + 4.65080673876 \cdot 10^{21} \cdot T^{11} \dots \\
& + (-5.00269403856 \cdot 10^{20} \cdot T^{10}) + 2.97964360343 \cdot 10^{19} \cdot T^9
\end{aligned}$$

$$\begin{aligned}
c3 := & -139880511826 \cdot T^4 + 6.34394295953 \cdot 10^{17} \cdot T^8 - 3.69777451831 \cdot 10^{14} \cdot T^6 \dots \\
& + (-2.51899598521 \cdot 10^{15} \cdot T^7) + 6043.73632539 T + 1.070099185451 \cdot 10^{13} \cdot T^5 \dots \\
& + 11902882.6303 T^3 + 3396575.59066 T^2 + 1.71254010855 \cdot 10^{21} \cdot T^{15} \dots \\
& + ((-2.21583385049 \cdot 10^{22} \cdot T^{14}) + 2.49703719587 \cdot 10^{22} \cdot T^{13}) - 9.60637580654 \cdot 10^{21} \cdot T^{12} \dots \\
& + 1.07020329752 \cdot 10^{21} \cdot T^{11} + 9.76154733966 \cdot 10^{19} \cdot T^{10} - 1.63902354394 \cdot 10^{19} \cdot T^9 - 4.
\end{aligned}$$

$$\begin{aligned}
c4 := & 1. + 46773466599.7 \cdot T^4 - 1.13712816468 \cdot 10^{17} \cdot T^8 + 1.87568814695 \cdot 10^{14} \cdot T^6 \dots \\
& + (-1.30056932254 \cdot 10^{15} \cdot T^7) - 2014.57877513 T - 4.44021504467 \cdot 10^{12} \cdot T^5 \dots \\
& + (-28281439.54 T^3) + 228719.39854 T^2 + 1.99372829639 \cdot 10^{22} \cdot T^{14} \dots \\
& + (-2.55644904832 \cdot 10^{22} \cdot T^{13}) + 1.15421382725 \cdot 10^{22} \cdot T^{12} - 2.06702478446 \cdot 10^{21} \cdot T^{11} \dots \\
& + 1.0547006755 \cdot 10^{20} \cdot T^{10} + 4.21916593595 \cdot 10^{17} \cdot T^9
\end{aligned}$$

and the coefficients d_k 's ($k=0,1,2,3$) in Equation (4-7) are

$$\begin{aligned}
d0 := & 1.54857677182 \cdot 10^{13} \cdot T^4 - 2.18276699881 \cdot 10^{21} \cdot T^8 + 1.39975596836 \cdot 10^{17} \cdot T^6 \dots \\
& + (-3.84649470837 \cdot 10^{18} \cdot T^7) + 4029.15755026 T - 2.11758552863 \cdot 10^{15} \cdot T^5 \dots \\
& + 1564460898.36 T^3 - 12458100.4438 T^2 + 8.12275445923 \cdot 10^{32} \cdot T^{15} \dots \\
& + 2.97754471886 \cdot 10^{31} \cdot T^{14} - 4.23153926222 \cdot 10^{29} \cdot T^{13} - 3.85166528128 \cdot 10^{28} \cdot T^{12} \dots \\
& + 3.28600447634 \cdot 10^{46} \cdot T^{26} - 6.48270154808 \cdot 10^{45} \cdot T^{25} + 2.01583471535 \cdot 10^{42} \cdot T^{22} \dots \\
& + (-4.9260040731 \cdot 10^{40} \cdot T^{21}) + 8.29903823211 \cdot 10^{44} \cdot T^{24} - 6.13921150044 \cdot 10^{43} \cdot T^{23} \dots \\
& + 1.80570805542 \cdot 10^{27} \cdot T^{11} - 3.72210830478 \cdot 10^{25} \cdot T^{10} + 4.16296032777 \cdot 10^{23} \cdot T^9 \dots \\
& + 1.1040592039 \cdot 10^{40} \cdot T^{20} - 9.84594662151 \cdot 10^{38} \cdot T^{19} + 2.14663598276 \cdot 10^{37} \cdot T^{18} \dots \\
& + 1.21070492634 \cdot 10^{36} \cdot T^{17} + 8.66377022529 \cdot 10^{46} \cdot T^{32} - 3.04964711931 \cdot 10^{47} \cdot T^{31} \dots \\
& + 4.80735282263 \cdot 10^{47} \cdot T^{30} - 4.47444225347 \cdot 10^{47} \cdot T^{29} + 2.72618004495 \cdot 10^{47} \cdot T^{28} \dots \\
& + (-1.13695762724 \cdot 10^{47} \cdot T^{27}) - 7.32272035205 \cdot 10^{34} \cdot T^{16}
\end{aligned}$$

$$\begin{aligned}
d1 := & -4.64839179739 \cdot 10^{13} \cdot T^4 + 6.79133187456 \cdot 10^{21} \cdot T^8 - 3.06846918824 \cdot 10^{17} \cdot T^6 \dots \\
& + 4.96347233749 \cdot 10^{18} \cdot T^7 - 12087.4726508 T + 5.43809251515 \cdot 10^{15} \cdot T^5 \dots \\
& + (-4467764411.47 \cdot T^3) + 37374301.3313 T^2 + 2.97004266133 \cdot 10^{33} \cdot T^{15} \dots \\
& + (-2.43167806675 \cdot 10^{32} \cdot T^{14}) + 5.17972099564 \cdot 10^{30} \cdot T^{13} + 1.81911438013 \cdot 10^{28} \cdot T^{12} \dots \\
& + 2.87791308246 \cdot 10^{46} \cdot T^{26} - 6.06611238384 \cdot 10^{45} \cdot T^{25} + 1.36037477702 \cdot 10^{43} \cdot T^{22} \dots \\
& + (-6.52187894985 \cdot 10^{41} \cdot T^{21}) + 1.05994914035 \cdot 10^{45} \cdot T^{24} - 1.46070401847 \cdot 10^{44} \cdot T^{23} \dots \\
& + (-3.54139543096 \cdot 10^{27} \cdot T^{11}) + 8.93608565568 \cdot 10^{25} \cdot T^{10} - 1.13094909635 \cdot 10^{24} \cdot T^9 \dots \\
& + 2.82806370526 \cdot 10^{39} \cdot T^{20} + 7.77506260959 \cdot 10^{38} \cdot T^{19} + 2.1879747343 \cdot 10^{37} \cdot T^{18} \dots \\
& + (-4.13791050121 \cdot 10^{36} \cdot T^{17}) + 1.73275404506 \cdot 10^{47} \cdot T^{32} - 5.34192319785 \cdot 10^{47} \cdot T^{31} \dots \\
& + 7.28535493111 \cdot 10^{47} \cdot T^{30} - 5.79790106626 \cdot 10^{47} \cdot T^{29} + 3.0043928263 \cdot 10^{47} \cdot T^{28} \dots \\
& + (-1.08197263938 \cdot 10^{47} \cdot T^{27}) + 1.11210013867 \cdot 10^{35} \cdot T^{16}
\end{aligned}$$

$$\begin{aligned}
d2 := & 4.65065745497 \cdot 10^{13} \cdot T^4 - 7.00053715594 \cdot 10^{21} \cdot T^8 + 1.98700494092 \cdot 10^{17} \cdot T^6 \dots \\
& + 1.04512379495 \cdot 10^{18} \cdot T^7 + 12087.4726508 T - 4.52309034055 \cdot 10^{15} \cdot T^5 \dots \\
& + 4243459631.02 T^3 - 37374301.3313 T^2 - 8.86027252851 \cdot 10^{33} \cdot T^{15} \dots \\
& + 3.93390145177 \cdot 10^{32} \cdot T^{14} - 8.68981065088 \cdot 10^{30} \cdot T^{13} + 6.95802669651 \cdot 10^{28} \cdot T^{12} \dots \\
& + (-1.81805422073 \cdot 10^{46} \cdot T^{26}) + 5.19958791252 \cdot 10^{45} \cdot T^{25} - 8.23845987475 \cdot 10^{42} \cdot T^{22} \dots \\
& + 3.96344021807 \cdot 10^{41} \cdot T^{21} - 9.30701123164 \cdot 10^{44} \cdot T^{24} + 1.08449992598 \cdot 10^{44} \cdot T^{23} \dots \\
& + 1.78425806707 \cdot 10^{27} \cdot T^{11} - 6.77755436997 \cdot 10^{25} \cdot T^{10} + 1.01238931792 \cdot 10^{24} \cdot T^9 \dots \\
& + (-1.69670020227 \cdot 10^{40} \cdot T^{20}) + 1.45883117036 \cdot 10^{39} \cdot T^{19} - 1.15788095854 \cdot 10^{38} \cdot T^{18} \dots \\
& + 4.29771463966 \cdot 10^{36} \cdot T^{17} + 8.66377022529 \cdot 10^{46} \cdot T^{32} - 2.28723533948 \cdot 10^{47} \cdot T^{31} \dots \\
& + 2.34152409895 \cdot 10^{47} \cdot T^{30} - 9.74032755626 \cdot 10^{46} \cdot T^{29} - 1.36023424025 \cdot 10^{46} \cdot T^{28} \dots \\
& + 3.49839714101 \cdot 10^{46} \cdot T^{27} + 2.19592925721 \cdot 10^{34} \cdot T^{16}
\end{aligned}$$

$$\begin{aligned}
d3 := & -1.55084242939 \cdot 10^{13} \cdot T^4 + 2.39461457752 \cdot 10^{21} \cdot T^8 - 3.1829717828 \cdot 10^{16} \cdot T^6 \dots \\
& + (-2.18631868333 \cdot 10^{18} \cdot T^7) - 4029.15755026 T + 1.20258928953 \cdot 10^{15} \cdot T^5 \dots \\
& + (-1340156117.99 T^3) + 12458100.4438 T^2 + 5.1551830109 \cdot 10^{33} \cdot T^{15} \dots \\
& + (-1.81967867983 \cdot 10^{32} \cdot T^{14}) + 3.97494551973 \cdot 10^{30} \cdot T^{13} - 4.97969525257 \cdot 10^{28} \cdot T^{12} \dots \\
& + (-1.63066252636 \cdot 10^{46} \cdot T^{26}) + 4.45402066274 \cdot 10^{45} \cdot T^{25} - 7.00306340599 \cdot 10^{42} \cdot T^{22} \dots \\
& + 2.60482899787 \cdot 10^{41} \cdot T^{21} - 8.01849610122 \cdot 10^{44} \cdot T^{24} + 9.44961651775 \cdot 10^{43} \cdot T^{23} \dots \\
& + (-4.54008474417 \cdot 10^{25} \cdot T^{11}) + 1.56402088463 \cdot 10^{25} \cdot T^{10} - 2.97872228769 \cdot 10^{23} \cdot T^9 \dots \\
& + 5.33014935165 \cdot 10^{39} \cdot T^{20} - 1.27362251677 \cdot 10^{39} \cdot T^{19} + 6.99296349504 \cdot 10^{37} \cdot T^{18} \dots \\
& + (-1.24095822617 \cdot 10^{36} \cdot T^{17}) + 5.04073904019 \cdot 10^{44} \cdot T^{31} - 1.91461107867 \cdot 10^{46} \cdot T^{30} \dots \\
& + 5.00227822666 \cdot 10^{46} \cdot T^{29} - 5.8310591552 \cdot 10^{46} \cdot T^{28} + 3.89183508634 \cdot 10^{46} \cdot T^{27} \dots \\
& + (-6.33298964556 \cdot 10^{34} \cdot T^{16})
\end{aligned}$$

The coefficients e_0 , e_1 , e_2 in Jury table could not have been calculated by means of Mathcad because Mathcad could not compute the results from such a large input

arguments and gave error. In order to overcome this problem, d_k 's are transferred to the Matlab then e_k 's are computed by using a dedicated program, namely juryt.m, written in Matlab.

After having the all coefficients defined in Jury table, the stability conditions given in Equations (4-9) to (4-15) are checked in order.

Characteristic polynomial at $z=1$ gives the polynomial below

$$Q(1) = 1 \cdot 10^{-7} \cdot T^2 + 2946275.51816 \cdot T^4$$

and the characteristic polynomial at $z=-1$ is

$$Q(-1) = 16 + 11781.9205236198 \cdot T + 99585.1644071 \cdot T^2 - 8570.98332554 \cdot T^3 + 2946275.518156 \cdot T^4$$

If it is taken into account that negative T is meaningless, it is seen that stability condition 1 and 2 are provided for all positive values of T .

The values of T which provide the conditions 3 to 7 are found by the file juryt.m. The file juryt.m also uses a similar logic with the juryk.m mentioned in Section 4.4.

The stability condition 3 gives the solution regions for T as follows

$$-0.008297 < T < 0.01096,$$

$$0.03731 < T < 0.04214,$$

and

$$0.399976 < T < 0.400023$$

The stability condition 4 requires the solution regions for T given below

$$\begin{aligned}
 &T < -0.02301, \\
 &-0.0004928 < T < 0.0005114, \\
 &0.05029 < T < 0.3951,
 \end{aligned}$$

and

$$T > 0.4046$$

The stability condition 5 is satisfied with the following regions for T

$$\begin{aligned}
 &T < -0.04027, \\
 &-0.008297 < T < -0.001008, \\
 &0 < T < 0.0004969, \\
 &0.0005165 < T < 0.01096, \\
 &0.03731 < T < 0.04214, \\
 &0.399976 < T < 0.400023,
 \end{aligned}$$

and

$$T > 0.544$$

The stability condition number 6 requires the following solution regions

$$\begin{aligned}
 &T < -0.1076, \\
 &-0.08159 < T < -0.04589, \\
 &-0.02598 < T < -0.008538, \\
 &-0.008237 < T < -0.001018, \\
 &-0.0004928 < T < 0, \\
 &0 < T < 0.0004969, \\
 &0.0004969 < T < 0.0005114, \\
 &0.008072 < T < 0.009256,
 \end{aligned}$$

and

$$T > 1.812$$

Finally, the stability condition number 7 gives the solution regions

$$\begin{aligned}
 &T < -0.1689, \\
 &-0.1689 < T < -0.1626, \\
 &-0.01393 < T < -0.01136, \\
 &-0.001882 < T < -0.0006432, \\
 &-0.0006432 < T < -0.0004678, \\
 &-0.0004678 < T < -0.0004516, \\
 &-0.0004516 < T < 0, \\
 &0 < T < 0.0006084, \\
 &0.0006084 < T < 0.002766, \\
 &0.002766 < T < 0.008429, \\
 &0.008429 < T < 0.01261, \\
 &0.01261 < T < 0.06025, \\
 &0.06025 < T < 0.1179, \\
 &0.1179 < T < 1.589, \\
 &\text{and} \\
 &1.888 < T < 2.325
 \end{aligned}$$

Since negative period is not practical case, we may not take into account negative value of period in the results above. Thus stability conditions 3 and 4 give the solution region

$$0 < T < 0.0005114$$

or in terms of frequency (Hz)

$$1955.4 < f < \infty$$

When this solution is combined with the result of stability condition 5, it is limited to

$$0 < T < 0.0004969$$

or in terms of frequency (Hz)

$$2012.47 < f < \infty$$

This solution region is not changed by the result of stability condition 6 and 7. As a consequence it is decided that chopping frequency must be kept in the range given below

$$2012.47 \text{ Hz} < f < \infty.$$

In order to control the result obtained from the stability analysis, the system will be analyzed without any limit on duty cycle for the frequency of 2010 Hz and 2020 Hz one of which is in stable and the other one is in the unstable region.

Figure 4 . 5 and Figure 4 . 6 give the speed and current responses respectively for the chopping frequency of 2010 Hz. As it is seen from these figures, both the speed and current responses are increasing in time and this shows the instability.

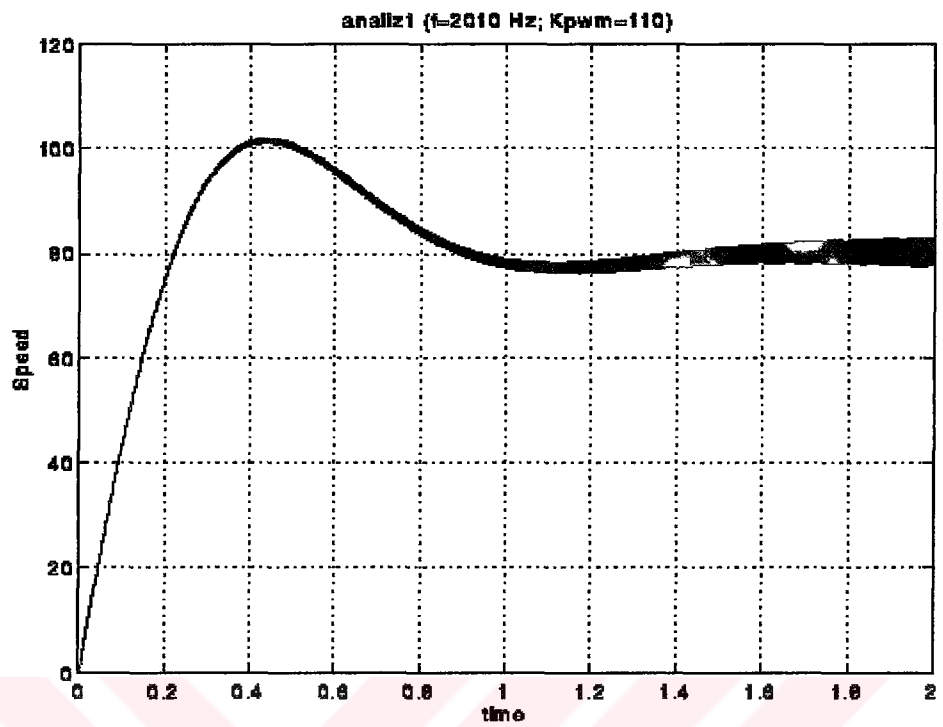


Figure 4 . 5 Speed of the motor showing unstability

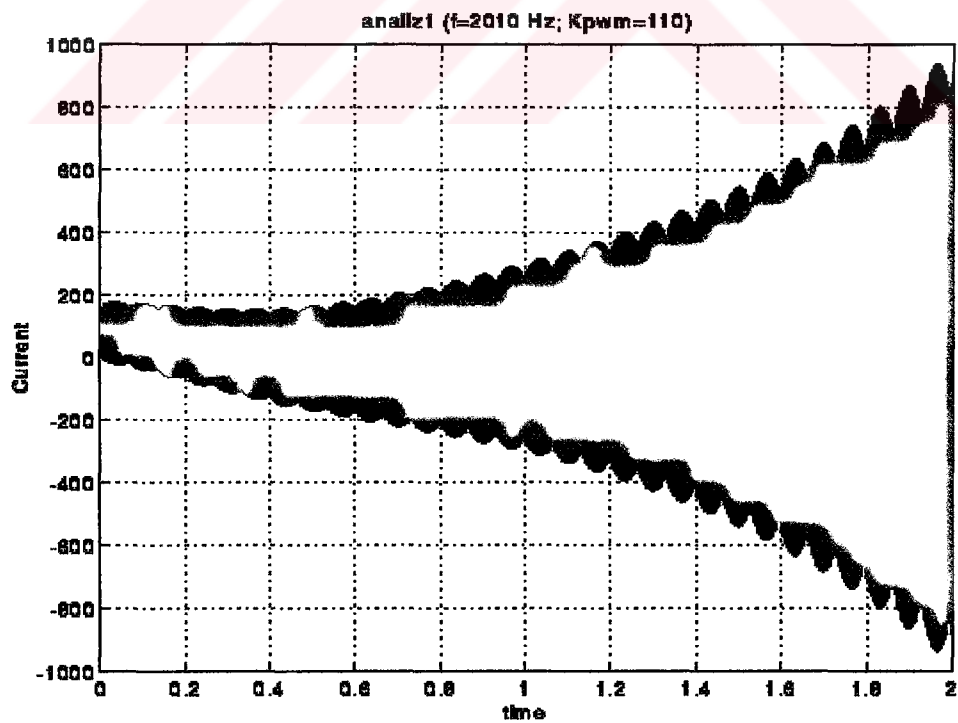


Figure 4 . 6 Armature current denoting unstability

Figure 4 . 7 and Figure 4 . 8 show the speed and current responses for the chopping frequency of 2020 Hz. In these figures both the speed and current response settle down and this denotes the stable operation for 2020 Hz.

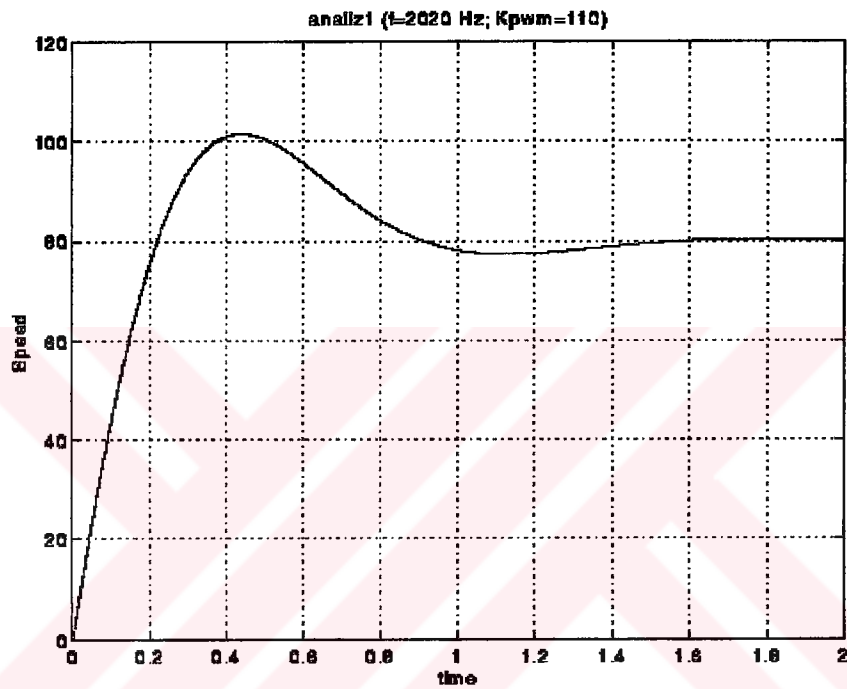


Figure 4 . 7 Speed of the motor showing stability

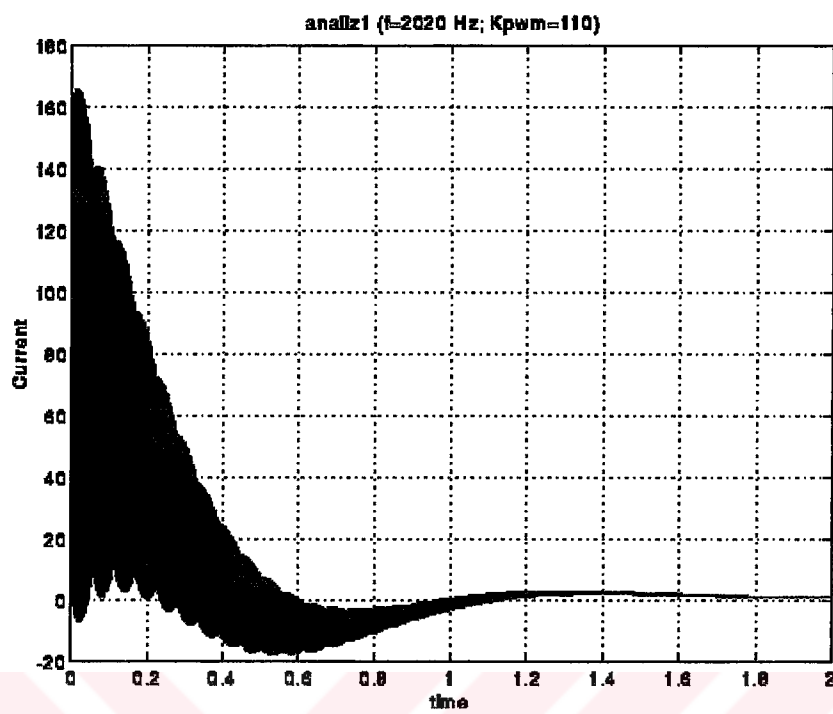


Figure 4 . 8 Armature current denoting stability

CHAPTER FIVE

REAL TIME SIMULATION OF THE SYSTEM

5.1 Introduction

Real-time simulation is a type of dynamic simulation of nonlinear systems. It can be used to analyze the system in detail after designing the controller parameters using the linearized model of the nonlinear system. Therefore, this detailed simulation can display the discrepancies between the linearized model and real system responses. The model given in Chapter 2 is developed to design the controller parameters by including the variation of PWM waveform in time into the model. The real time simulation mentioned in this chapter is carried out with the help of the software named Simulink (MathWorks, 1993) which is a program for simulating dynamic systems. This program uses the block diagrams to represent the DC motor drive. The numeric integration is performed by using the fifth order Runge-Kutta method in this study.

5.2 Real-time Simulation of the Closed-Loop Control of DC Drive

In this section, the closed-loop control of a separately excited DC motor given in Figure 2.1 will be simulated in z-domain with the help of Simulink. The Simulink model of the system, named classc, is given in Figure 5 . 1. The linear gains of current and speed transducers have been chosen unity. The transfer functions of the speed and current controllers in z-domain are given in Equation (2-29) and (2-38). These functions obtained as a result of applying trapezoidal rule in integration will be

employed to represent the PI controllers in dedicated blocks in Figure 5 . 1. The reference speed and load torque are defined as the step functions in their own blocks. These steps could be applied at any time during the simulation of the system. The step change of these inputs has been specified after the beginning of time at zero value. These two blocks have been identified by Step Fcn and Step Fcn1 in Figure 5 . 1.

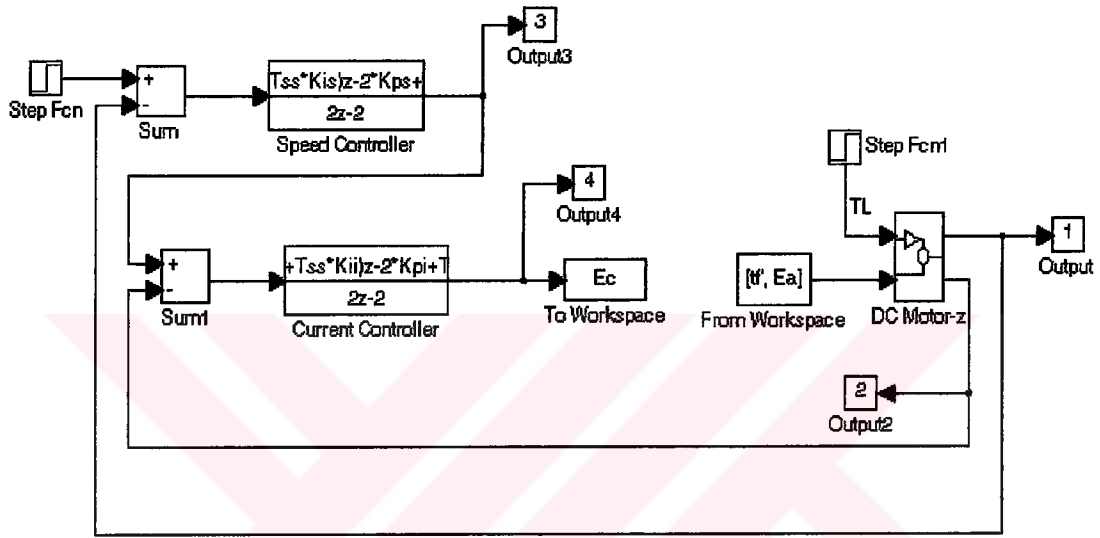


Figure 5 . 1 Block diagram representation of the real-time simulation model

Another block in Figure 5 . 1 is dedicated for the transfer function of dc motor having 2 inputs and 2 outputs. This transfer function in z-domain is obtained in two steps. The first step computes the transfer function $H(s)$ in s-domain from the state space model of the machine described in Section 2.2. Rewriting this state space forms;

$$\frac{d}{dt} \begin{bmatrix} i_a(t) \\ w(t) \end{bmatrix} = \begin{bmatrix} -R_a / L_a & -K_a \phi / L_a \\ K \phi / J & -B_v / J \end{bmatrix} \cdot \begin{bmatrix} i_a(t) \\ w(t) \end{bmatrix} + \begin{bmatrix} 0 & 1 / L_a \\ -1 / J & 0 \end{bmatrix} \cdot \begin{bmatrix} T_L(t) \\ V_a(t) \end{bmatrix}$$

or in the compact form

$$\frac{d}{dt} x_m(t) = A_m \cdot x_m(t) + B_{mm} \cdot u_m(t)$$

another function, named `c2dm`, of the same toolbox is used in order to obtain discrete transfer function from that value of it in s-domain.

Finally, the PWM waveform has been generated by comparing the output of current controller E_c to the sawtooth waveform. This comparison is performed by receiving the value of E_c from the simulation program running in Simulink package. The computation of the duty cycle depending on this value and peak value of sawtooth wave is made in a dedicated program written in Matlab. After receiving the duty cycle as a result of this computation, the PWM waveform has been generated and the data is transferred to the Simulink in order to continue to the simulation of the system. The detail of the estimation of PWM waveform is given in Section 5.2.1 below. This communication between Simulink and dedicated program is carried out via the blocks (To Workspace and From Workspace) given in Figure 5.1 once in every sampling period.

5.2.1 Estimation of PWM Waveform Using z-transformation

Let the number of samples in one period of the PWM signal be n which is integer. The number of samples during the high level of PWM waveform is the nearest integer to the value of t_{on}/T_s ratio where T_s is the sampling period used for the estimation of the PWM waveform.

If it is assumed that the PWM signal is high at the beginning of a period, then the z-transform of the PWM signal over one period whose amplitude is K_{pwm} Volts can be written by using the definition of z-transform (Phillips & Nagle, 1984) as given below;

$$V_a(z) = K_{pwm} \cdot \left\{ 1 \cdot z^0 + 1 \cdot z^{-1} + 1 \cdot z^{-2} + \dots + 1 \cdot z^{-(nos-1)} + 0 \cdot z^{-nos} + \dots + 0 \cdot z^{-(n-1)} \right\} \quad (5-3)$$

where the variable nos is the nearest integer to the value of t_{on}/T_s .

If Equation (5-3) is multiplied and divided by z^{n-1} , the following equation is obtained

$$V_a(z) = K_{pwm} \cdot \left\{ \frac{1 \cdot z^{n-1} + 1 \cdot z^{n-2} + 1 \cdot z^{n-3} + \dots + 1 \cdot z^{n-nos} + 0 \cdot z^{n-nos-1} + \dots + 0 \cdot z^0}{z^{n-1}} \right\} \quad (5-4)$$

Both Equation (5-3) and Equation (5-4) define the z-transform of the PWM waveform over one period. After finding the z-transform of the PWM waveform in the program `zzkare` given in Appendix 3, the PWM waveform has been generated by using the inverse z-transform of Equation (5-4), which is the advantage over Equation (5-3), in the program `classcm` written in Matlab.

5.3 Results of the Real-time Simulation

In this section, the simulation results for the controller gains of $K_{initial}$, K_{opt1} and K_{opt2} will be given in order to compare with the results of the analysis made in Chapter 3 by using the linear model.

Figure 5 . 3 to Figure 5 . 6 show the variation of rotor speed, armature current, reference current and duty cycle in time for $K_{initial}$. When these figures are compared with the Figure 3.15 to Figure 3.18 given in Section 3.5.2, the rise time, peak value and settling time of figures are almost the identical within the error in the range of 2%.

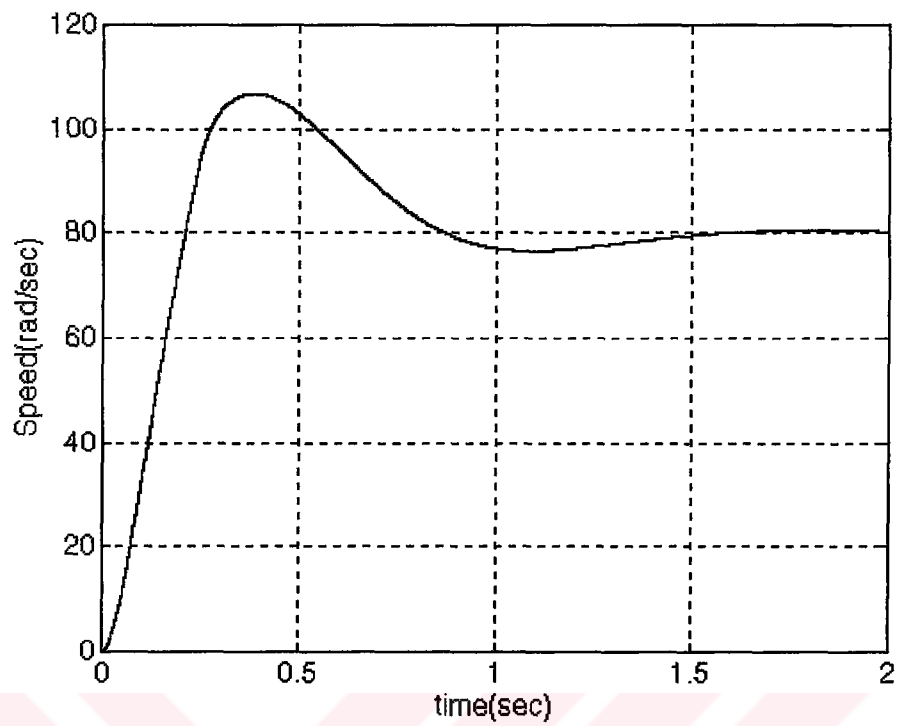


Figure 5 . 3 Rotor speed for $K_{initial}$

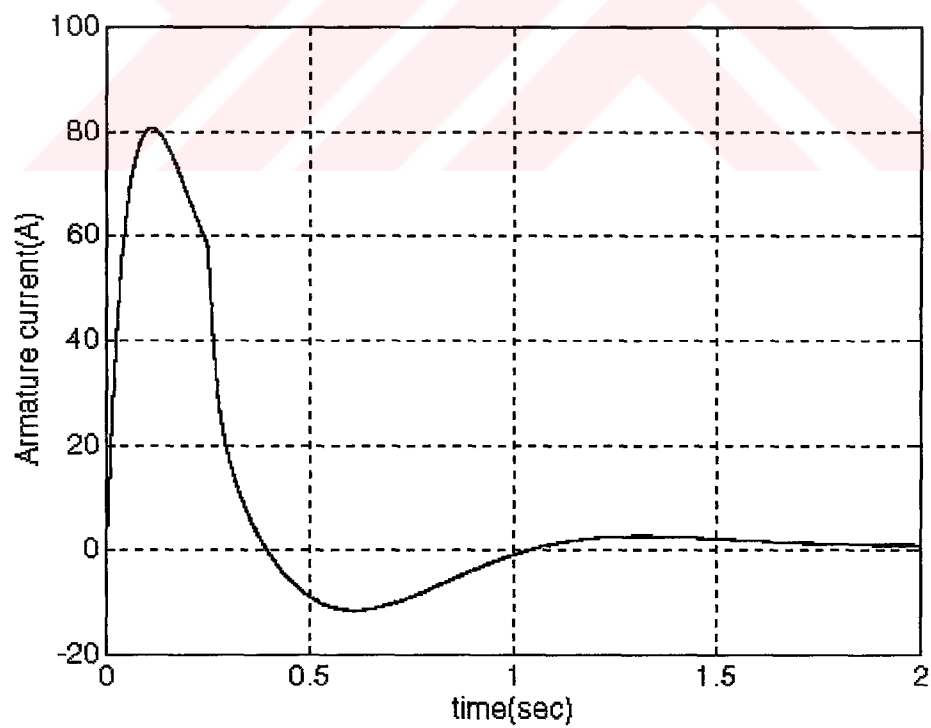


Figure 5 . 4 The armature current for $K_{initial}$

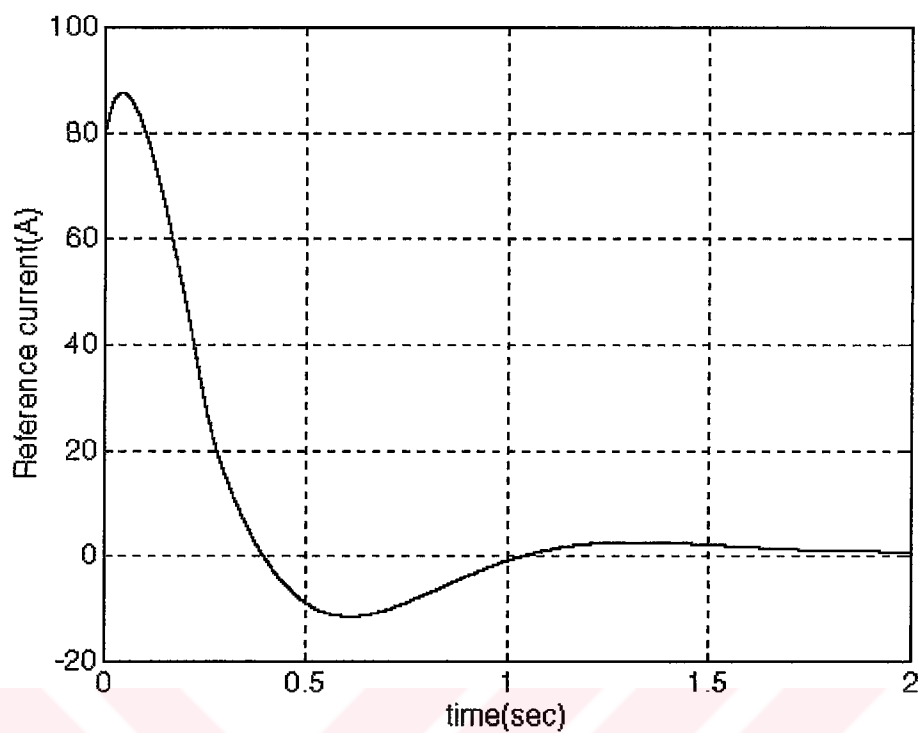


Figure 5 . 5 Reference current for $K_{initial}$

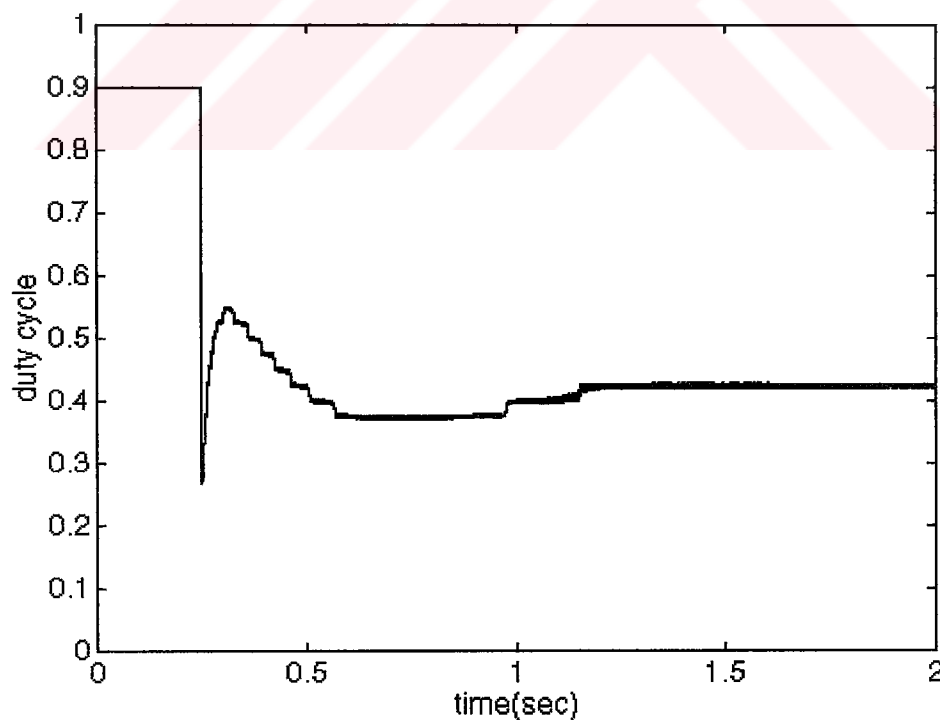


Figure 5 . 6 Variation of the duty cycle

Figure 5 . 7 to Figure 5 . 10 present the variation of rotor speed, armature current, reference current and duty cycle in time for K_{opt1} .

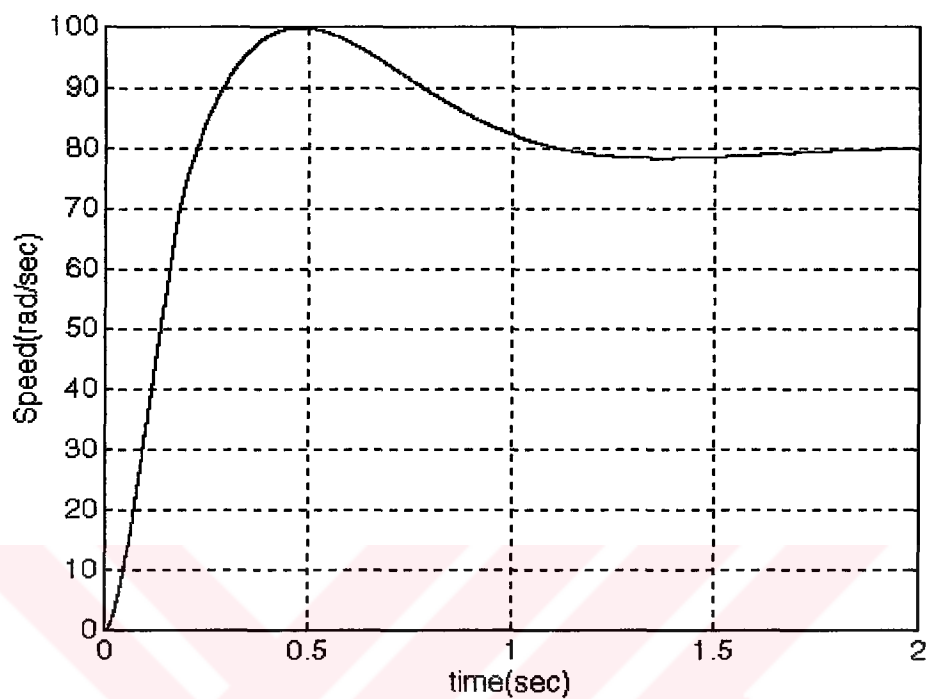


Figure 5 . 7 Rotor speed for K_{opt1}

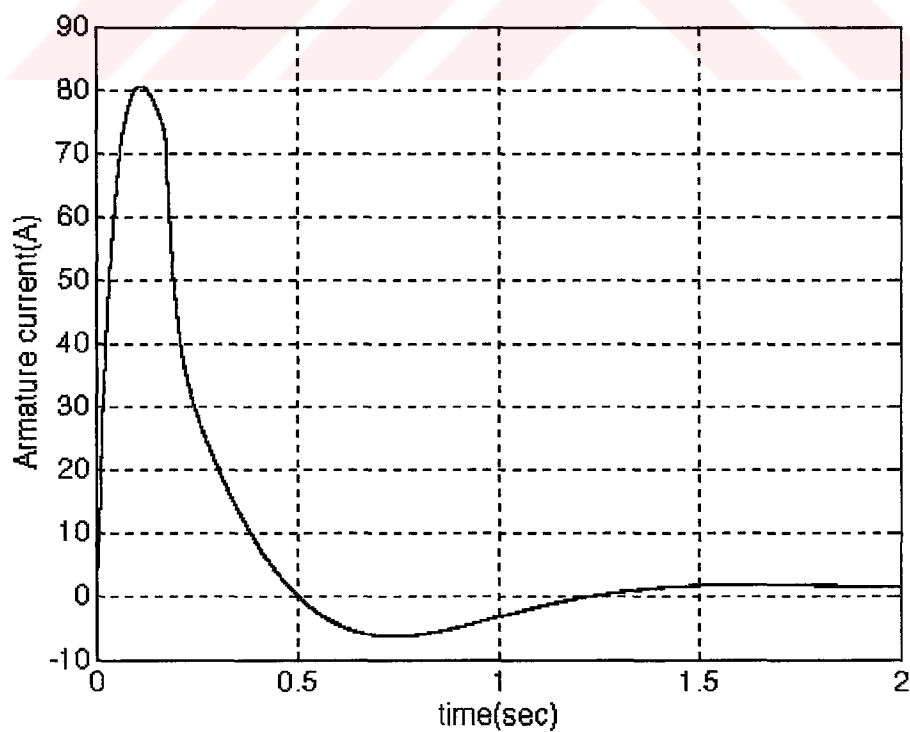


Figure 5 . 8 The armature current for K_{opt1}

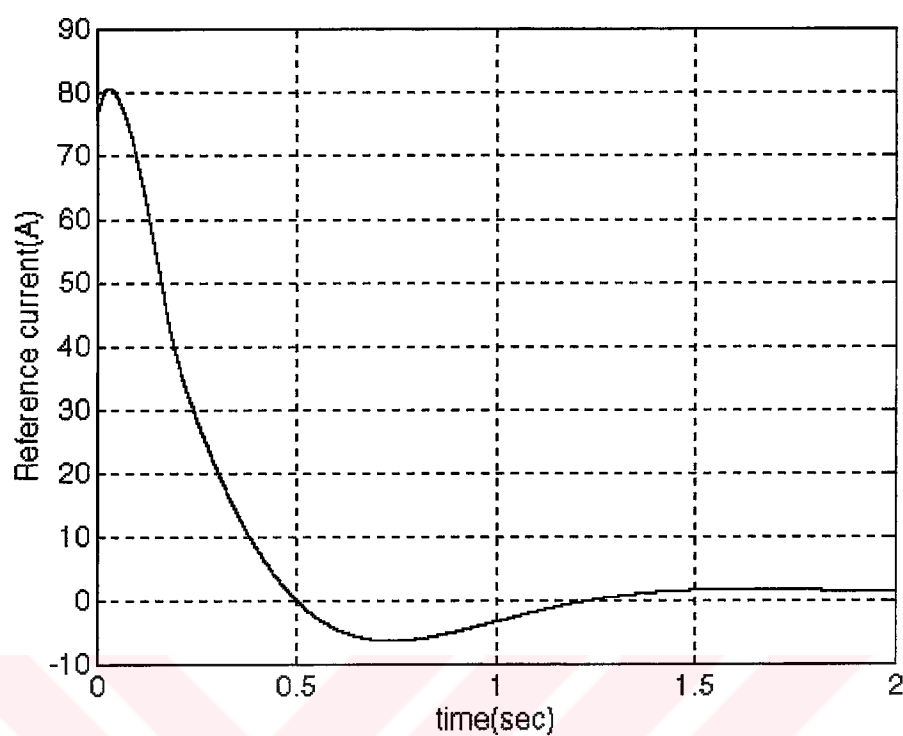


Figure 5 . 9 Reference current for K_{opt1}

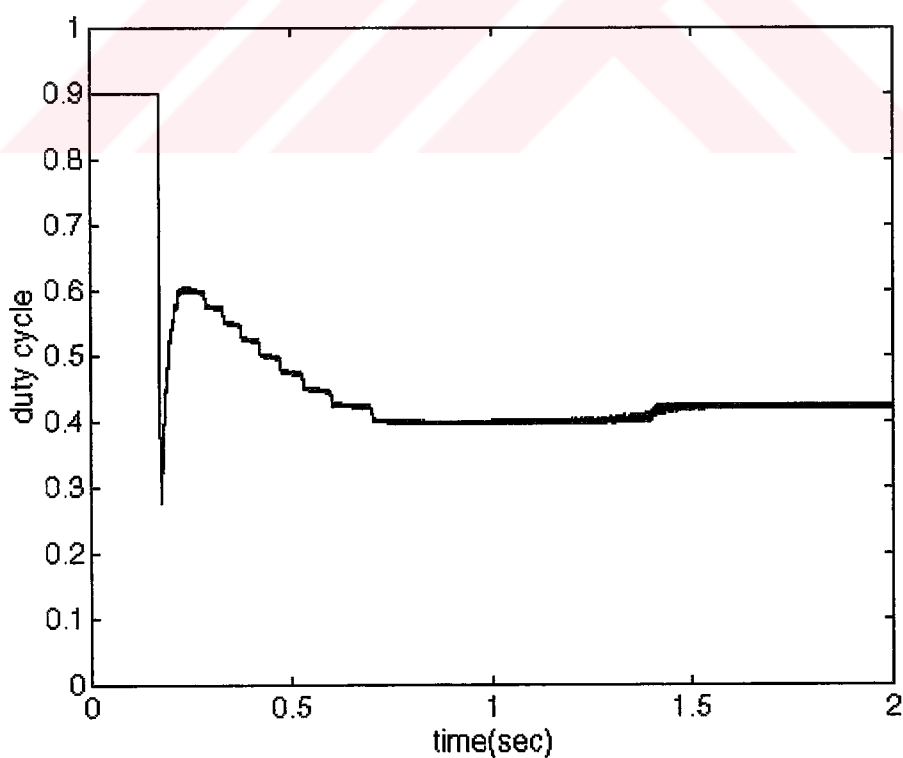


Figure 5 . 10 Variation of the duty cycle

Figure 5 . 11 to Figure 5 . 14 show the variation of rotor speed, armature current, reference current and duty cycle in time for K_{opt2} .

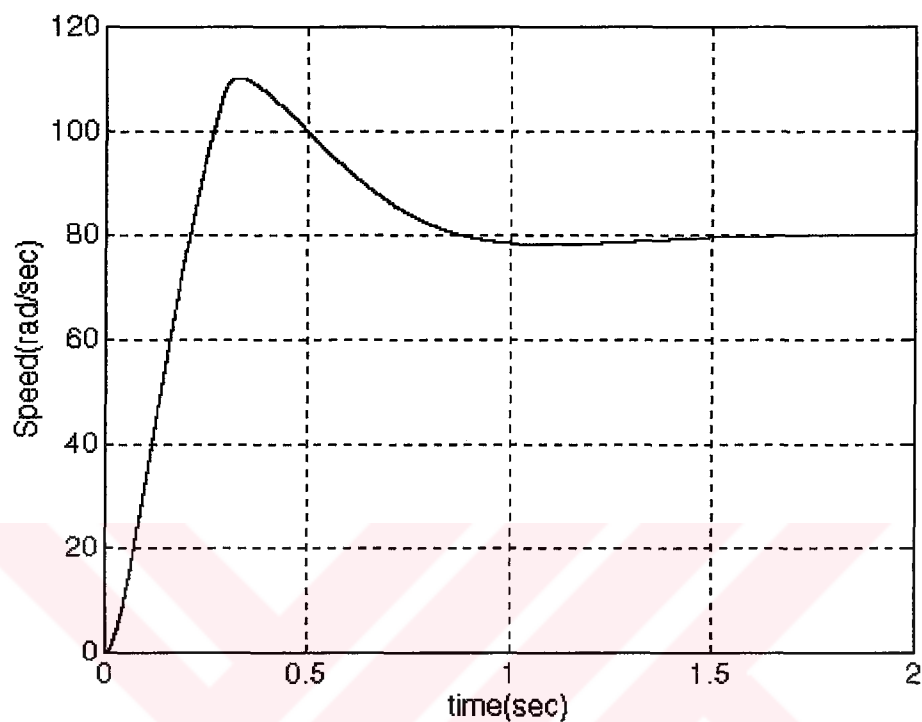


Figure 5 . 11 Rotor speed for K_{opt2}

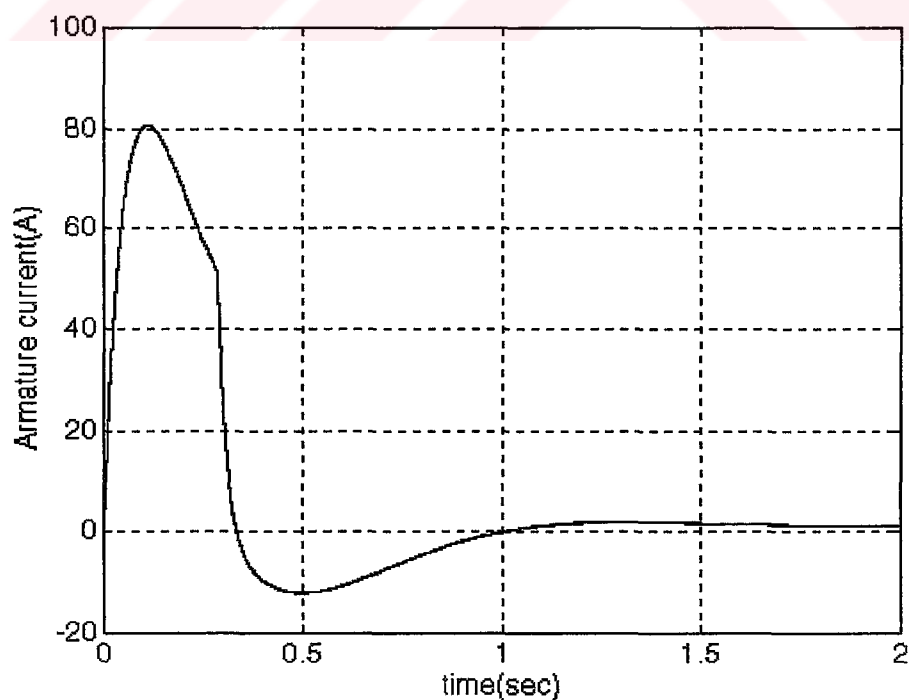


Figure 5 . 12 The armature current for K_{opt2}

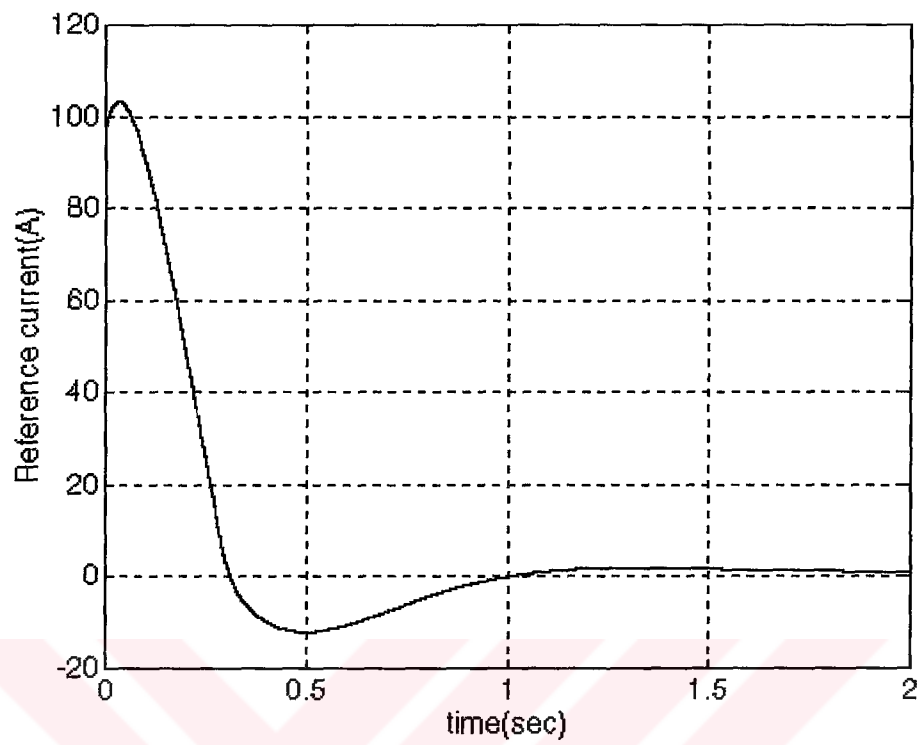


Figure 5 . 13 Reference current for K_{opt2}

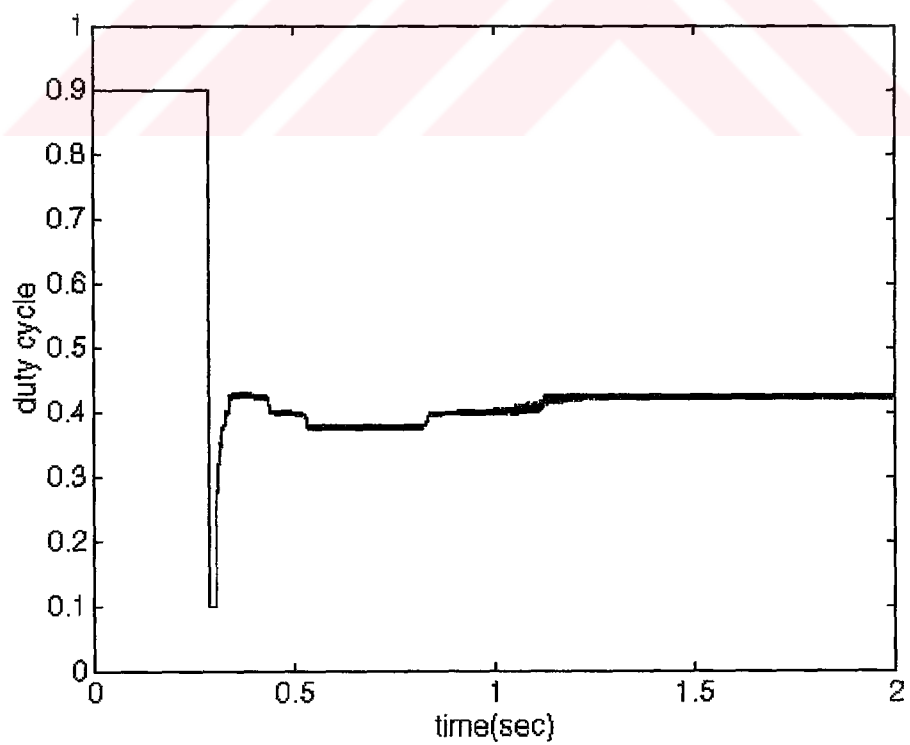


Figure 5 . 14 Variation of the duty cycle

CHAPTER SIX

CONCLUSION AND FURTHERWORK

6.1 Conclusions

In this thesis, first, a linear model of the closed-loop control of the dc motor fed by a class-C chopper in z-domain has been developed for the purpose of controller design. This model includes the time variation of pulsewidth modulated waveform at the output of the chopper. After establishing the model, the entire system has been considered as a discrete linear quadratic tracker problem with output feedback and the minimization has been performed on the cost function to obtain the optimum controller gains that stabilizes the system. Minimization requires the initial values of the variables. The root-locus method has been used for finding the initial values of the variables that stabilizes the system.

Two different state weighting matrices are considered for the optimum controller design. In the one of them, the error deviations on current and speed responses are equally weighted (Q_1) whereas in the other, the error deviation of speed is dominantly weighted against the error deviation of current (Q_2). The effects of these weightings are observed in the analysis results in Section 3.5.1 and Section 3.5.2. The speed response for K_{opt2} in Figure 3.12 which corresponds to the state weighting matrix Q_2 has less error deviation than the speed response for the K_{opt1} in Figure 3.9 corresponds to the Q_1 .

The analysis in Section 3.5.2 was carried out with limited duty cycle. Therefore the maximum value of the armature current waveforms in Figures 3.20 and 3.24 does not change for Q_1 and Q_2 , but the effect of the different weighting matrices can still be observed on the response times of the armature current waveforms.

As it is recognized from the results of analysis, the controller gains obtained as optimum values are very close to the initial values of the controller gains. In other words, the optimization method used in this thesis provided the local optimum values. This is the characteristic property of the hillclimbing methods which is a general term covering the method used in this thesis.

In Chapter 4, the effect of the variation of the amplitude and the chopping period of PWM waveform on the stability of overall system has been investigated. Stability limits obtained from root-locus method and the Jury test are confirmed by analyzing the model of the system. The linear model developed here for dc motor drive can be used to design optimal value of controllers in the stable operating region.

In Chapter 5, the real-time simulation of the system is performed to check the accuracy of the linear model developed in this thesis, and it is observed that the real-time simulation results and the analysis results of the linear model are in consistency.

6.2 Furtherwork

The following future works can be carried out on the basis of the study done in this thesis:

- 1) The genetic algorithm for numerical optimization of constrained problems (GENOCOP) has been developed by Zbigniew Michalewicz (Michalewicz, 1996) to find the global optimum of a function with additional linear equalities and inequalities constraints (Man, Tang & Kwong, 1996). The nonlinear cost function derived here

with Lyapunov equation can be optimized after some modifications made on current program available (Michalewicz, 1996).

2) The controller design method presented in this thesis can also be improved to apply on the alternative current machines as another future work.



APPENDIX 1

COMPUTER PROGRAMS FOR OPTIMAL CONTROLLER DESIGN

This Appendix gives the list of the Matlab files referred in Chapter 3 in addition to the explicit form of the cost function given in Equation (3-39).

tezana.m is the main program that finds the optimum controller gains using the SIMPLEX algorithm. State and input weighting matrices and initial K matrix are set in this routine. Then, it searches the controllability of (A, B) and the observability of (\sqrt{Q} , A), after that starts the searching process of finding the optimal gain matrix according to SIMPLEX method.

The file named **mtrpcsen.m** defines the motor parameters used in this thesis.

sysparam.m file includes some other system parameters except motor, such as chopper frequency, amplitudes of PWM and sawtooth signal, reference speed and load torque.

tezofmdl.m includes the system matrices given in Equations (3-5), (3-7), (3-12) and (3-15).

The function file **positdef.m** examines the positive definiteness of the matrix which is input to the function. It controls the positive definiteness of P during minimization

process. Positive definiteness of a matrix is decided according to the Sylvester's criterion (Ogata, 1990).

`tezana.m` and `dtractez.m` call the `tezfun1.m` for the evaluation of the cost function given in Equation (3-39).

`dtractez.m` is the simplex optimization routine that minimizes the cost function in Equation (3-39) subject to the Lyapunov constraint in Equation (3-40). This routine is obtained from the modification of a routine of MATLAB Optimization Toolbox named `fmins` in order to include a constraint defined by Lyapunov equation. In `dtractez.m`, Lyapunov equation is solved for P before the every evaluation of the cost function.

`tezana.m`

% Main program which finds the controller gains in the system

```
clear;
```

```
format short
```

```
mtrpcsen
```

```
sysparam
```

```
tezofmdl
```

```
Q=[1  0  0  0  0  0
    0  1  0  0  0  0
    0  0  0  .1  0  0
    0  0  .1  0  0  0
    0  0  0  0  0  .1
    0  0  0  0  .1  0];
```

```
R=[.1  0
    0  .1];
```

```
Kps=1;
```

```
Kis=5;
```

```
Kpi=10;
```

```
Kii=500;
```

```
Kinitial=[ 0    0  -Kps  -Kis
           -Kpi  -Kii   0    0];
```

```
K=Kinitial
```

```
Ac=A-B*K*C;
```

```
initial_eigenAc=(eig(Ac));
```

```
Act=Ac';
```

```
Ct=C';
```

```
Kt=K';
```

```
Clyap=Q+Ct*Kt*R*K*C;
```

```
P=dlyap(Act,Clyap);
```

```
positdef(P)
```

```
initialcost=tezfun1(K,A,B,C,E,F,r,Q,R,P)
```

```
[m,n]=size(A);
```

```
controllability=rank(ctrb(A,B))
```

```
    if controllability==n
```

```
        disp('(A,B) is controllable')
```

```
    else
```

```
        disp('(A,B) is NOT controllable')
```

```
    end
```

```
    disp(' ')
end
```

```
karekokQ=sqrtm(Q);
```

```

observability=rank(obsv(karekokQ,A))
    if observability==n
        disp('(kokQ,A) is observable')
    else
        disp('(kokQ,A) is NOT observable')
    end

options=[];
Pbos=1;
[Kopt,options]=dtrctez('tezfun1',K,options,[],A,B,C,E,F,r,Q,R,Pbos);

```

```

    Q
    R
    Nref
    TL
format short e
    Kinitial
    initialcost
    Kopt
    optcost=options(8)
format short

```

mtrpcsen.m

```

% DC motor parameter values
clc

Ra=1;
La=46e-3;

```



```

J=0.093;
Bv=0.008;
Kafi=0.55;

taua=La/Ra;
taum=J/Bv;

rlab='Bv= J= Kafi= La= Ra=';
clab='deger';
prmt=str2mat(Bv, J, Kafi, La, Ra);
printmat(prmt,'motor',rlab,clab);

disp('Electrical time constant (La/Ra) is ')
taua
disp('and mechanical time constant(J/Bv) is ')
taum
disp('second.')

```

sysparam.m

% The parameters used in the model of the system

```

f=1e4;
T=1/f;           % Chopping period
Kpwm=110;        % Amplitude of PWM signal
Esw=12;          % Amplitude of sawtooth signal
Nref=80;         % Reference speed
TL=0;            % Load torque

```

tezofmdl.m

% This file gives the matrices in the model given below

%

% $x(k+1) = A*x(k) + B*u(k) + E_r(k)$

% $y(k) = C*x(k) + F_r(k)$

% $z(k) = H*x(k)$

% $u(k) = -K*y(k)$

%

% where $r=[N_{ref}; TL]$ and $u = [I_{ref}; E_c]$

$ap11 = (L_a - R_a * T) / L_a;$ $ap12 = -K_{afi} * T / L_a;$

$ap21 = K_{afi} * T / J;$ $ap22 = (J - B_v * T) / J;$

$A = \begin{bmatrix} ap11 & ap12 & 0 & 0 & 0 & 0 \\ ap21 & ap22 & 0 & 0 & 0 & 0 \\ -1 & 0 & 0 & 0 & 0 & 0 \\ -T/2 & 0 & T/2 & 1 & 0 & 0 \\ 0 & -1 & 0 & 0 & 0 & 0 \\ 0 & -T/2 & 0 & 0 & T/2 & 1 \end{bmatrix};$

$B = [0 \ K_{pwm} * T / (L_a * E_{sw}); 0 \ 0; 1 \ 0; T/2 \ 0; 0 \ 0; 0 \ 0];$

$C = [0 \ 0 \ 1 \ 0 \ 0 \ 0$

$0 \ 0 \ 0 \ 1 \ 0 \ 0$

$0 \ 0 \ 0 \ 0 \ 1 \ 0$

$0 \ 0 \ 0 \ 0 \ 0 \ 1];$

$E = [0 \ 0; 0 \ -T/J; 0 \ 0; 0 \ 0; 1 \ 0; T/2 \ 0];$

$F = [0 \ 0; 0 \ 0; 0 \ 0; 0 \ 0];$

```
H=[1 0 0 0 0
    0 1 0 0 0];
r=[Nref;TL];
```

positdef.m

```
function positdef(A)

% Determines if the matrix A is positive definite or not

[m,n]=size(A);
LeadMinors=[];
for i=1:n
    minor = det(A(1:i,1:i));
    LeadMinors=[LeadMinors;minor];
end
LeadMinors;

if all(LeadMinors>0)
    disp(' positive definite')
else
    disp('NOT positive definite')
    disp(' press any key')
    pause
end
```

tezfun1.m

```
function costez1=tezfun1(K,A,B,C,E,F,r,Q,R,P9)
```

```
Ac=A-B*K*C;
```

```
Bc=E-B*K*F;
```

```
I=eye(size(A));
```

```
xbar=[-inv(Ac-I)]*Bc*r
```

```
X=xbar*xbar';
```

```
costez1=0.5*trace(P9*X);
```

dtractez.m

```
function [x, options] = dtractez(funfcn,x,options,grad,P1,P2,P3,P4,P5,P6,P7,P8,P9)
```

```
% -----
```

```
% This function implements the SIMPLEX optimization algorithm of the function
```

```
% funfcn under the constraint of discrete Lyapunov equation
```

```
% -----
```

```
if nargin<3, options=[]; end
```

```
options=foptions(options);
```

```
prnt=options(1);
```

```
tol=options(2);
```

```
tol2=options(3);
```

```
if (round(prnt) ~= prnt )
```

```
    if nargin<4, grad=0; end
```

```
    tol = prnt; tol2 = 1e10; prnt = grad;
```

```
end
```

```

evalstr = [funfcn];
if ~any(funfcn<48)
    evalstr=[evalstr, '(x)'];
    for i=1:nargin - 4
        evalstr = [evalstr,'P',int2str(i)];
    end
    evalstr = [evalstr, ')'];
end

```

```

n = prod(size(x));
if (~options(14))
    options(14) = 200*n;
end

```

% Set up a simplex near the initial guess.

```

xin = x(:);
v = 0.975*xin;
x(:) = v
Ac=P1-P2*x*P3;
eigen_Ac=eig(Ac)
Act=Ac';
Ct=P3';
Kt=x';
Clyap=P7+Ct*Kt*P8*x*P3;
P9=dlyap(Act,Clyap);
positdef(P9)
x
fv = eval(evalstr)
for j = 1:n
    j
    y = xin;

```

```

if y(j) ~= 0
    y(j) = 1.025*y(j);
end
v = [v y];
x(:) = y
Ac=P1-P2*x*P3;
eigen_Ac=eig(Ac)
Act=Ac';
Kt=x';
Clyap=P7+Ct*Kt*P8*x*P3;
P9=dlyap(Act,Clyap);
positdef(P9)
f = eval(evalstr);
fv = [fv f];
end
[fv,j] = sort(fv)
v = v(:,j)
cnt = n+1;
if prnt
    clc
    format compact
    format short e
    home
    cnt
    disp('initial ')
    disp(' ')
    v
    f
end

alpha = 0.75; beta = 0.5; gamma = 1.6;

```

```

[n,np1] = size(v);
onesn = ones(1,n);
ot = 2:n+1;
on = 1:n;

% Iterate until the diameter of the simplex is less than tol.
while cnt < options(14)
    if max(max(abs(v(:,ot)-v(:,onesn)))) <= tol & max(abs(fv(1)-fv(ot))) <= tol2,
break, end

%      One step of the Nelder-Mead simplex algorithm

vbar = (sum(v(:,on))/n)'; % Mean value
vr = (1 + alpha)*vbar - alpha*v(:,n+1);
x(:) = vr
Ac=P1-P2*x*P3;
Act=Ac';
Kt=x';
Clyap=P7+Ct*Kt*P8*x*P3;
P9=dlyap(Act,Clyap);
positdef(P9)
fr = eval(evalstr);
cnt = cnt + 1;
vk = vr; fk = fr; how = 'reflect ';
if fr < fv(n)
    if fr < fv(1)
        ve = gamma*vr + (1-gamma)*vbar;
        x(:) = ve
        Ac=P1-P2*x*P3;
        Act=Ac';
        Kt=x';

```

```

        Clyap=P7+Ct*Kt*P8*x*P3;
        P9=dlyap(Act,Clyap);
        positdef(P9)
        fe = eval(evalstr);
        cnt = cnt + 1;
        if fe < fv(1)
            vk = ve; fk = fe;
            how = 'expand ';
        end
    end
else
    vt = v(:,n+1); ft = fv(n+1);
    if fr < ft
        vt = vr; ft = fr;
    end
    vc = beta*vt + (1-beta)*vbar;
    x(:) = vc
    Ac=P1-P2*x*P3;
    Act=Ac';
    Kt=x';
    Clyap=P7+Ct*Kt*P8*x*P3;
    P9=dlyap(Act,Clyap);
    positdef(P9)
    fc = eval(evalstr);
    cnt = cnt + 1;
    if fc < fv(n)
        vk = vc; fk = fc;
        how = 'contract';
    else
        for j = 2:n
            v(:,j) = (v(:,1) + v(:,j))/2;

```



```

        x(:) = v(:,j)
        Ac=P1-P2*x*P3;
        Act=Ac';
        Kt=x';
        Clyap=P7+Ct*Kt*P8*x*P3;
        P9=dlyap(Act,Clyap);
        positdef(P9)
        fv(j) = eval(evalstr);

    end

    cnt = cnt + n-1;
    vk = (v(:,1) + v(:,n+1))/2;
    x(:) = vk
    Ac=P1-P2*x*P3;
    Act=Ac';
    Kt=x';
    Clyap=P7+Ct*Kt*P8*x*P3;
    P9=dlyap(Act,Clyap);
    positdef(P9)
    fk = eval(evalstr);
    cnt = cnt + 1;
    how = 'shrink ';

end

end

v(:,n+1) = vk;
fv(n+1) = fk;
[fv,j] = sort(fv);
cnt
v = v(:,j);

if prnt
    home

```

```

        cnt
        disp(how)
        disp(' ')
        v
        fv
    end
end
x(:) = v(:,1);
if prnt, format, end
options(10)=cnt;
options(8)=min(fv);
if cnt==options(14)
    if options(1) >= 0
        disp(['Warning:      Maximum      number      of      iterations
('int2str(options(14)),') has been exceeded']);
        disp('      (increase OPTIONS(14)).')
    end
end
end

```

analiz1.m

% Analyze the closed loop system by solving the state-space model according to a
 % given controller gain matrix . This program does not limit the duty cycle.

```

clear
mtrpcsen
sysparam
tezofmdl

```

Kps = 1.2172;

Kis = 4.8778;

Kpi = 10.668;

Kii = 500.93;

K=[0 0 -Kps -Kis
 -Kpi -Kii 0 0];

t=0;

tfinal=2;

x0=[0;0;0;0;0;0];

akim=[];

hiz=[];

kontrolinput=[];

zaman=[];

while t<=tfinal

 cikis=H*x0;

 akim=[akim cikis(1)];

 hiz=[hiz cikis(2)];

 u = -K*C*x0;

 kontrolinput=[kontrolinput u];

 xk = A*x0 + B*u + E*r;

 x0 = xk;

 zaman=[zaman t];

 t = t+T

end

Iref=kontrolinput(1,:);

Ec=kontrolinput(2,:);

figure

```
[dzaman, dhiz]=stairs(zaman,hiz);
plot(dzaman,dhiz,'k')
grid
ylabel('Speed')
xlabel('time')
title(['analiz1 (f=',num2str(1/T), ' Hz; Kps=', num2str(Kps),', Kis=',num2str(Kis),...
      ', Kpi=', num2str(Kpi),', Kii=',num2str(Kii),')'])
```

figure

```
[dzaman,dakim]=stairs(zaman,akim);
plot(dzaman, dakim, 'k')
grid
ylabel('Current')
xlabel('time')
title(['analiz1 (f=',num2str(1/T), ' Hz; Kps=', num2str(Kps),', Kis=',num2str(Kis),...
      ', Kpi=', num2str(Kpi),', Kii=',num2str(Kii),')'])
```

figure

```
[dzaman,diref]=stairs(zaman,Iref);
plot(dzaman,diref,'k')
grid
ylabel('Iref')
xlabel('time')
title(['analiz1 (f=',num2str(1/T), ' Hz; Kps=', num2str(Kps),', Kis=',num2str(Kis),...
      ', Kpi=', num2str(Kpi),', Kii=',num2str(Kii),')'])
```

anlzltd.m

% Analyze the closed loop system by solving the state-space model according to a
 % given controller gain matrix . This program limits the duty between 0.1 and 0.9.

```

clear
mtrpcsen
sysparam
tezofmdl

Kps = 1;      Kis = 5;
Kpi = 10;     Kii = 500;

K=[ 0   0  -Kps  -Kis
    -Kpi -Kii  0   0];

t=0;
tfinal=2;
x0=[0;0;0;0;0;0];
akim=[];
hiz=[];
kontrolinput=[];
zaman=[];

while t<=tfinal
    cikis=H*x0;
    akim=[akim cikis(1)];
    hiz=[hiz cikis(2)];
    u = -K*C*x0;
    if u(2)/Esw >= 0.9
        u(2)=0.9*Esw;
    end
    if u(2)/Esw <= 0.1
        u(2)=0.1*Esw;
    end
end

```

```

    kontrolinput=[kontrolinput u];
    xk = A*x0 + B*u + E*r;
    x0 = xk;
    zaman=[zaman t];
    t = t+T
end
Iref=kontrolinput(1,:);
Ec=kontrolinput(2,:);

figure
[dzaman, dhiz]=stairs(zaman,hiz);
plot(dzaman,dhiz,'k')
grid
ylabel('Speed')
xlabel('time')
title(['anlzltd (f=',num2str(1/T), ' Hz; Kps=', num2str(Kps),', Kis=',num2str(Kis),...
      ', Kpi=', num2str(Kpi),', Kii=',num2str(Kii),')'])

figure
[dzaman,dakim]=stairs(zaman,akim);
plot(dzaman, dakim, 'k')
grid
ylabel('Current')
xlabel('time')
title(['anlzltd (f=',num2str(1/T), ' Hz; Kps=', num2str(Kps),', Kis=',num2str(Kis),...
      ', Kpi=', num2str(Kpi),', Kii=',num2str(Kii),')'])

figure
[dzaman,dduty]=stairs(zaman,Ec/Esw);
plot(dzaman, dduty,'k')
ylabel('duty')

```

```

xlabel('time')
title(['anzltd (f=',num2str(1/T), ' Hz; Kps=', num2str(Kps),', Kis=',num2str(Kis),...
      ', Kpi=', num2str(Kpi),', Kii=',num2str(Kii),')'])
axis([0 tfinal 0 1])

```

```

figure
[dzaman,diref]=stairs(zaman,Iref);
plot(dzaman,diref,'k')
grid
ylabel('Iref')
xlabel('time')
title(['anzltd (Kps=', num2str(Kps),', Kis=',num2str(Kis),...
      ', Kpi=', num2str(Kpi),', Kii=',num2str(Kii),')'])

```

kinitial.mcd

Computes the characteristic equation, which is used in finding the matrix $K_{initial}$, of the closed loop system as a function of K_{is} .

```

La := 0.046      Ra := 1      J := 0.093      Bv := 0.008
Kafi := 0.55     T := (10)^-4  Kpwm := 110    Esw := 12
Kpi := 10        Kii := 500    Kps := 1      Kis := 1
z := 1

a11 := (La - Ra.T) / La      a12 := - (Kafi.T / La)      a21 := Kafi.T / J      a22 := (J - Bv.T) / J

a11 = 0.997826086957      a12 = -0.001195652174
a21 = 5.91397849462410^-4      a22 = 0.999991397849

```

Closed-loop system matrix defined in Equation (3-1) is evaluated for all the variables given above except Kis

$$A := \begin{bmatrix} 0.997826086957 & -0.001195652174 & \frac{110 \cdot 10^{-4} \cdot 10}{0.04612} & \frac{110 \cdot 10^{-4} \cdot 500}{0.04612} & 0 & 0 \\ 5.91397849462410^{-4} & 0.999991397849 & 0 & 0 & 0 & 0 \\ -1 & 0 & 0 & 0 & 1 & \text{Kis} \\ \frac{-10^{-4}}{2} & 0 & \frac{10^{-4}}{2} & 1 & \frac{10^{-4}}{2} & \frac{10^{-4} \cdot \text{Kis}}{2} \\ 0 & -1 & 0 & 0 & 0 & 0 \\ 0 & \frac{-10^{-4}}{2} & 0 & 0 & \frac{10^{-4}}{2} & 1 \end{bmatrix}$$

$$zI := \begin{bmatrix} z & 0 & 0 & 0 & 0 & 0 \\ 0 & z & 0 & 0 & 0 & 0 \\ 0 & 0 & z & 0 & 0 & 0 \\ 0 & 0 & 0 & z & 0 & 0 \\ 0 & 0 & 0 & 0 & z & 0 \\ 0 & 0 & 0 & 0 & 0 & z \end{bmatrix} - A$$

The matrix (zI-A):

$$\begin{bmatrix} z - .997826086957 & 1.19565217410^{-3} & -.199275362319 - 9.96376811594 & 0 & 0 \\ -5.9139784946210^{-4} & z - .999991397849 & 0 & 0 & 0 & 0 \\ 1. & 0 & z & 0 & -1. & -1. \cdot \text{Kis} \\ 5.0 \cdot 10^{-5} & 0 & -5.0 \cdot 10^{-5} & z - 1. & -5.0 \cdot 10^{-5} & -5.0 \cdot 10^{-5} \cdot \text{Kis} \\ 0 & 1. & 0 & 0 & z & 0 \\ 0 & 5.0 \cdot 10^{-5} & 0 & 0 & -5.0 \cdot 10^{-5} & z - 1. \end{bmatrix}$$

The statement $\det(zI-A)$ is as given below:

$$\left[\begin{aligned} & z^6 - 3.99781748481 \cdot z^5 + 6.19322673095 \cdot z^4 - 4.59177646291 \cdot z^3 + 1.59526082642 \cdot z^2 \dots \\ & + (-.199011166043 \cdot z) + 2.94627551815 \cdot 10^{-11} \cdot z \cdot K_{is} + 1.17556393174 \cdot 10^{-4} \dots \\ & + (-5.87781965872 \cdot 10^{-9} \cdot K_{is}) + 5.9072824139 \cdot 10^{-9} \cdot z^2 \cdot K_{is} \end{aligned} \right]$$

If it is arranged so that the terms including K_{is} and the others are grouped separately, it is obtained that

$$\begin{aligned} & (2.94627551815 \cdot 10^{-11} \cdot z - 5.87781965872 \cdot 10^{-9} + 5.9072824139 \cdot 10^{-9} \cdot z^2) \cdot K_{is} \dots \\ & + z^6 - 3.99781748481 \cdot z^5 + 6.19322673095 \cdot z^4 - 4.59177646291 \cdot z^3 \dots \\ & + 1.59526082642 \cdot z^2 - .199011166043 \cdot z + 1.17556393174 \cdot 10^{-4} \end{aligned}$$

Explicit Form of the Cost Function

The explicit form of the cost function given in Equation (3-39) is obtained with the help of the Mathcad and is given below:

$$\begin{aligned} \frac{1}{2} \text{trace}(P \cdot X) = & \frac{(T_L + B_v \cdot N_{ref})}{2 \cdot (K_a \phi)^2 \cdot K_{pwm} \cdot K_{ii} \cdot K_{is}} \cdot \{ p_{11} \cdot K_{pwm} \cdot K_{ii} \cdot K_{is} \cdot T_L + p_{11} \cdot K_{pwm} \cdot K_{ii} \cdot K_{is} \cdot B_v \cdot N_{ref} \\ & + p_{12} \cdot N_{ref} \cdot K_a \phi \cdot K_{pwm} \cdot K_{ii} \cdot K_{is} + p_{14} \cdot E_{sw} \cdot K_{is} \cdot R_a \cdot T_L + p_{14} \cdot E_{sw} \cdot K_{is} \cdot N_{ref} \cdot R_a \cdot B_v \\ & + p_{14} \cdot E_{sw} \cdot K_{is} \cdot N_{ref} \cdot (K_a \phi)^2 + p_{16} \cdot K_{pwm} \cdot K_{ii} \cdot T_L + p_{16} \cdot K_{pwm} \cdot K_{ii} \cdot B_v \cdot N_{ref} \} \\ & + \frac{N_{ref}}{2 \cdot K_a \phi \cdot K_{pwm} \cdot K_{ii} \cdot K_{is}} \cdot \{ p_{21} \cdot K_{pwm} \cdot K_{ii} \cdot K_{is} \cdot T_L + p_{21} \cdot K_{pwm} \cdot K_{ii} \cdot K_{is} \cdot B_v \cdot N_{ref} \\ & + p_{22} \cdot N_{ref} \cdot K_a \phi \cdot K_{pwm} \cdot K_{ii} \cdot K_{is} + p_{24} \cdot E_{sw} \cdot K_{is} \cdot R_a \cdot T_L + p_{24} \cdot E_{sw} \cdot K_{is} \cdot N_{ref} \cdot R_a \cdot B_v \end{aligned}$$

$$\begin{aligned}
& +p_{24} \cdot E_{sw} \cdot K_{is} \cdot N_{ref} \cdot (K_a \varphi)^2 + p_{26} \cdot K_{pwm} \cdot K_{ii} \cdot T_L + p_{26} \cdot K_{pwm} \cdot K_{ii} \cdot B_v \cdot N_{ref} \Big\} \\
& + \frac{E_{sw} (R_a \cdot T_L + N_{ref} \cdot R_a \cdot B_v + N_{ref} (K_a \varphi)^2)}{2 \cdot (K_a \varphi)^2 \cdot K_{pwm}^2 \cdot K_{ii}^2 \cdot K_{is}} \cdot \Big\{ p_{41} \cdot K_{pwm} \cdot K_{ii} \cdot K_{is} \cdot T_L \\
& + p_{41} \cdot K_{pwm} \cdot K_{ii} \cdot K_{is} \cdot B_v \cdot N_{ref} + p_{42} \cdot N_{ref} \cdot K_a \varphi \cdot K_{pwm} \cdot K_{ii} \cdot K_{is} + p_{44} \cdot E_{sw} \cdot K_{is} \cdot R_a \cdot T_L \\
& + p_{44} \cdot E_{sw} \cdot K_{is} \cdot N_{ref} \cdot R_a \cdot B_v + p_{44} \cdot E_{sw} \cdot K_{is} \cdot N_{ref} \cdot (K_a \varphi)^2 \\
& + p_{46} \cdot K_{pwm} \cdot K_{ii} \cdot T_L + p_{46} \cdot K_{pwm} \cdot K_{ii} \cdot B_v \cdot N_{ref} \Big\} \\
& + \frac{(T_L + B_v \cdot N_{ref})}{2 \cdot (K_a \varphi)^2 \cdot K_{is}^2 \cdot K_{pwm} \cdot K_{ii}} \cdot \Big\{ p_{61} \cdot K_{pwm} \cdot K_{ii} \cdot K_{is} \cdot T_L + p_{61} \cdot K_{pwm} \cdot K_{ii} \cdot K_{is} \cdot B_v \cdot N_{ref} \\
& + p_{62} \cdot N_{ref} \cdot K_a \varphi \cdot K_{pwm} \cdot K_{ii} \cdot K_{is} + p_{64} \cdot E_{sw} \cdot K_{is} \cdot R_a \cdot T_L + p_{64} \cdot E_{sw} \cdot K_{is} \cdot N_{ref} \cdot R_a \cdot B_v \\
& + p_{64} \cdot E_{sw} \cdot K_{is} \cdot N_{ref} \cdot (K_a \varphi)^2 + p_{66} \cdot K_{pwm} \cdot K_{ii} \cdot T_L + p_{66} \cdot K_{pwm} \cdot K_{ii} \cdot B_v \cdot N_{ref} \Big\}
\end{aligned}$$

where p_{ij} 's are the matrix elements of the positive definite matrix P and N_{ref} denotes the reference speed.

APPENDIX 2

COMPUTER PROGRAMS FOR STABILITY ANALYSIS

This Appendix includes the Matlab and Mathcad files referred in Chapter 4. The Matlab files have the extension m, whereas Mathcad files's extensions are mcd.

juryk.m

% Finds the solutions of the inequalities given in stability condition 4 to 7
% in Jury test for the amplitude of PWM signal.

%

% Stability condition number 4:

% $\text{abs}(b_0) > \text{abs}(b_5)$

% Stability condition number 5:

% $\text{abs}(c_0) > \text{abs}(c_4)$

% Stability condition number 6:

% $\text{abs}(d_0) > \text{abs}(d_3)$

% Stability condition number 7:

% $\text{abs}(e_0) > \text{abs}(e_2)$

%

% -----

clear

bsol=[1.14153691628e-12 0 -1];

```
bsag=[0 1.80492103986e-3 0];
```

```
csol=[1.30310653123e-24 0 -3.2577422432e-6 0 1];
```

```
csag=[2.21503322377e-21 3.48270266488e-12 -1.94153465874e-9 ...  
      -1.79085168507e-3 0.997818210612];
```

```
dsol=[-4.90637048432e-42 -1.54286042224e-32 -1.21292177412e-23 ...  
      1.35315094519e-20 1.0625354757e-11 -1.39042095128e-11 ...  
      -9.71875964704e-6 3.57388884774e-3 4.35881857107e-3];
```

```
dsag=[4.87900341191e-42 1.54288461522e-32 1.2197252417e-23 ...  
      -1.3531445195e-20 -1.0684953947e-11 1.36623411844e-11 ...  
      9.73695174216e-6 -3.57387140583e-3 -4.35881698352e-3];
```

```
esol=[2.67797035977e-85 8.4211070524e-76 -7.46580711026e-69 ...  
      -2.10526267157e-57 -1.65504350601e-48 3.68389085167e-45 ...  
      2.89967787006e-36 -1.60755308632e-33 -1.27007891017e-24 ...  
      -3.51036769834e-24 1.54723047165e-18 -4.21424801861e-16 ...  
      -3.56188980044e-13 1.29691281097e-10 2.8323175936e-10 ...  
      1.63399641547e-10 1.38396823247e-11];
```

```
esag=[2.6779662987e-85 8.42109427529e-76 -7.46579974599e-69 ...  
      -2.10525948644e-57 -1.65504100072e-48 3.68388197237e-45 ...  
      2.8996734767e-36 -1.60754774877e-33 -1.27007698409e-24 ...  
      -3.51037071474e-24 1.54722811791e-18 -4.21424153583e-16 ...  
      -3.56188437929e-13 1.29691082699e-10 2.83231250227e-10 ...  
      1.63399409175e-10 1.38399002782e-11];
```

```
format long e
```

```
disp('')
```

```
disp(' According to the stability condition number 4:')
```

```

disp(' ')
esitszlk(bsol,bsag)
disp('-----')

```

```

disp(' According to the stability condition number 5:')
disp(' ')
esitszlk(csol,csag)
disp('-----')

```

```

disp(' According to the stability condition number 6:')
disp(' ')
esitszlk(dsol,dsag)
disp('-----')

```

```

disp(' According to the stability condition number 7:')
disp(' ')
esitszlk(esol,esag)
format short

```

esitszlk.m

```

function esitszlk(bsol,bsag)
%
% Finds the solution of the inequality like  $\text{abs}(\text{bsol}) > \text{abs}(\text{bsag})$  for Kpwm.

kok1=roots(bsol-bsag);
kok2=roots(bsol+bsag);
kokler=[kok1;kok2];
koksayisi=length(kokler);

```

```

kokler=gercel(kokler);
koksirali=sort(kokler);
koksirali=natekrar(koksirali);
gercelkoksayisi=length(koksirali);

saglamanohtalari=koksirali(1)-1;
for i=1:(gercelkoksayisi-1)
    saglamanohtasi=(koksirali(i)+koksirali(i+1))/2;
    saglamanohtalari=[saglamanohtalari saglamanohtasi];
end
saglamanohtalari=[saglamanohtalari koksirali(gercelkoksayisi)+1];
koksirali=koksirali';

for i=1:gercelkoksayisi+1
    if abs(polyval(bsol,saglamanohtalari(i))) > ...
        abs(polyval(bsag,saglamanohtalari(i)))
        if(i==1)
            disp(['Kpwm < ', num2str(koksirali(1))])
            disp(' ')
        elseif(i==(gercelkoksayisi+1))
            disp(['Kpwm > ',num2str(koksirali(gercelkoksayisi))])
            disp(' ')
        else
            disp([num2str(koksirali(i-1)),' < Kpwm < ',...
                num2str(koksirali(i))])
            disp(' ')
        end
    end
end
end

```

gercel.m

```
function gercelkokler=gercel(a)
```

```
% Returns the only real elements of the vector a which may have
```

```
% both real and complex elements
```

```
j=1;
```

```
for i=1:length(a)
```

```
    if imag(a(i))==0
```

```
        gercelkokler(j)=a(i);
```

```
        j=j+1;
```

```
    end
```

```
end
```

```
gercelkokler=gercelkokler';
```

natekrar.m

```
function b=natekrar(a)
```

```
% Removes the repeated elements of the vector a of which elements are
```

```
% sorted and returns the different elements of a in b.
```

```
boyut=length(a);
```

```
i=1;
```

```
j=1;
```

```
b(i)=a(j);
```

```

while j <= boyut-1
    if a(j)==a(j+1)
        j=j+1;
    else
        i=i+1;
        j=j+1;
        b(i)=a(j);
    end
end
end

```

juryt.m

```

% Finds the solutions of the inequalities given in stability
% condition 3 to 7 in jury test for period of PWM signal.
%
%   Stability condition number 3:
%        $\text{abs}(a_0) < a_6$ 
%   Stability condition number 4:
%        $\text{abs}(b_0) > \text{abs}(b_5)$ 
%   Stability condition number 5:
%        $\text{abs}(c_0) > \text{abs}(c_4)$ 
%   Stability condition number 6:
%        $\text{abs}(d_0) > \text{abs}(d_3)$ 
%   Stability condition number 7:
%        $\text{abs}(e_0) > \text{abs}(e_2)$ 
%
% Calls the function czm_t.m.
% -----
clear
a0=[736568.879 -324090.307 11785.102 0 0];

```


$a6=[0 \ 0 \ 0 \ 0 \ 1];$

$b0=[542533714304 \ -477429668588 \ 122395605947 \ -7638874697.4 \dots$
 $138888630.862 \ 0 \ 0 \ 0 \ -1];$

$b5=[0 \ 0 \ 0 \ 16075727.7103 \ -11492733.4698 \ 1557858.36302 \dots$
 $-73560.4643914 \ 1992.75362319 \ 0];$

$c0=[2.94342831156e23 \ -5.18043382836e23 \ 3.60746573866e23 \dots$
 $-1.25159281293e23 \ 2.2425438715e22 \ -2.00254850069e21 \dots$
 $9.23508644806e19 \ -2.12153618799e18 \ 1.9106796379e16 \dots$
 $3.91280372286e13 \ -4.42660544274e12 \ 290275691199 \dots$
 $-11897774977.9 \ 293175763.879 \ -3971067.00274 \ 0 \ 1];$

$c4=[0 \ 0 \ 1.99372829639e22 \ -2.55644904832e22 \dots$
 $1.15421382725e22 \ -2.06702478446e21 \ 1.0547006755e20 \dots$
 $4.21916593595e17 \ -1.13712816468e17 \ -1.30056932254e15 \dots$
 $1.87568814695e14 \ -4.44021504467e12 \ 46773466599.7 \dots$
 $-28281439.54 \ 228719.39854 \ -2014.57877513 \ 1];$

$d0=[8.66377022529e46 \ -3.04964711931e47 \ 4.80735282263e47 \dots$
 $-4.47444225347e47 \ 2.72618004495e47 \ -1.13695762724e47 \dots$
 $3.28600447634e46 \ -6.48270154808e45 \ 8.29903823211e44 \dots$
 $-6.13921150044e43 \ 2.01583471535e42 \ -4.9260040731e40 \dots$
 $1.1040592039e40 \ -9.84594662151e38 \ 2.14663598276e37 \dots$
 $1.21070492634e36 \ -7.32272035205e34 \ 8.12275445923e32 \dots$
 $2.97754471886e31 \ -4.23153926222e29 \ -3.85166528128e28 \dots$
 $1.80570805542e27 \ -3.72210830478e25 \ 4.16296032777e23 \dots$
 $-2.18276699881e21 \ -3846494708370000000 \ 139975596836000000 \dots$
 $-2117585528630000 \ 15485767718200 \ 1564460898.36 \dots$
 $-12458100.4438 \ 4029.15755026 \ 0];$

d1=[1.73275404506e47 -5.34192319785e47 7.28535493111e47 ...
 -5.79790106626e47 3.0043928263e47 -1.08197263938e47 ...
 2.87791308246e46 -6.06611238384e45 1.05994914035e45 ...
 -1.46070401847e44 1.36037477702e43 -6.52187894985e41 ...
 2.82806370526e39 7.77506260959e38 2.1879747343e37 ...
 -4.13791050121e36 1.11210013867e35 2.97004266133e33 ...
 -2.43167806675e32 5.17972099564e30 1.81911438013e28 ...
 -3.54139543096e27 8.93608565568e25 -1.13094909635e24 ...
 6.79133187456e21 4.96347233749e18 -3.06846918824e17 ...
 5.43809251515e15 -4.64839179739e13 -4.46776441147e9 ...
 3.73743013313e7 -1.20874726508e4 0];

d2=[8.66377022529e46 -2.28723533948e47 2.34152409895e47 ...
 -9.74032755626e46 -1.36023424025e46 3.49839714101e46 ...
 -1.81805422073e46 5.19958791252e45 -9.30701123164e44 ...
 1.08449992598e44 -8.23845987475e42 3.96344021807e41 ...
 -1.69670020227e40 1.45883117036e39 -1.15788095854e38 ...
 4.29771463966e36 2.19592925721e34 -8.86027252851e33 ...
 3.93390145177e32 -8.68981065088e30 6.95802669651e28 ...
 1.78425806707e27 -6.77755436997e25 1.01238931792e24 ...
 -7.00053715594e21 1.04512379495e18 1.98700494092e17 ...
 -4.52309034055e15 4.65065745497e13 4.24345963102e9 ...
 -3.73743013313e7 1.20874726508e4 0];

d3=[0 5.04073904019e44 -1.91461107867e46 5.00227822666e46 ...
 5.8310591552e46 3.89183508634e46 -1.63066252636e46 ...
 4.45402066274e45 -8.01849610122e44 9.44961651775e43 ...
 -7.00306340599e42 2.60482899787e41 5.33014935165e39 ...
 -1.27362251677e39 6.99296349504e37 -1.24095822617e36 ...
 -6.33298964556e34 5.1551830109e33 -1.81967867983e32 ...
 3.97494551973e30 4.97969525257e28 -4.54008474417e25 ...

```

1.56402088463e25 -2.97872228769e23 2.39461457752e21 ...
-21863186833300000000 -318297178280000000 1202589289530000 ...
-15508424293900 -1340156117.99 12458100.4438 ...
-4029.15755026 0];

```

```

d0kare=conv(d0,d0);
d3kare=conv(d3,d3);
e0=d0kare-d3kare;

```

```

d0d2=conv(d0,d2);
d1d3=conv(d1,d3);
e2=d0d2-d1d3;

```

```

format long e
disp(' According to the stability condition number 3')
disp(' ')
czm_t(a0,a6,1)

```

```

disp('-----')
disp(' According to the stability condition number 4')
disp(' ')
czm_t(b0,b5,0)

```

```

disp('-----')
disp(' According to the stability condition number 5')
disp(' ')
czm_t(c0,c4,0)

```

```

disp('-----')
disp(' According to the stability condition number 6')
disp(' ')

```

```
czm_t(d0,d3,0)
```

```
disp('-----')
```

```
disp(' According to the stability condition number 7')
```

```
disp(' ')
```

```
czm_t(e0,e2,0)
```

```
format short
```

czm_t.m

```
function czm_t(bsol,bsag,thrd)
```

```
%
```

```
% If thrd=1, finds the solution of the inequality
```

```
%     abs(bsol) < bsag
```

```
%
```

```
% Otherwise, finds the solution of the inequality
```

```
%     abs(bsol) > abs(bsag)
```

```
% -----
```

```
kok1=roots(bsol-bsag);
```

```
kok2=roots(bsol+bsag);
```

```
kokler=[kok1;kok2];
```

```
koksayisi=length(kokler);
```

```
kokler=gercel(kokler);
```

```
koksirali=sort(kokler);
```

```
koksirali=natekrar(koksirali);
```

```
gercelkoksayisi=length(koksirali);
```

```
saglamanohtalari=koksirali(1)-1;
```

```

for i=1:(gercelkoksayisi-1)
    saglamanoktasi=(koksirali(i)+koksirali(i+1))/2;
    saglamanoktalari=[saglamanoktalari saglamanoktasi];
end
saglamanoktalari=[saglamanoktalari koksirali(gercelkoksayisi)+1];
koksirali=koksirali';

for i=1:gercelkoksayisi+1

    if(thrd==1)
        if abs(polyval(bsol,saglamanoktalari(i))) < ...
            polyval(bsag,saglamanoktalari(i))

            if(i==1)
                disp(['T < ', num2str(koksirali(1))])
                disp(' ')
            elseif(i==(gercelkoksayisi+1))
                disp(['T > ', num2str(koksirali(gercelkoksayisi))])
                disp(' ')
            else
                disp([num2str(koksirali(i-1)), '< T < ',...
                    num2str(koksirali(i))])
                disp(' ')
            end
        end
    end

    else

        if abs(polyval(bsol,saglamanoktalari(i))) > ...
            abs(polyval(bsag,saglamanoktalari(i)))
            if(i==1)
                disp(['T < ', num2str(koksirali(1))])

```

```
disp(' ')
elseif(i==(gercelkoksayisi+1))
    disp(['T > ', num2str(koksirali(gercelkoksayisi))])
    disp(' ')
else
    disp([num2str(koksirali(i-1)), '< T < ',...
        num2str(koksirali(i))])
    disp(' ')
end
end
end
end
```

chrceq_k.mcd

Computes the characteristic equation of the closed loop system by keeping the K_{pwm} as a parameter.

$$La := 0.046$$
$$Kafi := 0.55$$
$$Kpi := 10$$
$$z := 1$$
$$a11 := \frac{La - Ra \cdot T}{La}$$
$$a11 = 0.997826086957$$
$$a21 = 5.9139784946240^{-4}$$

$$Ra := 1$$
$$T := (10)^{-4}$$
$$Kii := 500$$
$$a12 := -\left(Kafi \cdot \frac{T}{La}\right)$$
$$a12 = -0.001195652174$$
$$a22 = 0.999991397849$$

$$J := 0.093$$
$$Kpwm := 110$$
$$Kps := 1$$
$$a21 := Kafi \cdot \frac{T}{J}$$
$$a22 = 0.999991397849$$

$$Bv := 0.008$$
$$Esw := 12$$
$$Kis := 5$$
$$a22 := \frac{J - Bv \cdot T}{J}$$

$$A := \begin{bmatrix} 0.997826086957 & -0.001195652174 \frac{K_{pwm} \cdot 10^{-4} \cdot 10}{0.04612} & \frac{K_{pwm} \cdot 10^{-4} \cdot 500}{0.04612} & 0 & 0 \\ 5.91397849462410^{-4} & 0.999991397849 & 0 & 0 & 0 & 0 \\ -1 & 0 & 0 & 0 & 1 & 5 \\ \frac{-10^{-4}}{2} & 0 & \frac{10^{-4}}{2} & 1 & \frac{10^{-4}}{2} & \frac{10^{-4} \cdot 5}{2} \\ 0 & -1 & 0 & 0 & 0 & 0 \\ 0 & \frac{-10^{-4}}{2} & 0 & 0 & \frac{10^{-4}}{2} & 1 \end{bmatrix}$$

$$zI := \begin{bmatrix} z & 0 & 0 & 0 & 0 & 0 \\ 0 & z & 0 & 0 & 0 & 0 \\ 0 & 0 & z & 0 & 0 & 0 \\ 0 & 0 & 0 & z & 0 & 0 \\ 0 & 0 & 0 & 0 & z & 0 \\ 0 & 0 & 0 & 0 & 0 & z \end{bmatrix}$$

$$\begin{bmatrix} z & 0 & 0 & 0 & 0 & 0 \\ 0 & z & 0 & 0 & 0 & 0 \\ 0 & 0 & z & 0 & 0 & 0 \\ 0 & 0 & 0 & z & 0 & 0 \\ 0 & 0 & 0 & 0 & z & 0 \\ 0 & 0 & 0 & 0 & 0 & z \end{bmatrix} - A$$

The matrix (zI-A):

$$\begin{bmatrix} z - .997826086957 & 1.19565217410^{-3} & -1.811594202910^{-3} \cdot K_{pwm} & -9.0579710144910^{-2} \cdot K_{pwm} & 0 & 0 \\ -.59139784946210^{-4} & z - .999991397849 & 0 & 0 & 0 & 0 \\ 1. & 0 & z & 0 & -1. & -5. \\ 5.0 \cdot 10^{-5} & 0 & -5.0 \cdot 10^{-5} & z - 1. & -5.0 \cdot 10^{-5} & -2.5 \cdot 10^{-4} \\ 0 & 1. & 0 & 0 & z & 0 \\ 0 & 5.0 \cdot 10^{-5} & 0 & 0 & -5.0 \cdot 10^{-5} & z - 1. \end{bmatrix}$$

The statement $\det(zI-A)$ is as given below:

$$z^6 - 3.99781748481z^5 + 5.99345318022z^4 - 3.99345390603z^3 + .997818210612z^2 \dots$$

$$+ 5.4312967758410^{-3} \cdot K_{pwm} \cdot z^2 - 1.8091924172410^{-3} \cdot K_{pwm} \cdot z + 1.0684273097810^{-6} \cdot K_{pwm} \dots$$

$$+ 1.8161231884110^{-3} \cdot K_{pwm} \cdot z^4 - 5.4392959716410^{-3} \cdot K_{pwm} \cdot z^3$$

chrceq_t.mcd

Computes the characteristic equation of the closed loop system by keeping T as a varying parameter.

$$\begin{aligned} La &:= 0.046 & Ra &:= 1 & J &:= 0.093 & Bv &:= 0.008 \\ Kafi &:= 0.55 & T &:= 0.0001 & Kpwm &:= 110 & Esw &:= 12 \\ Kpi &:= 10 & Kii &:= 500 & Kps &:= 1 & Kis &:= 5 \\ z &:= 1 \end{aligned}$$

$$A := \begin{bmatrix} \frac{La - Ra \cdot T}{La} & -\left(Kafi \cdot \frac{T}{La}\right) & \frac{Kpwm \cdot T \cdot Kpi}{La \cdot Esw} & \frac{Kpwm \cdot T \cdot Kii}{La \cdot Esw} & 0 & 0 \\ Kafi \cdot \frac{T}{J} & \frac{J - Bv \cdot T}{J} & 0 & 0 & 0 & 0 \\ -1 & 0 & 0 & 0 & Kps & Kis \\ -\frac{T}{2} & 0 & \frac{T}{2} & 1 & \frac{T \cdot Kps}{2} & \frac{T \cdot Kis}{2} \\ 0 & -1 & 0 & 0 & 0 & 0 \\ 0 & -\frac{T}{2} & 0 & 0 & \frac{T}{2} & 1 \end{bmatrix}$$

$$A := \begin{bmatrix} \frac{0.046 - 1 \cdot T}{0.046} & -\left(0.55 \cdot \frac{T}{0.046}\right) & \frac{110 \cdot T \cdot 10}{0.046 \cdot 12} & \frac{110 \cdot T \cdot 500}{0.046 \cdot 12} & 0 & 0 \\ 0.55 \cdot \frac{T}{0.093} & \frac{0.093 - 0.008 \cdot T}{0.093} & 0 & 0 & 0 & 0 \\ -1 & 0 & 0 & 0 & 1 & 5 \\ -1 \cdot \frac{T}{2} & 0 & \frac{T}{2} & 1 & \frac{T \cdot 1}{2} & \frac{T \cdot 5}{2} \\ 0 & -1 & 0 & 0 & 0 & 0 \\ 0 & -\frac{T}{2} & 0 & 0 & \frac{T}{2} & 1 \end{bmatrix}$$

$$zI := \begin{bmatrix} z & 0 & 0 & 0 & 0 & 0 \\ 0 & z & 0 & 0 & 0 & 0 \\ 0 & 0 & z & 0 & 0 & 0 \\ 0 & 0 & 0 & z & 0 & 0 \\ 0 & 0 & 0 & 0 & z & 0 \\ 0 & 0 & 0 & 0 & 0 & z \end{bmatrix} - A$$

The matrix (zI-A) is

$$\begin{bmatrix} z-1.0+21.7391304T & 11.9565217T & -1992.75362T & -99637.6812T & 0 & 0 \\ -5.91397849T & z-1.0+8.6021505410^{-2} \cdot T & 0 & 0 & 0 & 0 \\ 1. & 0 & z & 0 & -1. & -5. \\ .5 \cdot T & 0 & -.5 \cdot T & z-1. & -.5 \cdot T & -2.5 \cdot T \\ 0 & 1. & 0 & 0 & z & 0 \\ 0 & .5 \cdot T & 0 & 0 & -.5 \cdot T & z-1. \end{bmatrix}$$

Characteristic equation with respect to T is:

$$\begin{aligned} & -1992.75362T \cdot z + 21.8251519z^5 \cdot T + 6.0z^4 - 4.0z^3 + 26420.0562T^2 \cdot z + 5956.43571T \cdot z^2 \dots \\ & + (-38303.9972T^2 \cdot z^2) + 324090.307T^3 \cdot z^2 + 736568.879T^4 \cdot z^2 + 1473137.76T^4 \cdot z + 736568.879T^4 \dots \\ & + 1.0z^2 + 49891.4212z^4 \cdot T^2 - 49792.5822z^3 \cdot T^2 - 5912.7854T \cdot z^3 + 1927.27816T \cdot z^4 \dots \\ & + (-4285.49167T^3 \cdot z) + z^6 - 4.0z^5 - 324090.307T^3 + 11785.102T^2 + 4285.49167T^3 \cdot z^3 \end{aligned}$$

APPENDIX 3

COMPUTER PROGRAMS FOR REAL-TIME SIMULATION

This appendix gives the list of the programs mentioned in Chapter 5 for the real time simulation of dc drive.

Logic of the Simulation Program

In the simulation program, the minimum duty cycle is read in. This minimum duty cycle is saved for the variable `dutymin` in the program `classcm`. Then, the z-transform of PWM waveform is computed by using the duty ratio, period and amplitude of the waveform. This is accomplished via the routine `zzkare`. Then the data which defines the PWM waveform at the sampling instants are generated and thus the block of “From Workspace” will be released for the simulation step. Finally, the model presented in Figure 5.1 is simulated for the first period. After this simulation step the level of output of current controller will be available in the matrix E_c due to the block “To Workspace”. Thus the duty cycle required for the subsequent simulation step can be determined. These steps are repeated until the end of the simulation time.

`classcm.m`

```
% -----  
%  Simulates the closed-loop speed control of the DC
```

```

% motor driven by a class-C chopper in z-domain
% Note: T/Ts and adim/Ts should be integer.
% -----
clear;
mtrpcsen;
sysparam;
adim=T;           % duty control interval
tilk=0;
tfinal=2;
xi=[];
dutymin=0.1;
dutyvektor=dutymin;
duty=dutymin;
Ts=duty*T/4;
Tss=Ts;

Kps=1;
Kis=5;
Kpi=10;
Kii=500;

set_param('classc/Step Fcn', 'After', Nref)

ap11=-Ra/La;      ap12=-Kafi/La;
ap21=Kafi/J;      ap22=-Bv/J;

Am=[ap11 ap12;ap21 ap22];
Bm=[0 1/La;-1/J 0];
Cm=[0 1;1 0];
Dm=[0 0;0 0];

```

```
[numTL, denTL]=ss2tf(Am,Bm,Cm,Dm,1);      % s-domain tr. fnc. due to TL
[numVa, denVa]=ss2tf(Am,Bm,Cm,Dm,2);      % s-domain tr. fnc. due to Va
```

```
[dnumTL, ddenTL]=c2dm(numTL,denTL,Tss,'zoh');
[dnumVa, ddenVa]=c2dm(numVa,denVa,Tss,'zoh');
%-----
%[dnumTL, ddenTL]=c2dm(numTL,denTL,Tss,'tustin');
%[dnumVa, ddenVa]=c2dm(numVa,denVa,Tss,'tustin');
%-----
```

```
num1z=dnumVa(2,:);
den1z=ddenVa;
num2z=dnumTL(2,:);
den2z=ddenTL;
num3z=dnumTL(1,:);
den3z=ddenTL;
num4z=dnumVa(1,:);
den4z=ddenVa;
```

```
%-----
tekrar=adim/T;
[numchop, denchop]=zzkare(T, duty, Ts, Kpwm, tekrar);
[Ea, Xa]=dimpulse(numchop, denchop, adim/Ts);
tf=0:Ts:(adim-Ts);
```

```
% -----
```

```
% writing to file
```

```
fidwrite=fopen('sonuc', 'w');
fprintf(fidwrite, '%4.4f %4.4fn', [], []);
fclose(fidwrite);
fidappend=fopen('sonuc', 'a');
```

```
fidwriteEa=fopen('sonucEa', 'w');
fprintf(fidwriteEa, '%4.4fn', []);
```

```

fclose(fidwriteEa);
fidappendEa=fopen('sonucEa', 'a');

fidwritedy=fopen('sonucdy', 'w');
fprintf(fidwritedy, '%4.4f\n', duty);
fclose(fidwritedy);
fidappenddy=fopen('sonucdy', 'a');
% -----
tol=1e-3;          minstep=Tss;          maxstep=Tss;
i=0;
oran=adim/Tss;
tson=oran*Tss;
while (tson<=tfinal)
    [t,x,N]=rk45('classc',[tilk (tson-Ts)],xi,[tol minstep maxstep]);
    i=i+1;
    sx=size(x);
    xi=x(sx(1),:);          % last row of x
    tN=[t N];
    fprintf(fidappend, '%4.8f %4.8f %4.8f %4.8f %4.8f\n', tN);
    fprintf(fidappendEa, '%4.4f\n', Ea);
    hatasabit=Ec(sx(1));
    alfa=hatasabit/Esw;
% -----
    if(alfa<dutymin) duty=dutymin;
        elseif(alfa>(1-dutymin)) duty=(1-dutymin);
    else    duty=alfa;
end
% -----
fprintf(fidappenddy, '%4.4f\n', duty);
tilk=oran*i*Tss
tson=oran*(i+1)*Tss;

```

```

[numchop, denchop]=zzkare(T,duty, Ts, Kpwm, tekrar);
[Ea, Xa]=dimpulse(numchop, denchop, (tson-tilk)/Ts);
tf=tilk:Ts:(tson-Ts);

end

fclose(fidappend);
fclose(fidappendEa);
fclose(fidappenddty);
disp(' Data files has been closed')
load sonuc;
load sonucdty;

figure
plot(sonuc(:,1),sonuc(:,2),'k')
grid;
ylabel('Speed(rad/sec)');
xlabel('time(sec)')

figure
plot(sonuc(:,1),sonuc(:,3),'k')
grid;
ylabel('Armature current(A)');
xlabel('time(sec)')

figure
plot(sonuc(:,1),sonuc(:,4),'k')
grid;
ylabel('Reference current(A)');
xlabel('time(sec)')

```

```

figure
zaman=[0:T:tfinal];
[dzaman,dsonucdty]=stairs(zaman,sonucdty);
plot(dzaman,dsonucdty,'k')
ylabel('duty cycle')
xlabel('time(sec)')
title(['classcm.m (f=', num2str(1/T), ' Hz)'])
axis([0 2 0 1])

```

zzkare.m

```

function [nz, dz]=zzkare(T,duty, Ts, genlik, tekrar)
% Returns the z-transform of the PWM signal whose period,
% duty cycle, amplitude and the number of period of the signal
% to be generated are the input arguments to the function

n=T/Ts;           % number of samples in one period
N=n*tekrar;
sample1s=floor(T*duty/Ts);
sample0s=n-sample1s;
numperT=[ones(1,sample1s) zeros(1,sample0s)];

num=numperT;
for i=1:(tekrar-1)
    num=[num numperT];
end

nz=genlik*num;
dz=[1 zeros(1,(N-1))];

```

REFERENCES

- Al-Assadi, Salem A.K. & Al-Chalabi, Lamy A.M. (1987) Optimal Gain for Proportional-Integral-Derivative Feedback, IEEE Control System Magazine, December, pp. 16-19.
- Bose, Bimal K. (1988) Technology Trends in Microcomputer Control of Electrical Machines, IEEE Transactions on Industrial Electronics, vol. 35, n.1, pp. 160-177.
- Chen, Chi-Tsong (1984) Linear System Theory and Design Holt, Rinehart and Winston.
- Damle, P.D. & Dubey, G.K. (1975) A Digital Computer Program for Chopper-Fed DC Motors, IEEE Trans.on Industrial Electronics and Control Instrumentation, vol. IECI-22, n.3, pp.408-412.
- Dorf, Richard C. (1992) Modern Control Systems (6th ed.), Addison Wesley.
- Dubey, Gopal K.(1989) Power Semiconductor Controlled Drives, Prentice-Hall.
- Dubey, G.K. & Shepherd, W. (1975) Analysis of d.c. series motor controlled by power pulses, IEE Proceedings, vol. 122, n.12, pp.1397-1398.
- Egami, T.; Wang, J. & Tsuchiya, T. (1985) Efficiency Optimized Speed Control System Synthesis Method Based on Improved Optimal Regulator Theory-

- Application to Separately Excited DC Motor System, IEEE Transactions on Industrial Electronics, vol. IE-32, n.4, pp.372-380.
- Fallside, F. & Wortley, A.T. (1969) Steady-state oscillation and Stabilization of variable-frequency inverter-fed induction-motor drives, Proceedings of IEE, vol.116, n.6, pp.991-998.
- Franklin, G.F., Powell, J.D., Workman, M.L. (1990) Digital Control of Dynamic Systems (2nd ed.), Addison-Wesley.
- Fu, M.; Olbrot, A.W. & Polis, M.P. (1989) Comments on “Optimal Gain for Proportional-Integral-Derivative Feedback”, IEEE Control System Magazine, January, pp.100-101.
- Grace, Andrew (1992) Optimization Toolbox For Use with MATLAB, The MathWorks Inc.
- Houpis, Constantine H. & Lamont, Gary B. (1987) Digital Control Systems Theory, Hardware, Software, McGraw-Hill.
- Huang, Lin & Li, Zhong (1989) Fundamental theorem for optimal output feedback problem with quadratic performance index, Int. Journal of Control, vol. 50, n.6, pp. 2341-2347.
- Jing-Ping Jiang, Shen Chen & Pradip K. Sinha, (1990) Optimal Feedback Control of Direct-Current Motors, IEEE Transactions on Industrial Electronics, vol. 37, n.4, pp. 269-274.
- Kettleborough, J.G.; Smith, I.R.; Vadher, V.V.; & Antunes, F.L.M. (1991) Microprocessor-Based DC Motor Drive with Spillover Field Weakening, IEEE Transactions on Industrial Electronics, vol. 38, n.6, pp.469-475.

Kojori, H.A.; Lavers, J.D. & Dewan, S. (1993) A Critical Assesment of the Continuous-System Approximate Methods for the Stability Analysis of a Sampled Data System, IEEE Transactions on Power Electronics, vol. 8, n.1, pp.76-84.

Krause, P.C. (1986) Analysis of Electric Machinery, Mc Graw-Hill.

Lewis, F.L. (1992) Applied Optimal Control & Estimation Digital Design & Impementation, Prentice-Hall.

Lipo, Thomas A. & Krause, Paul C. (1969) Stability Analysis of a Rectifier-Inverter Induction Motor Drive, IEEE Transactions on Power Apparatus and Systems, vol.PAS-88, n.1, pp.55-66.

Luenberger, David G. (1973) Introduction to Linear and Nonlinear Programming, Addison-Wesley Publishing Company.

Man, K.F.; Tang, K.S. & Kwong, S. (1996) Genetic Algorithms:Cocepts and Applications, IEEE Transactions on Industrial Electronics, vol. 43, n.5, pp.519-534.

MathSoft (1993) Mathcad User's Guide (4th printing), The MathSoft Inc.

MathWorks (1993) Matlab Control System Toolbox ver 3.0b, The MathWorks Inc.

MathWorks (1993) MATLAB High Performance Numeric Computation and Visualization Software User's Guide, The MathWorks Inc.

MathWorks (1993) SIMULINK Dynamic System Simulation Software User's Guide
The MathWorks Inc.

- Michalewicz, Zbigniew (1996) Genetic Algorithms + Data Structures = Evolution Programs (3rd, revised and extended ed.), Springer-Verlag.
- Mota, Philippe; Rognon, Jean Pierre & Le-Huy, Hoang (1984) Position Servo System: A State Variable Feedback System, IEEE Transactions on Industry Applications, vol. IA-20, November/December, pp. 1473-1481.
- Muir, P.F. & Neuman, C.P. (1985) Pulsewidth Modulation Control of Brushless DC Motors for Robotic Applications. IEEE Transactions on Industrial Electronics, vol. IE-32, n.3, pp.222-229.
- Nelder, J.A. & Mead, R. (1965) A Simplex method for function minimization, Computer Journal, vol.7, pp.308-313.
- Nitta, K.; Okitsu, H.; Suzuki, T. & Kinouchi, Y. (1970) Dynamic Response of Separately Excited DC Motor Driven by a Thyristor Pulsating Power Supply, Electrical Engineering in Japan, vol. 90, n.4, pp.95-102.
- Ogata, Katsuhiko (1990) Modern Control Engineering (2nd ed.), Prentice-Hall.
- Phillips, C.L. & Nagle, H.T. (1984) Digital Control System Analysis and Design, Prentice-Hall.
- Press W.H., Flannery B.P., Teukolsky S.A & Vetterling W.T (1992) Numerical Recipes in Fortran, The Art of Scientific Computing (2nd ed.), Cambridge University Press.
- Rao, S.S. (1984) Optimization, theory and applications (2nd ed.), Wiley Eastern Limited.

Rashid, Muhammad H. (1993) Power Electronics Circuits, Devices, and Applications. (2nd ed.), Prentice-Hall.

Saadat, Hadi (1993) Computational Aids in Control Systems using Matlab, McGraw-Hill Inc.

Sen, Paresh C. (1990) Electric Motor Drives and Control-Past, Present and Future, IEEE Transactions on Industrial Electronics, vol. 37, n.6, pp. 562-575.

Sen, Paresh C. (1991) Thyristor DC Drives (Reprint edition), Krieger Publishing Company.

Slemon G.R. & Straughen A. (1980) Electric Machines, Addison-Wesley Publishing Company.

Turner, W.W. (1988) Simulation of the Response of a dc Motor Driven from an SCR-Controlled Sources, IEEE Transactions on Education, vol. 31,n.3, pp.231-234.

Umanand, L. & Bhat, S.R. (1996) Optimal and robust digital current controller synthesis for vector-controlled induction motor drive systems IEE Proc. Electr. Power Appl. vol. 143, n.2, pp. 141-150.

Walsh G.R. (1979) Methods of Optimization, John Wiley and Sons.

Wester, G. W. & Middlebrook, R. D. (1973) Low-Frequency Characterization of Switched dc-dc Converters, IEEE Transactions on Aerospace and Electronic Systems, vol. AES-9, n.3, pp.376-385.